Novel, Rapid and Cost-effective Methods for Concentration, Detection and Monitoring of Waterborne Pathogens in Resource-Limited Settings

Thesis by

Xunyi Wu

In Partial Fulfillment of the Requirements for the degree of

Doctor of Philosophy

CALIFORNIA INSTITUTE OF TECHNOLOGY

Pasadena, California

2021

(Defended 06/02/2021)

Xunyi Wu

ORCID: 0000-0001-9710-6896

ACKNOWLEDGEMENTS

It is with tears and smiles that I write this acknowledgement section of my thesis: I have so many words of gratitude to all of you who have helped me during this long and incredible journey that I don't know where to begin. I feel so blessed that I've spent six years with inspiring mentors and brilliant peers. It was you who helped me become a qualified PhD and a better person. Therefore, I'll have a long list in this section for everyone I am thankful for. If I happened to miss some of you in this list, please forgive my forgetfulness and please know that I am always so thankful for all the support I have received from everyone.

First and foremost, I would like to thank my advisor Professor Michael R. Hoffmann, a most cheerful, encouraging advisor. He is always there, ready to guide me when I am in doubt, yet allow me to explore my interest in the field of environmental microbiology. Mike never hesitates to share words of wisdom in navigating the academia and the larger life beyond. Besides my advisor, other members of my committee, Professor Jared R. Leadbetter, Professor Alex L. Sessions, and Professor David A. Tirrell all offered me important advices towards my thesis work. I would like to thank them for their valuable time and comments.

I would also like to thank the Bill and Melinda Gates Foundation for the continuous funding support towards our group and my own research. It was an honor for me to work

with the Foundation and develop technologies that help better control deadly pathogens and save lives in developing countries.

My thesis work would never have been finished without the day-to-day guidance and hand-by-hand help from senior researchers in our Lab: Dr. Xing Xie, Dr. Eric Huang, and Dr. Jing Li. I was a newbie in environmental microbiology when I started six years go. I could never imagine myself performing my experiments independently without learning every little experimental technique and tricks from you. Besides the lab techniques and scientific knowledge, you also advised me on how to plan and carry out research projects. Thank you for being the role models for me as intelligent and professional researchers.

I am proud to say that I worked with the most excellent lab mates who are not only great researchers but also sincere friends: Jieun Shin, Eunkyung Kim, Dr. Yanzhe Zhu, Dr. Siwen Wang, Dr. Yang Yang, Dr. Cody Finke, Dr. Clément Cid, Dr. Eric Huang, Dr. Sara Li, Dr. Xingyu Lin, Dr. Katharina Urmann, Eitam Shafran, Dr. Leda Katebian, Hugo Leandri, Léopold Dobelle, Axl LeVan, Sam Zhang, Heng Dong, Dr. Lei Guo, Alan Gu, Sean Kim, Dr. Su Young Ryu, Dr. Sean McBeath, Dr. A. J. Colussi, Dr. Nathan Dalleska, and many others including visiting research scholars. Thank you for always being there for me. I will never forget all the little favors such as opening chemical bottles, unscrewing centrifuge rotors, etc. and I enjoyed all the great group meetings we had with beers and snacks.

I would like to say a big ‘thank you’ for all the great friends in my life! I still remember when I first met Dr. Yanzhe Zhu, Dr. Stephanie Kong, Dr. Siteng Fan, and Dr. Hao Xie during orientation and how we got drunk together days after. It is so moving to see us all grow up so much during these years and succeed in our respective fields. Caltech has introduced so many great friend into my life: Dr. Xiaomin Li, Dr. Yi Xu, Dr. Jia He, Dr. Zhaoyi Shen, Dr. Yuanlong Huang, Dr. Liuchi Li, Dr. Jinglin Huang, Dr. Yu Su, Dr. Ruohan Wang, Dr. Ke Yu, Sam Zhang, Hao Liu, Heng Dong and so many others. Hanging out with you made my life much more enjoyable. I am delighted to be friends with you.

Many thanks also go out to my old friends since college: Jiawei Chen, Wendy Jiang, Sharine Chen, Pingbo Yang, and Xiaotian Shen. Although we are currently scattered all around the world, we always have so much to talk about when we see each other and I am really happy to witness so many great things happen in your lives. I really hope I can see you soon when the current COVID situation gets better so that I can go back to China.

I should also thank my snowboarding buddies. I used to hate sports, especially difficult outdoor sports such as snowboarding, but my friends encouraged me to try. You were very patient when I started to learn. Dr. Siteng Fan, Dr. Yu Su, Dr. Ke Yu and Dr. Zhicai Zhang were my first coaches who instilled passion of snowboarding in me with the unforgettable quote “It’s gonna be fast but it’s okay”. I still repeat that quote to myself when I practice. My other snowboarding and skiing buddies include but not limited to: Dr. Xiaomin Li, Dr.

Yi Xu, Dr. Cindy Ren, Fangzhou Xiao, Dr. Jinglin Huang, Dr. Liuchi Li, Yang Gao etc. Drinking hot chocolate and mulled wine, and having authentic Chinese hotpots at Mammoths with you are some of my best experiences.

I also met many great friends through Dragon Nest (an online MMO game): Yi Zhao, Haiqin Liu, Weili Zhu, Jinge Qin, Qi Fen, and so many other members in our guild. From teammates who work back-to-back together and slay evil dragons, to real-life friends that hang out and travel together. I feel so lucky that a game could brought me so much and I could proudly say that I never regretted joining and leading our guild! I would also like to thank TWICE, the idol group debuted shortly after I started my PhD student life back in 2015. Those nine girls always bring me so much happiness and energy when I watch their stages and TV shows, and their songs cheered me up when I was low on momentum. Although the closest physical distance we had was when I went to your concerts, in my heart, you have always been one of my best friends.

A special thanks goes to my boyfriend Dr. Fei Dai, a man with a smart mind and a warm heart. Thank you for being my best friend, always listening to my problems and encouraging me to face new challenges. When we are together, we always have endless things to share and talk about and we have similar opinions towards this chaotic world. I feel lucky to have met you and to understand you, and I will always support you just as you support me. I love you.

Finally, I would like to thank my parents and my other family members. My parents, Xiaoping Gao and Guo'er Wu, are so supportive of all my important decisions in life. They encouraged me to come to the U.S. for college when I was 18. They hoped that I could see a bigger world. I am grateful that my ten years here in the U.S. made me grow up so much. My grandparents are my biggest fans, always telling everyone how smart and how sweet their granddaughter is. When I go home, they always prepare my favorite childhood dishes and tell me they are always proud of me. In fact, I am so proud of my family members and their love is the ultimate reason for all the successes I've achieved and I'll achieve in the future.

ABSTRACT

Waterborne pathogenic organisms including bacteria, viruses, protozoa and helminths, are responsible for a series of diseases which is a major public health concern worldwide. This issue is extremely severe in developing regions due to the scarcity of clean water supply and poor sanitation. Therefore, point-of-use (POU) detection and quantification processes as well as a monitoring program of waterborne pathogens are needed to ensure the safety of water and protect human health. However, the polymerase chain reaction (PCR) technology and its related detection platforms rely on complicated thermal cycling, centralized laboratory equipment and trained personnel, thus making PCR-based systems incapable of POU testing of environmental waters. In this dissertation, we develop a portable 3D-printed system with super-absorbent polymer (SAP) microspheres for sample enrichment, and a membrane-based in-gel loop-mediated isothermal amplification (mgLAMP) system for absolute quantification of pathogens. We also explored the interactions between microbial indicator of *Escherichia coli* (*E. coli*) and waterborne pathogen *Vibrio Cholerae* (*V. Cholerae*). The main results are as follows:

1. The application of detection and quantification methods is often hindered by the low pathogen concentrations in natural waters. Rapid and efficient sample concentration methods are urgently needed. Here we present a novel method to pre-concentrate microbial pathogens in water using a portable 3D-printed system with super-absorbent polymer (SAP) microspheres,

which can effectively reduce the actual volume of water in a collected sample. The SAP microspheres absorb water while excluding bacteria and viruses by size exclusion and charge repulsion. The 3D-printed system with optimally-designed SAP microspheres could rapidly achieve a 10-fold increase in the concentration of *E. coli* and bacteriophage MS2 within 20 minutes with concentration efficiencies of 87% and 96%, respectively. Fold changes between concentrated and original samples from qPCR and RT-qPCR results were found to be 11.34-22.27 for *E. coli* with original concentrations of 10^4-10^6 cell·mL^{-1}; and 8.20-13.81 for MS2 with original concentrations of 10^4-10^6 PFU·mL^{-1}. Furthermore, SAP microspheres can be reused 20 times without performance loss thereby significantly decreasing the cost of our concentration system.

2. Following sample concentration, accurate quantification methods for waterborne pathogens are needed, especially at the point of sample collection. The surge of COVID-19 in late 2019 called for a more urgent need for a rapid and cost-effective quantification of SARS-CoV-2 in environmental waters. Quantification results contribute to wastewater-based epidemiology (WBE) which helps the monitoring of prevalent infections within a community and early detections of contamination. Here we demonstrated the usage of our portable membrane-based in-gel loop-

mediated isothermal amplification (mgLAMP) system for absolute quantification of SARS CoV-2 in wastewater samples within a one-hour timeframe for point-of-use (POU) testing and data management. The limit of detection (LOD) of mgLAMP for SARS-CoV-2 quantification in Milli-Q water was observed to be down to 1 copy/mL, and that in surface water collected from Kathmandu, Nepal was down to 100 copies/mL. Both were 100-fold lower than that of RT-qPCR in corresponding matrices. Compared to alternative detection methods, our platform has a very high level of tolerance against inhibitors thanks to the restriction of the hydrogel matrix. This enables the highly sensitive detection in either clinical or environmental samples.

3. Regular environmental surveillance of waterborne pathogens is key to ensure the safety of water and protect public health. Due to the diversity of pathogenic bacteria in environmental waters, regular monitoring of so many pathogens for individuality is impractical. Therefore, microbial indicators are used to gauge the total pathogen concentration; and manage waterborne health risks. In this study, the interactions of *V. cholerae*, the etiologic agent of reemerging cholera, with *E. coli*, the most commonly used indicator for waterborne pathogens. Specifically, we investigated through evaluating the survival and growth of both bacteria under different temperature and

nutrition deprivation using plate culturing and real-time polymerase chain reaction (qPCR). During co-growth, it was challenging for *V. Cholerae* to maintain initial population advantages as *E. coli* consumes nutrition more effectively. Whereas during co-existence, *V. Cholerae* soon fell into a viable-but–non-culturable state under environmental stress in 3-5 days while *E. coli* stay viable more than 14 days. We found that *V. cholerae* interacts with *E. coli* differently depending on the composition of the water that is sampled and analyzed. This suggests that bacterium-bacterium interactions influenced by the intrinsic chemical and biological parameters of ambient water will be a contributing mechanism in regulating the proliferation of *V. cholerae*.

In summary, two platforms for environmental sample concentration and detection have been developed and tested using ambient and engineered waters. In addition, interactions between a microbial indicator, *E. coli,* and the pathogenic bacteria, *V. Cholerae,* were studied. The chapters in this thesis describe in detail: (1) A hand-pressed 3D-printed system to produce SAP microspheres was developed with the goal of achieving efficient concentrations of environmental microorganisms for subsequent analysis. The simplified concentration procedure and can be easily integrated into various detection platforms; (2) A portable membrane-based in-gel loop-mediated isothermal amplification (mgLAMP) system was developed for absolute quantification of SARS-CoV-2 in environmental water

samples within one hour, enabling a 100-fold lower detection limit compared to the gold-standard of RT-qPCR; and (3) Differences in bacterium-bacterium interactions of *V. cholerae* and *E. coli* under as a function of water composition indicated that environmental stress presented in ambient water matrices should be taken into consideration while using a microbial indicator such as *E. coli* to estimate the risk of waterborne pathogens. These collective advances allow for the rapid and ultrasensitive POU testing of waterborne pathogens that should provide for more effective monitoring strategies in terms of the use of indicator microorganisms.

PUBLISHED CONTENTS AND CONTRIBUTIONS

[6] **Xunyi Wu**, Jing Li, Michael R. Hoffmann. **(2021).** "Co-occurrence patterns of *Vibrio cholerae* and *Escherichia coli* in various environmental settings." In preparation.

M.R.H, J.L., and X.W. conceived the concept for this study. J.L. and X.W. designed the study, X.W. performed experiments, and X.W. wrote the paper.

[5] **Xunyi Wu**, Yanzhe Zhu, Jing Li, Michael R. Hoffmann. **(2021).** "Membrane-Based in-Gel Loop-Mediated Isothermal Amplification (mgLAMP) System Enables SARS-CoV-2 Quantification in Milliliters of Environmental Waters." In preparation.

M.R.H. and J.L. conceived the concept for this study. J.L. and Y.Z. designed the study, J.L. X.W. and Y.Z. performed experiments, J.L. X.W. and Y.Z. analyzed the data, and X.W. wrote the manuscript.

[4] **Xunyi Wu**, Xiao Huang, Yanzhe Zhu, Jing Li, Michael R. Hoffmann. **(2020)**. "Synthesis and Application of Superabsorbent Polymer Microspheres for the Concentration and Quantification of Microbial Pathogens in Ambient Water." *Separation and Purification Technology*, 239:116540.

M.R.H, X.H., and X.W. conceived the concept for this study. J.L., X.H. and X.W. designed the study, X.W. performed experiments, and J.L. X.W. and Y.Z. wrote the paper.

[3] Jing Li, Yanzhe Zhu, **Xunyi Wu**, and, Michael R. Hoffmann. **(2020).** "Rapid Detection Methods for Bacterial Pathogens in Ambient Waters at the Point of Sample Collection: A Brief Review." *Clinical Infectious Diseases*.**2020**, *71* (Suppl. 2), S84–S90.

X.W. reviewed cell-based technologies and contributed to compiling the technology summary table, manuscript writing, and editing.

[2] Sunny Jiang, Hamsa Gowda, Huang Xiao, **Xunyi Wu**, Marc Madou, Michael R. Hoffmann. (2019) "Portable Pathogen Analysis System for Detecting Waterborne Pathogens" US Patent 20190105653A1

X.W. participated in developing the pretreatment technology, and contributed to the patent writing, and editing.

[1] Yanzhe Zhu, Xiao Huang, Xing Xie, Janina Bahnemann, Xingyu Lin, **Xunyi Wu**, Siwen Wang, and Michael R. Hoffmann. (**2018**). "Propidium monoazide pretreatment on a 3D-printed microfluidic device for efficient PCR determination of 'live versus dead' microbial cells". *Environmental Science: Water Research & Technology* 4(7): 956-963.

X.W. participated in the manuscript editing.

TABLE OF CONTENTS

LIST OF ILLUSTRATIONS AND/OR TABLES

Number ***Page***

Chapter 1

INTRODUCTION

1.1. Introduction

Multiple diseases caused by waterborne pathogens are responsible for high morbidity and mortality in developing regions of the world[1,2]. According to the World Health Organization (WHO), global mortality attributable to water-related diseases is currently 3.4 million per year, most of which are impacting children[3]. Unsafe water supplies and poor sanitation conditions exacerbate the spread of these waterborne disease particularly among those with relatively weak immune systems[4]. Moreover, diseases caused by waterborne pathogens can potentially cause regional outbreaks posing serious risks to many local communities[5,6]. Therefore, regular detection and monitoring of these pathogens is essential for evaluating the health risk and ensuring the safety of water[7].

1.1.1. Concentration Methods of Waterborne Pathogens

Concentration methods are crucial for detecting pathogens in environmental waters, because the concentrations of pathogens in environmental water samples are usually orders of magnitudes lower than those in clinical samples. Small sample volumes in detection assays make the direct detection of pathogens in

environmental water samples difficult[7,8]. Pathogen concentrations below the detection limit of detection do not guarantee the safety of water as many pathogens have very low infectious doses [1,9]. Therefore, numerous techniques for pathogen concentration have been developed including traditional techniques such as polyethylene glycol (PEG) coagulation and precipitation, membrane filtration, centrifugation, and evaporation[10,11], in-plane evaporation[12], magnetic nanoparticle platforms on a chip[13], or magnetic separators[14,15]. However, these concentration methods may require complicated setups, are time-consuming, or limited for use in a laboratory, or are incapable of handling field samples with volumes less than 1 or 2 liters[14–16] or up to 100 liters in the case of polio virus detection in remote ambient waters.

A novel concentration method uses Super-absorbent polymer (SAP) microspheres. SAPs are a class of cross-linked hydrogels that can absorb and retain water up to 1000 times the initial dry weight of the SAP materal[17,18]. By controlling the pore sizes of the hydrogel down to several nanometers, SAPs can absorb water but at the same time exclude particles with sizes above several nanometers, such as bacteria and viruses[19,20]. In order to use SAPs for microbial sample concentration, the SAPs were synthesized as small spherical microspheres using a milli-fluidic flow system.

Itaconic acid is added to the polymer to obtain negatively charged polymer surface. These polymeric microspheres have uniform spherical shapes, which minimize electrostatic adsorption of microorganisms on the surface of the microspheres[21]. Furthermore, SAP microspheres absorb water through osmosis, which is driven by polyelectrolyte counter ions attached to the polymer. The maximum water absorbencies and water absorption rates of the SAPs are determined by the equilibrium of the osmotic forces and the retention forces of the polymer network. For a given SAP formulation with a fixed number of polyelectrolyte counter ions, the osmotic force generated by the SAPs decreases with an increase of ionic strength, which effectively lowers the maximum water absorbency and water absorption rate of a specific SAP formulation. Therefore, the ionic strength of environmental water samples has a significant impact on the performance of the SAP microspheres.

1.1.2 Detection Platforms of Waterborne Pathogens

Following sample concentration, accurate detection and quantification methods for waterborne pathogens are needed at the point of sample collection[8,22]. However,

to date, monitoring sites and sample frequencies are limited due to the high demands and workload of standard laboratory methods. Also, collected water samples need to be refrigerated and transported to centralized laboratories for analysis. This may result in sample degradation during the transportation[7]. Regular detection methods include phenotypic methods based on cultivation, which is a standard approach for the identification and quantification of pathogenic bacteria and viruses[23,24]. However, phenotypic methods can only identify the concentration of live and culturable organisms at the genus level. The use of molecular methods such as enzyme-linked immunosorbent assay (ELISA), biosensors, and the polymerase chain reaction (PCR) technique have become routine due to their sensitivity, specificity, and short sample-to-result time (usually under 2 hours)[25–29]. Among the molecular methods, the most wildly used technique is PCR or RT-PCR (Reverse Transcription PCR) which amplifies target nucleic acids to a large amount within a short time. The technique is highly sensitive and can produce millions to billions of copies for subsequent fluorescence analysis. Evolving from the preliminary qualitative analysis, current real-time PCR (qPCR) can achieve relative quantification using internal controls, reference genes, or standard curves[30,31]. Digital PCR can provide an absolute quantification without calibration[32,33]. Digital PCR works by separating the sample into a large number of partitions, in which the

reaction is carried out in each partition individually. After the reaction, a back-calculation using the final proportion of positive and negative reactions in each partition based on a Poisson distribution is made to obtain sensitive and accurate measurement of nucleic acid amounts without calibration[34].

Microfluidic chips with reaction chambers based on polydimethylsiloxane (PDMS), glass or silicon materials have been developed and the partition of sample and reaction mix can be partitioned using vacuums, valves, or pumps.[35–38]. Compared to physical chambers, another form of digital PCR uses water-in-oil droplets in which each droplet becomes a mini-reactor for PCR[39]. There are also commercial digital PCR systems developed commercially for use of either droplets or physical chambers. However, these platforms are often complicated to use and expensive. They often require trained researchers with professional skills to perform the assays. Another major challenge to apply digital PCR in the field is that amplification of PCR relies on the thermo-cycling, which requires temperature controlling elements. Therefore, an alternative amplification method, Loop-mediated Isothermal Amplification (LAMP) has been developed and widely used[40,41]. The LAMP amplification method is performed at a constant temperature, which simplifies the analytical system design. LAMP amplification readily

achieves a high degree of specificity and a tolerance toward inhibitors present in environmental samples.

Covid-19 is an unparalleled pandemic. As of May 10th, 2021, 158,612,000 cases and more than 3,299,000 deaths have been reported according to COVID-19 Dashboard presented by the Center for Systems Science and Engineering at Johns Hopkins University. The number continue to grow. The quantification of SARS-CoV-2, the causative virus leading to COVID-19, is routinely present in wastewater, thus wastewater-based epidemiology (WBE) has become an importance source tracing tool. Quantification of SARS-CoV-2 in wastewater provides the ability to monitor the prevalence of infections among target populations[42,43] and allows for early detection of viral contamination. However, SARS-CoV-2 quantification relies on the availability of specialized equipment and personnel for environmental[44] water sample preparation, processing, and analysis. Thus, ultrasensitive, rapid, and cost-effective microbial detection platforms for point-of-sampling testing (POST) are urgently needed.

1.1.3. Monitoring Strategies of Waterborne Pathogens

Regular environmental surveillance of waterborne pathogens is required to ensure the safety of recreational and drinking water in order to protect human health. As mentioned above, precise detection and quantification methods for waterborne pathogens including traditional culture-based methods and more recent nucleic acid amplification diagnosis are regularly used in surveillance programs to periodically measure the concentrations of target pathogens and to evaluate the potential risks[42]. Due to the diverse range of pathogenic bacteria in environmental waters, regular monitoring for specific pathogens is often impractical. Therefore, microbial indicators are most often used to manage waterborne health risks[23,43]. Microbial indictors are microorganisms that are more abundant and more easily detected, and are indicative of the potential presence of other pathogenic organisms. The most commonly used microbial indicator is *Escherichia coli* (*E. coli*) due to its high correlation with fecal contaminations[44–46]. There is a high concentration of *E. coli* in the intestine of vertebrate animals. Therefore, the presence of *E. coli* in environmental waters is used as indicator of fecal contamination and associated pathogenic risks[47,48]. Compared to many pathogenic bacteria ,which usually have very low concentration in environmental waters and are thus difficult to be detected,

E. coli's concentration is relatively high in both food or environmental samples. Furthermore, there are well-established detection protocols for *E. coli* using both cultivation-based and nucleic acid analysis methods.

One of the leading etiologic pathogenic bacteria that need to be frequently monitored is *Vibrio cholerae* (*V. cholerae*). Some strains of *V. cholerae* that can secrete cholera toxin (CT); they are also the causative agent of the reemerging cholera as a disease[49,50]. During bacterial infection of the human intestine, mucous production is enhanced, leading to diarrhea and vomiting which will cause extreme dehydration. Cholera is estimated to cause around 2.8 million cases of illness and 91,000 deaths worldwide annually[51]. Similar other pathogenic bacteria, *V. cholerae* is mainly transmitted through the fecal-oral route, in which fecal matter is secreted by infected persons is passed on to healthy individuals though untreated drinking water or contaminated food[22]. Moreover, after being released to the environment. *V. cholerae* can persist in aquatic reservoirs for weeks or months, which further increase the difficulty to eradicate the transmission of the disease[52,53]. Testing the concentration of the microbial indicator *E. coli* in environmental waters should give useful information for the presence of *V. cholerae*, which will help evaluating the risk of this pathogenic bacteria and design better bottom-up control practices.

However, the growth, persistence, and survival of this indicator bacteria with other fecal contaminants can vary as a function of environmental location. In addition, the correlation between *E. coli* with *V. cholerae* and its relationship to other pathogenic bacteria needs to be studied in order to provide better methods for monitoring waterborne pathogens[43,47].

1.2. Thesis outline

The structure of this thesis has three parts. The schematic roadmap of the thesis is shown in **Figure 1.1.**

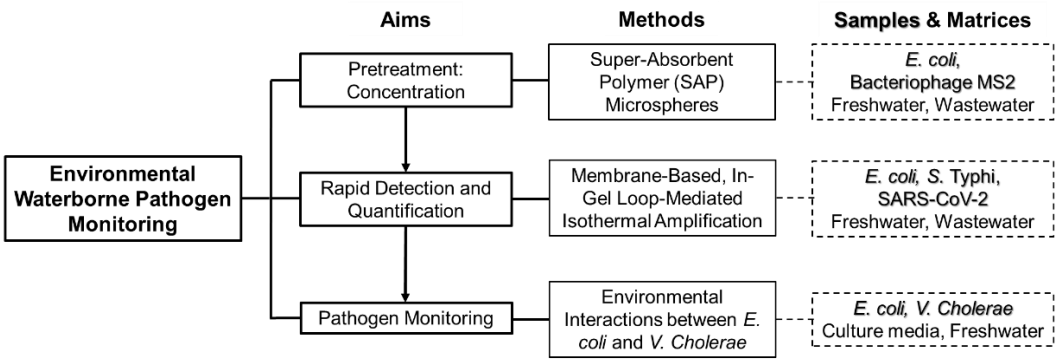

Figure 1.1 Roadmap of this thesis dissertation.

Even though numerous methods have been developed for the detection and quantification of waterborne pathogens, the application of these methods is often hindered by the very low pathogen concentrations in natural waters. Therefore, rapid and efficient sample concentration methods are urgently needed. In **Chapter**

2, we present a novel method to pre-concentrate microbial pathogens in water using a portable 3D-printed system with super-absorbent polymer (SAP) microspheres, which can effectively reduce the actual volume of water in a collected sample. The SAP microspheres absorb water while excluding bacteria and viruses by size exclusion and charge repulsion. SAP microspheres can be reused for 20 times without performance loss. This capability significantly decreases the cost of a 'point of use' concentration system.

Following the SAP concentration step, **Chapter 3** explores the use of a membrane-based, in-gel loop-mediated isothermal amplification (mgLAMP) platform for digital detection of SARS-CoV-2 and several pathogenic bacteria in ambient water samples. Since the detection and quantification of many pathogenic microorganisms still relies primarily on either culture-based assays, which takes a relatively long time, or polymerase chain reaction (PCR) assays, which are often constrained to use in a laboratory. In this study, we report on an on-membrane in-gel loop-mediated isothermal amplification (mgLAMP) system using QUASR or molecular beacon probes. Viral or bacterial particles in environmental water samples are initially filtered through a PCTE membrane and then immobilized with LAMP reagents in a polyethylene glycol hydrogel. Amplification of the target

nucleic acids through the LAMP reaction is restricted by the hydrogel matrix. Finally, we used the number of fluorescent amplicon dots, which are imaged by a smartphone, to quantitatively determine the initial concentration of SARS-CoV-2 or pathogenic bacterial concentration in a water sample.

Chapter 4 explores the potential antagonistic interactions of *Vibrio cholerae* (*V. cholerae*) and *Escherichia coli* (*E. coli*) in terms of their relative dominance, and growth in competition for substrates and nutrients as functions of temperature, salinity, pH using plate culturing and real-time polymerase chain reaction (qPCR) as quantification tools. *V. cholerae* interacts *E. coli* differently based on a given water conditions. This suggests that competitive microbial interactions are also influenced by environmental stressors present in ambient waters and that various inhibitors or anthropogenic contaminants may actually regulate the proliferation of *V. cholerae*.

References

(1) Bridle, H. *Waterborne Pathogens*; 2014.

(2) World Health Organization. Drinking-water http://www.who.int/news-room/fact-sheets/detail/adolescent-pregnancy.

(3) World Health Organization. *Water for Health: Taking Charge*; 2001.

(4) Rusin, P. A.; Rose, J. B.; Haas, C. N.; Gerba, C. P. Risk Assessment of Opportunistic Bacterial Pathogens in Drinking Water. *Rev. Environ. Contam. Toxicol.* **1997**, *152*, 57–83.

(5) Diseases, W. Water Sanitation Hygiene Water-Related Diseases. **2020**, 3–5.

(6) Gunda, N. S. K.; Mitra, S. K. Rapid Water Quality Monitoring for Microbial Contamination. *Electrochem. Soc. Interface* **2017**, *25* (4), 73–78.

(7) Aw, T. G.; Rose, J. B. Detection of Pathogens in Water: From Phylochips to QPCR to Pyrosequencing. *Curr. Opin. Biotechnol.* **2012**, *23* (3), 422–430.

(8) Ramírez-Castillo, F.; Loera-Muro, A.; Jacques, M.; Garneau, P.; Avelar-González, F.; Harel, J.; Guerrero-Barrera, A. Waterborne Pathogens: Detection Methods and Challenges. *Pathogens* **2015**, *4* (2), 307–334.

(9) Schmid-Hempel, P.; Frank, S. A. Pathogenesis, Virulence, and Infective Dose. *PLoS Pathog.* **2007**, *3* (10), 1372–1373.

(10) Stevens, K. A.; Jaykus, L. A. Bacterial Separation and Concentration from Complex Sample Matrices: A Review. *Critical Reviews in Microbiology*. **2004**, pp 7–24.

(11) Borchardt, M. A.; Kieke, B. A.; Spencer, S. K. Ranking Filter Methods for Concentrating Pathogens in Lake Water. *Appl. Environ. Microbiol.* **2013**, *79* (17), 5418–5419.

(12) Choi, J. W.; Hosseini Hashemi, S. M.; Erickson, D.; Psaltis, D. A Micropillar Array for Sample Concentration via In-Plane Evaporation. *Biomicrofluidics* **2014**, *8* (4), 1–9.

(13) Zhang, Y.; Riley, L. K.; Lin, M.; Hu, Z. Lanthanum-Based Concentration and Microrespirometric Detection of Microbes in Water. *Water Res.* **2010**. 44(11), 3385-92.

(14) Rotariu, O.; Ogden, I. D.; MacRae, M.; Bădescu, V.; Strachan, N. J. C. An Immunomagnetic Separator for Concentration of Pathogenic Micro-Organisms from Large Volume Samples. *J. Magn. Magn. Mater.* **2005**, *293* (1), 589–596.

(15) Chen, G. D.; Alberts, C. J.; Rodriguez, W.; Toner, M. Concentration and Purification of Human Immunodeficiency Virus Type 1 Virions by Microfluidic Separation of Superparamagnetic Nanoparticles. *Anal. Chem.* **2009**, *82* (2), 723–728.

(16) Park, S.; Zhang, Y.; Wang, T.-H.; Yang, S. Continuous Dielectrophoretic Bacterial Separation and Concentration from Physiological Media of High Conductivity. *Lab Chip* **2011**, *11* (17), 2893.

(17) Kiatkamjornwong, S. Superabsorbent Polymers and Superabsorbent Polymer Composites. *ScienceAsia* **2007**, *33* (1), 39–43.

(18) Lee, W.-F.; Wu, R.-J. Superabsorbent Polymeric Materials. I. Swelling Behaviors of Crosslinked Poly(Sodium Acrylate-Co-Hydroxyethyl Methacrylate) in Aqueous Salt Solution. *J. Appl. Polym. Sci.* **1996**, *62* (7), 1099–1114.

(19) Valade, D.; Wong, L. K.; Jeon, Y.; Jia, Z.; Monteiro, M. J. Polyacrylamide Hydrogel Membranes with Controlled Pore Sizes. *J. Polym. Sci. Part A Polym. Chem.* **2013**, *51* (1), 129–138.

(20) Mark Elliott. Superabsorbent Polymers. **1994**, *573*, 128–140.

(21) Xie, X.; Bahnemann, J.; Wang, S.; Yang, Y.; Hoffmann, M. R. "Nanofiltration" Enabled by Super-Absorbent Polymer Beads for Concentrating Microorganisms in Water Samples. *Sci. Rep.* **2016**, *6* (2), 1–8.

(22) Leclerc, H.; Schwartzbrod, L.; Dei-Cas, E. Microbial Agents Associated with Waterborne Diseases. *Crit. Rev. Microbiol.* **2002**, *28* (4), 371–409.

(23) Straub, T. M.; Chandler, D. P. Towards a Unified System for Detecting Waterborne Pathogens. *J. Microbiol. Methods* **2003**, *53* (2), 185–197.

(24) Lin, X.; Huang, X.; Zhu, Y.; Urmann, K.; Xie, X.; Hoffmann, M. R. Asymmetric Membrane for Digital Detection of Single Bacteria in Milliliters of Complex Water Samples. *ACS Nano* **2018**. *12* (10), 10281–10290.

(25) Cheng, C. M.; Martinez, A. W.; Gong, J.; Mace, C. R.; Phillips, S. T.; Carrilho, E.; Mirka, K. A.; Whitesides, G. M. Paper-Based Elisa. *Angew. Chemie - Int. Ed.* **2010**. *49* (28):4771-4.

(26) Nasseri, B.; Soleimani, N.; Rabiee, N.; Kalbasi, A.; Karimi, M.; Hamblin, M. R. Point-of-Care Microfluidic Devices for Pathogen Detection. *Biosens. Bioelectron.* **2018**, *117* (5), 112–128.

(27) Vikesland, P. J.; Wigginton, K. R. Nanomaterial Enabled Biosensors for Pathogen Monitoring - A Review. *Environ. Sci. Technol.* **2010**, *44* (10), 3656–3669.

(28) Justino, C. I. L.; Duarte, A. C.; Rocha-Santos, T. A. P. Recent Progress in Biosensors for Environmental Monitoring: A Review. *Sensors (Switzerland)* **2017**, *17* (12).

(29) Marx, V. PCR Heads into the Field. *Nat. Methods* **2015**, *12* (5), 393–397.

(30) Shipley, G. The MIQE Guidelines Uncloaked. In *PCR Troubleshooting and Optimization: The Essential Guide*; **2011**; 149–162.

(31) Morley, A. A. Digital PCR: A Brief History. *Biomol. Detect. Quantif.* **2014**, *1* (1), 1–2.

(32) Taylor, S. C.; Laperriere, G.; Germain, H. Droplet Digital PCR versus QPCR for Gene Expression Analysis with Low Abundant Targets: From Variable Nonsense to Publication Quality Data. *Sci. Rep.* **2017**, *7* (1), 1–8.

(33) Whale, A. S.; Huggett, J. F.; Tzonev, S. Fundamentals of Multiplexing with Digital PCR. *Biomol. Detect. Quantif.* **2016**, *10*, 15–23.

(34) Lin, X.; Huang, X.; Urmann, K.; Xie, X.; Hoffmann, M. R. Digital Loop-Mediated Isothermal Amplification on a Commercial Membrane. *ACS Sensors* **2019**, *4* (1), 242–249.

(35) Xu, T.; Wu, L.; Wang, X.; Zhu, X.; Bao, Y.; Cai, S.; Li, G.; Li, X. A PDMS-Based Digital PCR Chip with Vacuum Aspiration and Water-Filling Cavity Integrated for Sample Loading and Evaporation Reduction. *Proc. IEEE Int. Conf. Micro Electro Mech. Syst.* **2018**, 1142–1145.

(36) Du, W.; Li, L.; Nichols, K. P.; Ismagilov, R. F. SlipChip. *Lab Chip* **2009**, *9* (16), 2286.

(37) Shen, F.; Du, W.; Kreutz, J. E.; Fok, A.; Ismagilov, R. F. Digital PCR on a SlipChip. *Lab Chip* **2010**, *10* (20), 2666.

(38) Yin, X.; Zhang, J.; Wang, X. Sequential Injection Analysis System for the Determination of Arsenic by Hydride Generation Atomic Absorption Spectrometry. *Fenxi Huaxue* **2004**, *32* (10), 1365–1367.

(39) Hindson, B. J.; Ness, K. D.; Masquelier, D. A.; Belgrader, P.; Heredia, N. J.; Makarewicz, A. J.; Bright, I. J.; Lucero, M. Y.; Hiddessen, A. L.; Legler, T. C.; et al. High-Throughput Droplet Digital PCR System for Absolute Quantitation of DNA Copy Number. *Anal. Chem.* **2011**, *83* (22), 8604–8610.

(40) Notomi, T. Loop-Mediated Isothermal Amplification of DNA. *Nucleic Acids Res.* **2000**. *28*(12): E63.

(41) Huang, X.; Lin, X.; Urmann, K.; Li, L.; Xie, X.; Jiang, S.; Hoffmann, M. R. Smartphone-Based in-Gel Loop-Mediated Isothermal Amplification (GLAMP)

System Enables Rapid Coliphage MS2 Quantification in Environmental Waters. *Environ. Sci. Technol.* **2018**, *52* (11), 6399–6407.

(42) Ahmed, W.; Angel, N.; Edson, J.; Bibby, K.; Bivins, A.; O'Brien, J. W.; Choi, P. M.; Kitajima, M.; Simpson, S. L.; Li, J.; et al. First Confirmed Detection of SARS-CoV-2 in Untreated Wastewater in Australia: A Proof of Concept for the Wastewater Surveillance of COVID-19 in the Community. *Sci. Total Environ.* **2020**, *728*, 138764.

(43) Gonzalez, R.; Curtis, K.; Bivins, A.; Bibby, K.; Weir, M. H.; Yetka, K.; Thompson, H.; Keeling, D.; Mitchell, J.; Gonzalez, D. COVID-19 Surveillance in Southeastern Virginia Using Wastewater-Based Epidemiology. *Water Res.* **2020**, *186* (1), 116296.

(44) Randazzo, W.; Truchado, P.; Cuevas-Ferrando, E.; Simón, P.; Allende, A.; Sánchez, G. SARS-CoV-2 RNA in Wastewater Anticipated COVID-19 Occurrence in a Low Prevalence Area. *Water Res.* **2020**, *181*, 115942.

(45) Leclerc, H.; Edberg, S.; Pierzo, V.; Delattre, J. M. Bacteriophages as Indicators of Enteric Viruses and Public Health Risk in Groundwaters. *Journal of Applied Microbiology*. **2000**. *88*(1), 5-21

(46) Abia, A. L. K.; Ubomba-Jaswa, E.; Momba, M. N. B. Competitive Survival of Escherichia Coli, Vibrio Cholerae, Salmonella Typhimurium and Shigella Dysenteriae in Riverbed Sediments. *Microb. Ecol.* **2016**, *72* (4), 881–889.

(47) Ashbolt, N.; Grabow, W.; Snozzi, M. Indicators of Microbial Water Quality. In *WHO Water Quality: Guidelines, Standards and Health*; **2001**.

(48) Saxena, G.; Bharagava, R. N.; Kaithwas, G.; Raj, A. Microbial Indicators, Pathogens and Methods for Their Monitoring in Water Environment. *J. Water Health* **2015**, *13* (2), 319–339.

(49) Edberg, S. C.; Rice, E. W.; Karlin, R. J.; Allen, M. J. Escherichia Coli: The Best Biological Drinking Water Indicator for Public Health Protection. *J. Appl. Microbiol.* **2000**. *(29)*, 106S-116S.

(50) Truchado, P.; Hernandez, N.; Gil, M. I.; Ivanek, R.; Allende, A. Correlation between E. Coli Levels and the Presence of Foodborne Pathogens in Surface Irrigation Water: Establishment of a Sampling Program. *Water Res.* **2018**, *128*, 226–233.

(51) Price, R. G.; Wildeboer, D. E. Coli as an Indicator of Contamination and Health Risk in Environmental Waters. In *Escherichia coli - Recent Advances on Physiology, Pathogenesis and Biotechnological Applications*; InTech, **2017**; Vol. i, p 13.

(52) Silva, A. J.; Benitez, J. A. Vibrio Cholerae Biofilms and Cholera Pathogenesis. *PLoS Negl. Trop. Dis.* **2016**, *10* (2), 1–25.

(53) Gómez-Aldapa, C. A.; Refugio Torres-Viela, M.; Amaya-Acosta, M. A.; Rangel-Vargas, E.; Villaruel-López, A.; Castro-Rosas, J. Behavior of Thirteen Foodborne Bacteria on Whole Hass Avocado and Potential of Roselle Calyx Extracts as Alternative Disinfectant Agents of Avocado. *J. Food Saf.* **2017**, *37* (4), 1–8.

(54) Ali, M.; Nelson, A. R.; Lopez, A. L.; Sack, D. A. Updated Global Burden of Cholera in Endemic Countries. *PLoS Negl. Trop. Dis.* **2015**, *9* (6), 1–13.

(55) Vezzulli, L.; Pruzzo, C.; Huq, A.; Colwell, R. R. Environmental Reservoirs of Vibrio Cholerae and Their Role in Cholera. *Environ. Microbiol. Rep.* **2010**, *2* (1), 27–33.

(56) Lutz, C.; Erken, M.; Noorian, P.; Sun, S.; McDougald, D. Environmental Reservoirs and Mechanisms of Persistence of Vibrio Cholerae. *Front. Microbiol.* **2013**, *4* (12), 1–15.

(57) Truchado, P.; Hernandez, N.; Gil, M. I.; Ivanek, R.; Allende, A. Correlation between E. Coli Levels and the Presence of Foodborne Pathogens in Surface Irrigation Water: Establishment of a Sampling Program. *Water Res.* **2018**, *128*, 226–233.

Chapter 2

SYNTHESIS AND APPLICATION OF SUPERABSORBENT POLYMER MICROSPHERES FOR RAPID CONCENTRATION AND QUANTIFICATION OF MICROBIAL PATHOGENS IN AMBIENT WATER

Xunyi Wu, Xiao Huang, Yanzhe Zhu, Jing Li, and, Michael R. Hoffmann*

Author Statement

The manuscript was written through contributions of all authors. M.R.H, X.H., and X.W. conceived the concept for this study. J.L., X.H. and X.W. designed the study, X.W. performed experiments, and J.L. Y.Z. and X.W. wrote the paper. This manuscript has been read and approved by all named authors.

2.0. Abstract

Even though numerous methods have been developed for the detection and quantification of waterborne pathogens, the application of these methods is often hindered by the very low pathogen concentrations in natural waters. Therefore, rapid and efficient sample concentration methods are urgently needed. Here we present a novel method to pre-concentrate microbial pathogens in water using a portable 3D-printed system with super-absorbent polymer (SAP) microspheres, which can effectively reduce the actual volume of water in a collected sample. The SAP microspheres absorb water while excluding bacteria and viruses by size exclusion and charge repulsion. To improve the water absorption capacity of SAP in varying ionic strength waters (0-100 mM), we optimized the formulation of SAP to 180 $g \cdot L^{-1}$ Acrylamide, 75 $g \cdot L^{-1}$ Itaconic Acid and 4.0 $g \cdot L^{-1}$ Bis-Acrylamide for the highest ionic strength water as a function of the extent of cross-linking and the concentration of counter ions. Fluorescence microscopy and double-layer agar plating respectively showed that the 3D-printed system with optimally-designed SAP microspheres could rapidly achieve a 10-fold increase in the concentration of *Escherichia coli* (*E. coli*) and bacteriophage MS2 within 20 minutes with concentration efficiencies of 87% and 96%, respectively. Fold changes between

concentrated and original samples from qPCR and RT-qPCR results were found to be respectively 11.34-22.27 for *E. coli* with original concentrations from 10^4 to 10^6 cell·mL^{-1}, and 8.20-13.81 for MS2 with original concentrations from 10^4-10^6 PFU·mL^{-1}. Furthermore, SAP microspheres can be reused for 20 times without performance loss, significantly decreasing the cost of our concentration system.

2.1. Introduction

Waterborne pathogens, including various pathogenic bacteria, viruses, and protozoa, are responsible for a series of diseases, and thus have been a major public health concern worldwide[1–3]. According to the World Health Organization (WHO), global mortality attributable to water-related diseases is currently 3.4 million per year, most of which are children[4]. This issue is especially severe in developing regions of the world due to the scarcity of clean water supplies and poor sanitation conditions[1,4–6]. Sensitive detection and quantification methods for waterborne pathogens, including traditional culture-based methods, or more recently, nucleic acid amplification tests[3,7–10], are thus indispensable to ensure water safety and to protect the public health.

Testing for pathogens in environmental waters has two main challenges: 1) the concentrations of pathogens in environmental water samples are usually magnitudes lower than those in clinical samples; and 2) the small sample volume being analyzed in each assay makes the direct detection of pathogens in environmental water samples nearly impossible[1,3]. Pathogen concentrations below the detection limit of the methods mentioned above, do not guarantee the

safety of water, as they may still pose a health risk considering their low infectious doses [5,11].

Numerous techniques for pathogen concentration have been developed. Traditional techniques including polyethylene glycol (PEG) coagulation and precipitation, membrane filtration, centrifugation, and evaporation are most commonly used[12,13]. However, these concentration methods require complicated setups and are often time-consuming, which means water samples have to be transported to centralized laboratories with inevitable sample degradation even under continuous cold chain[1]. For field-studies, marine biologists use three steps of Tangential Flow Filtration (TFF) to concentrate water samples with a volume of 120 L[14]. The use of filtration cartridges and membranes, as well as pumping systems, are inevitable and the first TFF step for 60-fold concentration alone takes four hours[15]. The Bag-Mediated Filtration System (BMFS) provides another in-field concentration method that uses gravity as the driving force to filter and concentrate water samples. However, filters and an elution step followed by PEG/NaCl precipitation were also required[16]. Some new techniques are emerging, such as in-plane evaporation[17], magnetic nanoparticle platform on chip[18] or magnetic separators[19,20]. However, these new methods are still limited to laboratory use

and are incapable of handling field samples with volumes of at least 1 or 2 liters[19–21].

Super-absorbent polymer (SAP) microspheres are a class of cross-linked hydrogels that can absorb and retain water up to 1000 times the initial dry weight of the SAP beads[22,23]. SAP materials are widely used in personal disposable hygiene products (e.g., diapers), and for agricultural water preservation or waste fluid spill control[24,25]. By controlling the pore sizes of the hydrogel down to several nanometers, SAPs can absorb water but at the same time exclude particles with sizes above several nanometers, such as bacteria and viruses[24,26]. In order to use SAPs for microbial sample concentration, the SAPs were synthesized as small spherical microspheres using a milli-fluidic flow system. Itaconic acid is added to the polymer to obtain negatively charged polymeric microspheres that have uniform spherical shapes, which minimize electrostatic adsorption of microorganisms on the surface of the microspheres[27].

SAP microspheres absorb water through osmosis, which is driven by polyelectrolyte counter ions attached to the polymer. However, the extent of water absorption is limited by the retention force of the polymer networks due to cross-linking. The maximum water absorbencies and water absorption rates of the SAPs

are determined by the equilibrium of the osmotic forces and the retention forces. For a given SAP formulation with a fixed number of polyelectrolyte counter ions, the osmotic force generated by the SAPs decreases with an increase of ionic strength, which effectively lowers the maximum water absorbency and water absorption rate of a specific SAP formulation. Therefore, the ionic strength of environmental water samples may have a significant impact on the performance of the SAP microspheres.

Here we have adjusted the composition of the SAP microspheres to achieve optimal performances in freshwater or saline waters and further demonstrated that bacteria and viruses collected from environmental water samples can be rapidly concentrated using optimized SAP microspheres. We have further developed a 3D-printed portable, hand-pressed centrifuge system to realize the single-step concentration using SAP microspheres for onsite water concentration in limited-resource settings and without trained personnel. Our study highlights that concentration of the microbial samples using SAPs provides an alternative sample concentration method that avoids a typical multi-step procedure that is often tedious, time-consuming, and inappropriate for use in underdeveloped parts of the world.

2.2. Materials and Methods

2.2.1. SAP preparation and characterization

Monomers used for synthesis of the polymeric beads were acrylamide and itaconic acid, which were dissolved in deionized water with concentrations of 180 $g \cdot L^{-1}$ and 20 $g \cdot L^{-1}$, respectively. Bis-acrylamide (4.0 $g \cdot L^{-1}$) was added to the monomer solution as a cross-linker and potassium persulfate (2.6 $g \cdot L^{-1}$) was added as the initiator of the polymerization reaction[27–29]. Itaconic acid in the monomer solution was fully neutralized by sodium hydroxide prior to the polymerization. All chemicals were purchased from Sigma-Aldrich and were used as received.

SAP microspheres with diameter of 500 μm were prepared by a two-step polymerization using a milli-fluidic system as shown in Fig. 1. Droplets of the monomer solution were generated through a T-junction with an inner diameter of 1/16 inch into the carrying silicon oil of 500 cSt. For the generation of water phase droplets, oil phase and water phase were injected at 0.5 $mL \cdot min^{-1}$ and 0.2 $mL \cdot min^{-1}$, respectively, using two syringe pumps (74905-02, Cole-Parmer, US), into the tubing with 1/16-inch inner diameter. Generated droplets first underwent preliminary polymerization in the tube for 30 seconds at 95°C. Subsequently, full

polymerization of the microspheres was achieved after the microspheres left the tube and settled in the hot oil bath at 95°C for 1.5 hours. This system can generate microspheres of diameters ranging from 500 μm to 2000 μm. Another fabrication method, inverse suspension polymerization, can be used to generate microspheres of diameters ranging from 10 μm to 500 μm, which can be used in smaller concentration systems with smaller starting sample volumes (see Fig. S1). After the polymerization, fabricated microspheres were washed using 95% ethanol to wash off residual oil. Microspheres were soaked in DI water for 24 hours to remove any remaining monomers and subsequently dried under vacuum overnight. Weight analyses of dried SAP microspheres were performed using an analytical balance (AT469, Mettler, USA).

2.2.2. Water absorbency evaluation

The water absorbency Q (g/g) is defined as the swollen weight of SAP (g) divided by the dried weight of SAP (g). To simplify the experimental procedures and to evaluate the water absorbency more easily and precisely, larger SAP blocks (~1×10^{-2} g/block) (Fig. S7) were fabricated with varying monomer and cross-linker ratios

(see Table 1). SAP blocks were fabricated under the same condition for SAP beads fabrication, and they share the same adsorption properties with SAP beads. Na^+ content in the polymer was changed by varying the proportion of sodium itaconate in the monomer solution. SAP blocks were tested for their absorbency in sodium chloride solutions with a series of ionic strengths of 0, 100, 200 and 500 $mmol \cdot L^{-1}$ [30]. The ionic strength S of all solutions was calculated using the following equation:

$$S = \frac{1}{2} \sum_{i=1}^{n} c_i z_i^2 \qquad (1)$$

where c is the concentration of the dissolved salt ion in $mol \cdot L^{-1}$, and z is the valence of the ion. For the dissolved salts, a complete dissociation was assumed[30]. After absorbing water overnight, polymer blocks were drained and the remaining water on the surface of the SAP was gently removed with a paper tissue. The weight of the fully swollen SAP blocks was determined, and their corresponding water absorbency (gram water absorbed by gram dried polymer) was calculated.

To measure the absorption rate, completely dried SAP microspheres were soaked in water. Their diameter changes upon swelling were recorded and measured with a light microscope (Leica M205FA, Leica Co., Germany). The water absorption

rates were evaluated by three models with MATLAB (see supplementary information) and compared to the experimental results.

2.2.3. Microbial sample preparation

E. coli (ATCC 10798) was used as model bacteria in this study and cultured in Luria-Bertani broth (BD Difco™, USA). Before each concentration test, cells were harvested, washed and serially diluted to 10^4-10^6 cells·mL^{-1} using phosphate-buffered saline (pH 7.4) (Corning™, USA). Coliphage MS2 (ATCC 15597-B1) was chosen as model virus. The growth and purification procedures of MS2 are described in our previous work[10]. Before spiking MS2 in water samples, host *E. coli* cells were removed through centrifugation at 12000 rpm (13523 g) for 2 min (Eppendorf 5424, US). Briefly, MS2 suspension was diluted to 10^5-10^7 PFU·mL^{-1} for seeding studies. Environmental water samples were collected from a turtle pond on the Caltech campus and from the primary effluent from a local wastewater treatment plant (with ionic strengths of 15 and 20 mmol·L^{-1}, respectively[31]). The conductivities and pH values of environmental water samples were measured with

an electrical pH/conductivity meter (Orion Star A215, Thermo Scientific, US) and ionic strengths were quantified using Griffin's equation[32].

2.2.4. Concentration experiments

A manual hand-powered tube system was designed and fabricated for field use in resource-limited settings (see Fig. 4). A 3D-printed filter with a mesh size of 300 μm (Fig. S4A) was inserted into a 50 mL commercial centrifuge tube (SuperClear™ Ultra High Performance Centrifuge Tubes, VWR, USA). The filter was fabricated using a high-resolution 3D printer (ProJet™ MJP 2500 Plus) with Visijet M2 RCL Clear Material (3D Systems, Rock Hill, SC). Subsequently, the tube was divided into two chambers: the upper chamber (filled with 0.5 g SAP microspheres) for sample concentration; and the lower chamber for concentrated sample collection. 40 mL water sample was added into the tube and was kept in the upper chamber. The sample water would not enter the lower chamber through the filter due to the surface tension of the liquid. The tube was left standing for 15 minutes for SAP microspheres to absorb water. Then the residual water (~4 mL) was transferred to the lower chamber by centrifugation (~500 rpm). The hand-press

centrifuge was adapted from a commercially-available salad spinner (32480, OXO, USA). The filter and microspheres were taken out of the centrifuge tube. Subsequently, the concentrated sample was collected and its volume was measured. The concentrations of *E. coli* and MS2 in samples before and after concentration were measured and compared as described in section 2.5. Concentration experiments of *E. coli* solutions with initial concentrations of 10^4, 10^5 and 10^6 cell·mL^{-1} were performed as independent triplicates. The difference before and after each microsphere-concentration experiment was compared using qPCR assays. The qPCR assays of *E. coli* solutions of 10^5, 10^6 and 10^7 cell·mL^{-1} were also performed as positive controls. Concentration experiments using MS2 with initial concentrations of 10^5, 10^6 and 10^7 PFU·mL^{-1} were performed in triplicate. The RT-qPCR assays of MS2 solutions of 10^6, 10^7 and 10^8 PFU·mL^{-1} were also performed as positive controls.

2.2.5. Concentration efficiency analyses

In this study, we use concentration efficiency to evaluate the performance of the concentration system. Here, we define the concentration efficiency as the

percentage of microorganisms that remain in concentrated samples. Concentration efficiencies for *E. coli* and MS2 were analyzed using both of microcopy and culturing methods at the level of cell. The performance of the system was further evaluated by the fold-change using PCR-based molecular methods. *E. coli* cell concentrations were quantified using fluorescence microscopy (Leica DMi8, Leica Co., Germany) after SYBR-Green (Invitrogen™, USA) staining according to the manufacturer's protocol[10]. Fluorescence pictures were processed and the cell numbers were counted by ImageJ software (ImageJ 1.51j8, Wayne Rasband National Institutes of Health, USA). The number of *E. coli* was also evaluated by plating on Luria-Bertani agar (BD Difco™, USA). Colonies were counted after 14 h of incubation at 37°C. Total environmental bacterial concentrations in environmental water samples (pond water and wastewater) were enumerated by fluorescence microscope counting and plate counting on LBA as well. The MS2 concentration was determined by the double agar layer method[33].

Concentration efficiencies of *E. coli* and MS2 were quantified by quantitative PCR (qPCR) and quantitative reverse transcription PCR (RT-qPCR) using a 6300 Realplex4 qPCR platform (Eppendorf, Hamburg, Germany). Relevant primer sets and probes are listed in Table S1. For *E. coli*, the qPCR assay targeting the 16s

rRNA gene was carried out in a 20-µL reaction mixture consists of 10 µL PerfeCTa® qPCR ToughMix® (Quanta BioSciences Inc.), 0.25 µM forward primer, 0.25 µM reverse primer, 0.25 µM TaqMan probe, 2 µL of template DNA, and nuclease-free-water. The qPCR thermocycling involves 3 minutes of initialization at 95 °C, and 40 cycles of denaturation at 95 °C for 15 seconds followed by annealing/extension at 55 °C for 30 seconds. For MS2, the RT-qPCR reactions were performed using QIAGEN OneStep RT-PCR Kit (Germantown, MD). Each 25-µL reaction mix included 800 nM forward and reverse primers, 300 nM TaqMan probe, 0.5 mg·mL^{-1} BSA, 1x RT-PCR buffer, 0.4 mM dNTP, 1 U enzyme mix, 3 µL of template RNA, and nuclease-free water.[10] The RT-qPCR thermocycling involves an initial reverse transcription step at 50 °C for 30 minutes, followed by an initial denaturation at 95 °C for 15 minutes, then 45 cycles of 94 °C for 15 seconds and 60 °C for 60 seconds. The nuclease-free water was used as negative controls for all qPCR and RT-qPCR assays. Here for each concentration assay, the concentration efficiency was evaluated by the fold change value:

$$\text{Fold change} = \frac{C(after\ the\ concentration)}{C(before\ the\ concentration)} \times 100\% \qquad (2)$$

where $C_{(before\ the\ concentration)}$ and $C_{(after\ the\ concentration)}$ are concentrations of sample before and after concentration calculated with standard curves performed on each

plate. Concentrations of *E. coli* and MS2 standard samples were respectively evaluated using the fluorescence microscopy and the double-layer agar as described in Section 2.5. All qPCR and RT-qPCR reactions performed in this study reached efficiency between 90% and 110%, indicating the high reliability of our performed assays[34]. Quantification data of samples before and after concentration experiments for the fold change calculations for both *E. coli* and MS2 can be found in Table S3 in the supporting information. All samples were run in triplicate.

2.2.6. Reusability test

To reuse the SAP microspheres after the concentration tests, the microspheres were washed under running tap water for two minutes to remove the remaining bacteria and viruses from the surfaces of the microspheres. The SAP microspheres were subsequently washed in 30 mL Milli-Q water and followed by being dried for subsequent reuse. The synthesized SAP microspheres were fully loaded with water via absorption and then dried using a vacuum oven (VO914A, Thermo Scientific, USA) for 20 consecutive cycles. The gross weights and water absorbencies were measured to test their reusability after successive swelling and drying cycles.

2.3. Results and Discussion

2.3.1. Synthesis of SAP microspheres

Uniform poly (acrylamide-co-itaconic acid) (P(AM-co-IA)) microspheres were fabricated using a system as illustrated in Fig. 1. Monomer solution-in-oil droplets were generated with two syringe pumps, using a T-junction. After the generation of monomer solution droplets, the P(AM-co-IA) microspheres required at least 1.5 hours at 95°C to achieve complete polymerization: the polymerization reaction was catalyzed by free radicals from persulfate generated by heating and dissociating potassium persulfate. The persulfate free radicals convert monomers of acrylamide and itaconic acid with double bonds to free radicals that react with other monomers to begin the polymerization chain reaction. The elongating polymer chains are randomly cross-linked by bis-acrylamide, resulting in a gel matrix structure[35]. The two-step polymerization system was designed such that the polymer microspheres would only undergo preliminary polymerization in the tube, so they would not fuse into each other and block the tube. When the partially polymerized microspheres left the tube, they were immersed in an oil bath for 1.5 hours allowing for complete polymerization. The characteristics of washed and fully-dried SAP microspheres presented uniform spherical shape with a characteristic diameter of

500 ± 8 μm, white color, and smooth surfaces as shown in Fig. 1. Each SAP microspheres have the same formula and are formed with the same amount of monomers, being very uniform after absorbing water. The slight difference in the shape of the sphere when they are dried was most likely due to the inconsistent shape change during the drying process. When the microspheres were fully dried, their density was slightly lower than that of water due to that voids presented in the polymer structure. Variances in the porous polymer structure during drying of each polymer microspheres may also lead to slight density inconsistency between microspheres, but these slight differences in shape and density would not influence the performance of SAP microspheres on water absorption as they became uniform after they start to absorb water. Smaller size microspheres can be fabricated by inverse suspension polymerization method and shared similar SAP properties (see Fig. S1B).

2.3.2. Optimization of SAP for various water matrices

SAP microspheres used in the previous research with fixed composition can only work in deionized water, since both the maximum capacity, and the rate of water

absorption would decrease drastically in high ionic strength water. Hence, the composition of the SAP beads needs to be adjusted to achieve optimal performances for different water matrices. SAP blocks fabricated according to the original monomer solution recipe (180 $g \cdot L^{-1}$ AM, 20 $g \cdot L^{-1}$ IA and 4.0 $g \cdot L^{-1}$ Bis-A) could absorb water of around 80 times their own weight (water absorbency ($Q \sim 80$), and a maximum absorbency of 96% was reached under 20 minutes in DI water (see Fig. 2). Although the polymer is stable and tolerant to different environmental conditions, the maximum water absorbency and water absorption rate of the polymer were significantly reduced in higher ionic strength water samples due to the decreased osmotic force. For environmental waters, the average ionic strength of freshwater and wastewater are around 5 $mmol \cdot L^{-1}$ and 50 $mmol \cdot L^{-1}$, respectively, and can be as high as 150 $mmol \cdot L^{-1}$ for untreated wastewater[36–39]. In water with an ionic strength of 100 $mmol \cdot L^{-1}$, the same SAP's absorbency decreased to 30% of its maximum absorbency. Less than 80% of maximum water absorbency was achieved, and equilibrium could not be reached for more than 30 minutes (see Fig. 2). Therefore, the SAP composition requires optimization to improve its performance in saline water.

The water absorbency of SAP is determined by the balance of three forces: (1) the osmosis potential between the solution within the polymer network and the external solution; (2) the electrostatic repulsion resulting from the fixed charges on the polymer chains; and (3) the elastic retractile response of the polymer network[40]. Forces (1) and (2) increase the absorption of SAP while force (3) restricts the absorption. The high sodium cation (polyelectrolyte counter ion) concentration within the polymer network provides osmotic pressure, which quickly drives water into the polymer. As the water penetrates the polymer, the sodium cation is diluted, and the concentration of sodium cation in the polymer decreases, leading to a decrease of osmotic force[22,23]. At the same time, the retention force of the polymer is increasing with the expansion of the polymer network. When the balance between the osmotic force and retention force is reached, the SAP is at equilibrium. For the cross-linked polymer, the water absorbency, Q, can be expressed as a function using elasticity gel theory of Flory[35,40], which has the following form:

$$Q^{\frac{5}{3}} = \left[\left(\frac{i}{2V_u S^{\frac{1}{2}}}\right)^2 + \left(\frac{1}{2} - X_1\right)V_1\right] V_e/V_0 \qquad (4)$$

where Q: maximum water absorbency (g/g); V_e/V_0: crosslinking density of polymer (amount cross-linker/total polymer); $(1/2\text{-}X_1)/V_1$: affinity between polymer and

external solution (X_1: interaction parameter of polymer with solvent; V_1: molar volume of solvent in a real network); V_u: volume of structural unit; i: electronic/ionic charge present on the polymer backbone per polymer unit; i/V_u: fixed charge per unit volume of polymer; S: Ionic strength of external solution ($mol \cdot L^{-1}$). Since the affinity of the polymer to water does not change in our case, and the volume of the structural unit is fixed, the maximum water absorbency is solely controlled by the crosslinking density, fixed-charge density and external ionic strength.

Two methods were explored to improve the performance of SAP in water at different ionic strengths: one was to reduce the retention force of the polymer by decreasing the cross-linking degree; and the other was to increase the osmotic pressure by increasing the sodium content in the polymer. The recipe changes of SAP also varied the pore size of the fabricated SAP, which was still small enough to exclude bacteria and viruses with high concentration efficiencies (see section 3.4 for results and discussion).

Fig. 3 shows the change of SAP absorption performance induced by varying cross-linking degrees and counter ion concentrations. As shown in Fig. 3A, SAP with the lowest cross-linking degree (C1) could reach water absorbency of 50 in the highest

ionic strength solution (500 $mmol \cdot L^{-1}$), while the absorbency of the original microspheres (O1) decreased to less than 20. However, it should be noted that when loosening the structure of the polymer to reduce the retention force, the mechanical strength of the SAP is also reduced. If the cross-linking degree were modified to an amount smaller than 1 g Bis-A per 1000 g total monomer, then the SAP microspheres broke easily during the centrifugation step and the debris of the broken SAP microspheres entered the residual water sample, influencing the experimental results. Thus, broken SAP microspheres cannot be reused.

Increasing the Na^+ content in the polymer also significantly improved the absorption rate of SAP in saline water, by providing an increased osmotic force (see Fig. 3B). Before the centrifugation step, the microspheres needed to reach at least 90% of their maximum absorbency. At this stage, the absorption rate slows down and the weight of SAP did not change a lot (Fig. 2), which was important for the following centrifugal step. For a successful concentration step, a small volume of sample must remain after the water absorption through SAP. Therefore, a slow water absorption rate of SAP microspheres during centrifugation would be desirable. Otherwise, the SAP microspheres would continue to rapidly absorb the remaining water during centrifugation and the sample water could be totally

absorbed by SAP microspheres at a fast absorption rate, leading to the failure of the concentration process. For the original SAP microspheres, less than 80% of the maximum water absorbency was obtained at 20 minutes in 100 $mmol \cdot L^{-1}$ water while still swelling rapidly. If we were to use SAP microspheres made with this recipe, the concentration process would take more than 30 minutes. However, the microspheres with the S2 recipe would reach 95% maximum water absorbency in 20 minutes, which was much faster than the microspheres with the original recipe (~35 minutes). The improvement of the absorption rate was further confirmed using three models (see supplementary information). By applying the models to our experimental data to calculate the diffusion coefficients, all three models show the increase of the diffusion coefficients by around 50% after using the optimized recipe. Since the resulting linear fits of $Q^{5/3}$ versus the cross-linking density and the fixed charge density (i/V_u) are consistent with the predictions of the Flory theory[39,40] (Fig. 3), the SAP formulations could be easily customized to suit different ionic strengths of the respective water matrices.

2.3.3. Tube concentration system

Furthermore, the previous concentration method introduced in Xie et al. (2015) required five manual and consecutive operations of using pipettes to collect concentrated samples (each step concentrating about 20% of the sample volume), which made this approach tedious, time-consuming and not applicable in field. Therefore, our study remarkably developed a portable, hand-pressed centrifuge system with one-step operation to facilitate the efficient use of SAP beads for onsite concentration for waterborne microorganism in low-resource settings, thus allowing our concentration method to be easily performed by people without any prior training. Fig. 4 schematically illustrates the tube system for microbial pathogen concentration. Each tube contains 0.5 g SAP microspheres and a 3D-printed filter. The 3D-printed filter divided the tube into two chambers and the water samples are restricted in the upper chamber before centrifugation by the filter due to the surface tension of the sample. After adding the sample, the tube only need to be left to stand for 20 minutes for the full absorption of water by the SAP. Non-absorbed water is transferred to the lower chamber using a hand-press centrifuge. After 20 minutes, more than 90% of the sample was adsorbed and continued absorption became very slow. Thus, a remaining water sample (~4 mL) could be collected by centrifugation. The hand-press centrifuge was adapted from a salad spinner, which can reach an average rotation speed of 500 rpm. This spinning speed

was fast enough, as evident, as the concentration efficiency (percentage of microorganisms recovered after concentration) did not change when using a commercial centrifuge with up to 1200 rpm (data not shown). This hand-pressed spinner reduced the cost of the system and made the system totally off-grid and suitable for field use. Moreover, our system may be a promising tool in field studies, as it can rapidly concentrate environmental samples. One example of applications could be in-field sequencing when coupled with the new sequencing technology, MinION sequencer[41].

2.3.4. Microorganism concentration performance

The concentration factor (hereinafter referred to as the ratio of the sample volumes before and after the concentration) of SAP microspheres were maintained in a range of 1.3–2.1 for each step, so that the swollen SAP microspheres could be suspended after the concentrating step. When the concentration factor exceeded 4, the concentration efficiency decreased substantially due to that the microorganisms trapped in remaining liquids on the microsphere surface and/or in the voids among the microspheres. The concentration efficiency dropped to 38% when the

concentration factor increased an order of magnitude[27]. When using the hand-pressed centrifuge centrifuging step, the concentrate was transferred to the collection chamber. This step substantially improved the concentration factors (the ratio of the sample volumes before and after concentration) and concentration efficiencies. A concentration efficiency of 87 ± 6% was achieved with a concentration factor of 9-10 for *E. coli* in DI water within 20 min (see Fig. 5). By using different SAP formulations, we were able to achieve similar concentration efficiencies of *E. coli* in water with high ionic strengths up to 100 $mmol \cdot L^{-1}$. S2 SAP microspheres were used for the concentration of *E. coli* in 100 $mmol \cdot L^{-1}$ ionic strength water and an average of 89 ± 17% concentration efficiency was achieved. Additionally, qPCR targeting 16S rRNA gene and RT-qPCR were respectively performed to evaluate the concentration efficiencies of *E. coli* and MS2. As shown in Fig. 6, the fold change values between 10-fold concentrated samples and original samples were found to be 11.34, 22.27 and 17.97, respectively, from *E. coli* solutions with initial concentrations of 10^4, 10^5 and 10^6 $cell \cdot mL^{-1}$. As positive controls, the fold changes between *E. coli* solutions of 10^5 and 10^4, 10^6 and 10^5, 10^7 and 10^6 $cell \cdot mL^{-1}$ were 3.03, 8.50 and 9.34, respectively, which implied the concentration efficiencies of SAP microsphere-based concentration system were respectively 275%, 162% and 92% higher than they were supposed to be by qPCR

assays. For the samples of 10^4, 10^5 and 10^6 cell·mL^{-1}. Fold change values between samples of 10^5 (both concentrated and serially diluted) and 10^4 cell·mL^{-1} were relatively low because the concentration of 10^4 cell·mL^{-1} is much close to the detection limit of 16S rRNA qPCR. Our results showed that the tube concentration system based on SAP microspheres could achieve satisfactory concentration efficiencies of *E. coli* solutions with a range of initial concentrations.

The bacterial concentrations of original samples did not affect the concentration efficiency as evaluated by microscopic cell counts. Experimental results showed very similar concentration efficiencies (between 85% - 90%) for water samples with different initial concentrations from 10^4 -10^8 cells·mL^{-1}, thus allowing total concentration efficiencies of higher than 60% for 100- or 1000-time concentration, although 2 or 3 sequential concentration steps may be required. It should be noted that these sequential concentration steps may require multiple formulations of SAP microspheres due to the increasing ionic strength during concentration. It's extremely difficult to achieve 100-1000 times concentration in one step due to the difficulty in concentrated sample collection and the sample loss on the microspheres' surface.

Concentration tests using bacteriophage MS2 resulted in a similar level of concentration efficiency (see Fig. 5) evaluated by plaque forming unit quantification. The average concentration efficiency of one concentration step was 101 ± 12% in DI water using O1 SAP. For a 100-mmol·L^{-1} ionic strength water sample, the concentration efficiency of MS2 was 90 ± 10%, using S2 SAP microspheres (Fig. 5). The value of >100% was likely caused by the well-known large standard deviation of the double agar layer method, imprecisions in experimental procedures and the MS2 aggregation during experiments. RT-qPCR was performed to evaluate the recovery rates of MS2. As shown in Fig. 6, the fold changes between concentrated samples and original samples were found to be 13.81, 9.83 and 8.20, respectively, for the samples with initial concentrations of 10^4, 10^5 and 10^6 PFU·mL^{-1}. Meanwhile, the fold change values between 10^6 and 10^5, 10^7 and 10^6, 10^8 and 10^7 were 7.64, 11.22 and 10.69, respectively, which implied the concentration efficiencies of SAP microsphere-based concentration system were respectively 180%, 88% and 77% comparing to what they were supposed to be by qPCR assays. Fold change values between 10-fold concentrated MS2 samples and original samples are similar to fold change values of between positive control MS2 samples with 10-fold dilution, indicating high concentration efficiencies of the tube concentration system. In summary, results from qPCR and RT-qPCR assays

indicate that the SAP microsphere-based concentration method completely meets the requirements for nucleic acid amplification-based environmental monitoring and surveillance. It should be noted that compared to conventional virus concentration methods, such as ultracentrifugation, electropositive or electronegative filters or ultrafiltration[42–44], the SAP microspheres concentration method neither uses complicated instruments or expensive filters, nor requires the preconditioning of water samples.

Furthermore, the concentration efficiencies of SAP microspheres used for concentrating the native bacteria in the Caltech pond water (ionic strength 15 $mmol \cdot L^{-1}$, pH = 7.75) and the wastewater from the wastewater treatment plant (ionic strength 20 $mmol \cdot L^{-1}$, pH = 8.02) were investigated. As shown in Fig. 5, average bacterial concentration efficiencies of 112% and 83%, respectively, were achieved for pond water and wastewater samples. The concentration processes were completed in less than 20 minutes. Presence of other substances in real water samples such as natural organic matters or algae would not influence the performance of our system according to our tests on real environmental waters, which was discussed in section 3.4.

It should be noted that we introduced itaconic acid to our customized SAP formula to add a negative surface charge and minimize the electrostatic adsorption of microorganisms. Although bacteria and viruses may not always have negative surface charge in environmental waters, which depends on their isoelectric points[45,46]. As most bacteria have low isoelectric points and will be negatively charged in environmental waters[45,47], they should be repelled by the SAP beads as what happened to our model bacterium *E. coli*. However, viruses have a broader range of isoelectric points[46]. Our model virus, MS2, has a low isoelectric point (~ 3.5)[46] and thus, a high concentration efficiency is expected due to electrostatic repulsion. Although accounting for a small part, there are still viruses whose surface charges in natural water may not be strong enough for electrostatic repulsion and therefore the concentration efficiency might be impaired, e.g., somatic coliphage ΦX174 (isoelectric point ~ 7)[46].

2.3.5. Reusability of SAP microspheres

Reusing the microspheres can significantly decrease the cost of our concentration system. After use, the microspheres can be washed and dried for subsequent

applications requiring sample concentration. Simple washing with running tap water was sufficient for the reuse of SAP microspheres, as no bacteria or viruses were detected using membrane filtration from the final washing water before the next use. For more sensitive applications, SAP microspheres could be autoclaved as well. To demonstrate their reusability, the SAP microspheres were dried and rehydrated for more than 20 times. Fig. S3 shows the weight change of 100 SAP microspheres for 20 cycles of full drying and swelling. For 20 cycles, the weight change for both dried and swollen microspheres was less than 5%, whereas the decrease of water absorbency was less than 2%. The concentration efficiencies of *E. coli* and MS2 using recycled microspheres (after 20 cycles) were still up to 84 ± 7% and 90 ± 11%, respectively (Fig. 5). Slight efficiency losses during reusing recycled microspheres were most likely attributed to the inevitable breaks of some SAP microspheres during the recycling process, which became much more severe with the increase of recycling times as observed. Damaged spheres might trap much more pathogens due to the increased surface area.

2.4. Conclusion

In this study, tailored SAP microspheres coupled with a hand-powered tube system were developed to achieve efficient and rapid concentration for environmental microorganisms. In order to overcome the performance loss of SAP in high ionic strength water samples, we have been able to improve the water absorption ability of SAP microspheres by optimizing the degree of polymer cross-linking and controlling the counter ion concentrations using the Flory model as a guide. Optimally synthesized SAP microspheres were shown to absorb more water at higher absorption rates compared to other commercially available water-absorbing microspheres, making our synthetically-tailored SAP microspheres able to concentrate bacteria and viruses from high ionic strength water samples and environmental water samples within a short time. In addition, we developed a low-cost, portable, hand-powered portable centrifuge tube system based on our tailored SAP microspheres to facilitate concentrating water in low-resource settings in the field. Results from our study highlight that we provide a cost-effective, easy-to-use and off-grid system with tailored SAP microspheres for various water samples. We envision that this system could be applied to the field for efficient microbial concentration and promote rapid on-site microbial analysis.

Acknowledgements

The authors acknowledge the financial support provided by the Bill and Melinda Gates Foundation (grant no. OPP1111252). The authors thank Dr. Katharina Urmann, Dr. Xingyu Lin and Dr. Xing Xie for their helpful advices and discussions.

Tables and Figures

Table 1. SAP recipes with varying cross-linking degree and sodium content

	Acrylamide ($g \cdot L^{-1}$)	Itaconic Acid ($g \cdot L^{-1}$)	Bis-Acrylamide ($g \cdot L^{-1}$)
(O1) Original Recipe	180	20	4
C1	180	20	0.2
C2	180	20	0.4
C3	180	20	1
C4	180	20	2
S1	180	50	4
S2	180	75	4
S3	180	100	4

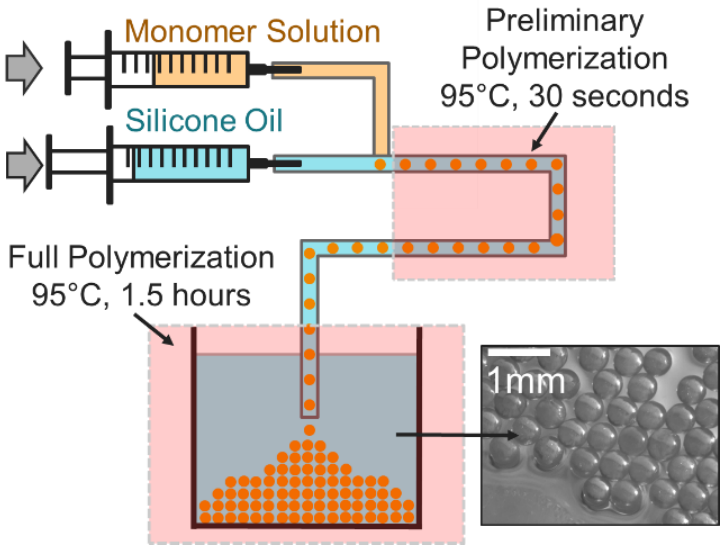

Figure 1. A schematic illustration of the synthesis steps producing SAP microspheres.

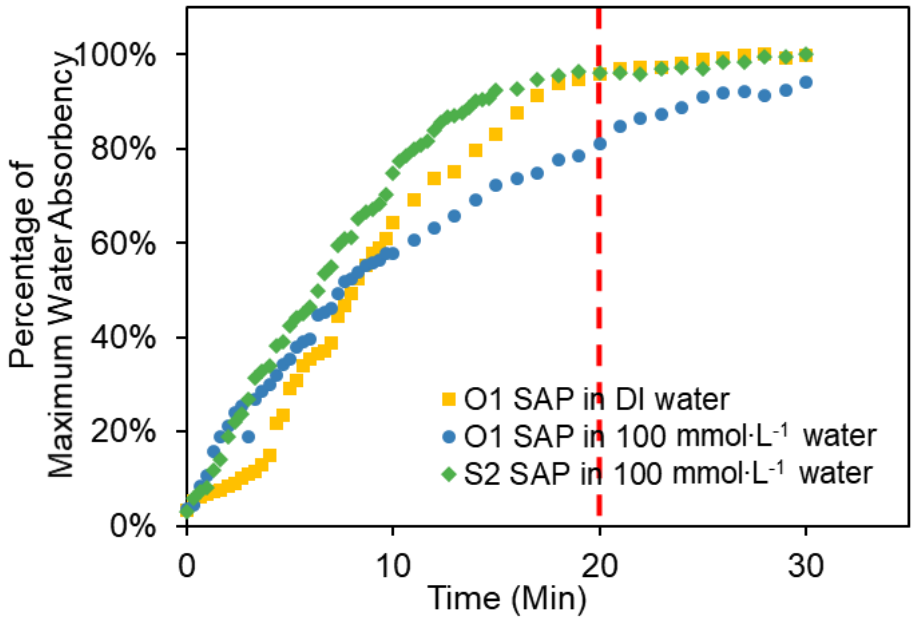

Figure 2. Water absorbency of original microspheres (O1) and revised microspheres (S2) in DI water and saline water (100 mmol·L^{-1}) over time.

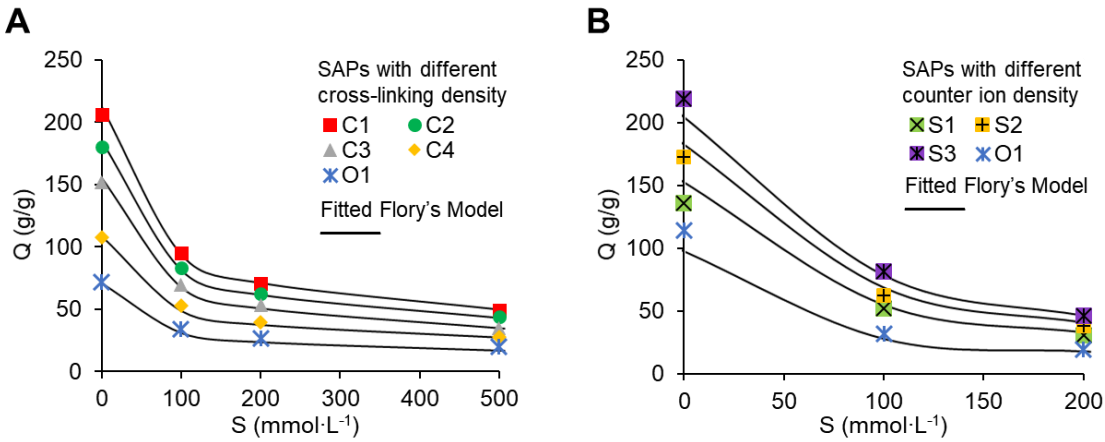

Figure 3. Change of maximum water absorbency (Q) vs. ambient ionic strengths (S), and the impacts of changing cross-linking density (A) and counter ion density (B) on maximum water absorbency. Error bars are all smaller than 1% and are not shown on graphs.

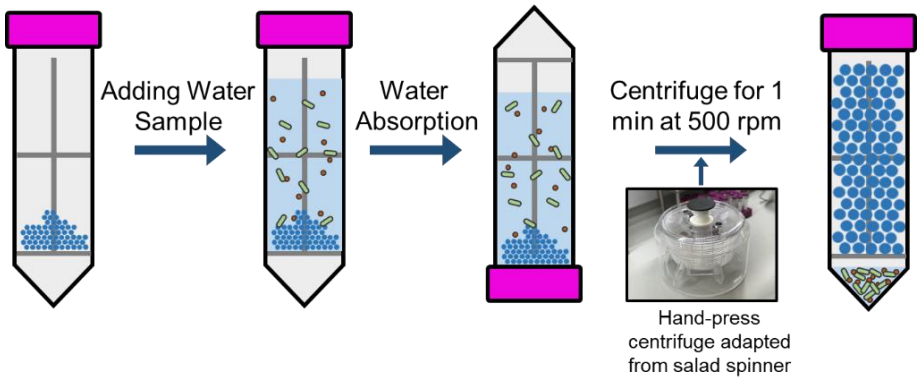

Figure 4. The tube system designed for microbial pathogen concentration using SAP microspheres. The tube is composed of 0.5 g SAP microspheres and a 3D-printed filter. After adding the water sample, the tube is left to stand for 20 minutes for the full absorption of water by SAP. Non-absorbed water is pushed to the lower chamber using a hand-press centrifuge.

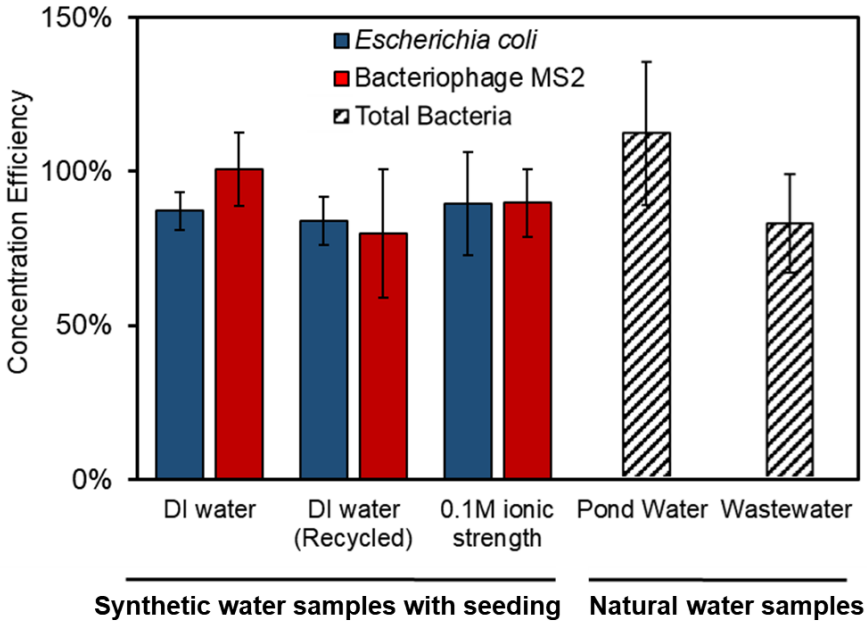

Figure 5. Concentration efficiencies of *E. coli*, MS2 and total bacteria using the tube concentration system calculated by microscopic cell counts, plague forming unit quantification. *E. coli* and MS2 were concentrated using new SAP microspheres and recycled SAP microspheres after 20 drying- swelling cycle, and in DI and 0.1 M ionic strength water. Total bacteria were concentrated from pond water and wastewater samples.

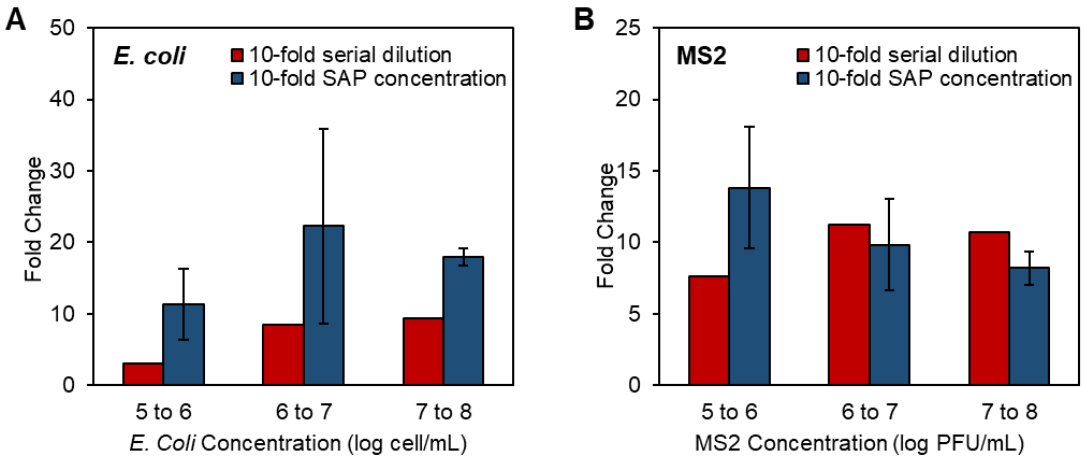

Figure 6. Fold Changes of qPCR and RT-qPCR of *E. coli* (A) and MS2 (B) for samples in varying magnitude of orders with serially diluted samples (red bars) and concentrated samples (blue bars) using the tube concentration system; wherein standard deviations (error bars) were calculated from fold change values of triple independent concentration experiments. Fold change values were calculated from quantification data according to the standard curve performed on each plate.

References

[1] F. Ramírez-Castillo, A. Loera-Muro, M. Jacques, P. Garneau, F. Avelar-González, J. Harel, A. Guerrero-Barrera, Waterborne Pathogens: Detection Methods and Challenges, Pathogens. 4 (2015) 307–334. doi:10.3390/pathogens4020307.

[2] T.M. Straub, D.P. Chandler, Towards a unified system for detecting waterborne pathogens, J. Microbiol. Methods. 53 (2003) 185–197. doi:10.1016/S0167-7012(03)00023-X.

[3] T.G. Aw, J.B. Rose, Detection of pathogens in water: From phylochips to qPCR to pyrosequencing, Curr. Opin. Biotechnol. 23 (2012) 422–430. doi:10.1016/j.copbio.2011.11.016.

[4] World Health Organization, Water for health: Taking charge, 2001. doi:10.1017/CBO9781107415324.004.

[5] H. Bridle, Waterborne Pathogens, 2014. doi:10.1016/B978-0-444-59543-0.00002-5.

[6] A. Malik, A. Yasar, A.B. Tabinda, M. Abubakar, Water-borne diseases, cost of illness and willingness to pay for diseases interventions in rural communities of developing countries, Iran. J. Public Health. 41 (2012) 39–49. doi:Export Date 9 July 2012\nSource Scopus.

[7] J.. S.D. Madigan, M.; Martinko, Brock. Biology of Microorganisms, 2012. doi:10.1007/s13398-014-0173-7.2.

[8] G. Shipley, The MIQE Guidelines Uncloaked, in: PCR Troubl. Optim. Essent. Guid., 2011: pp. 149–162. doi:10.1373/clinchem.2008.112797.

[9] M. Burns, H. Valdivia, Modelling the limit of detection in real-time quantitative PCR, Eur. Food Res. Technol. 226 (2008) 1513–1524. doi:10.1007/s00217-007-0683-z.

[10] X. Huang, X. Lin, K. Urmann, L. Li, X. Xie, S. Jiang, M.R. Hoffmann, Smartphone-Based in-Gel Loop-Mediated Isothermal Amplification (gLAMP) System Enables Rapid Coliphage MS2 Quantification in Environmental Waters, Environ. Sci. Technol. 52 (2018) 6399–6407. doi:10.1021/acs.est.8b00241.

[11] P. Schmid-Hempel, S.A. Frank, Pathogenesis, virulence, and infective dose, PLoS Pathog. 3 (2007) 1372–1373. doi:10.1371/journal.ppat.0030147.

[12] K.A. Stevens, L.A. Jaykus, Bacterial separation and concentration from complex sample matrices: A review, Crit. Rev. Microbiol. 30 (2004) 7–24. doi:10.1080/10408410490266410.

[13] M.A. Borchardt, B.A. Kieke, S.K. Spencer, Ranking filter methods for concentrating pathogens in lake water, Appl. Environ. Microbiol. 79 (2013) 5418–5419. doi:10.1128/AEM.01430-13.

[14] A. Sundbergh, S. Craig Cary, K.E. Wommack, R.R. Helton, K. Portune, S.J. Williamson, B.T. Glazer, An instrument for collecting discrete large-volume water samples suitable for ecological studies of microorganisms, Deep Sea Res. Part I Oceanogr. Res. Pap. 51 (2004) 1781–1792. doi:10.1016/j.dsr.2004.05.011.

[15] K.E. Gibson, K.J. Schwab, Tangential-flow ultrafiltration with integrated inhibition detection for recovery of surrogates and human pathogens from large-volume source water and finished drinking water, Appl. Environ. Microbiol. 77 (2011) 385–391. doi:10.1128/AEM.01164-10.

[16]C.S. Fagnant, L.M. Sánchez-Gonzalez, N.A. Zhou, J.C. Falman, M. Eisenstein, D. Guelig, B. Ockerman, Y. Guan, A.L. Kossik, Y.S. Linden, N.K. Beck, R. Wilmouth, E. Komen, B. Mwangi, J. Nyangao, J.H. Shirai, I. Novosselov, P. Borus, D.S. Boyle, J.S. Meschke, Improvement of the Bag-Mediated Filtration System for Sampling Wastewater and Wastewater-Impacted Waters, Food Environ. Virol. 10 (2018) 72–82. doi:10.1007/s12560-017-9311-7.

[17] J.W. Choi, S.M. Hosseini Hashemi, D. Erickson, D. Psaltis, A micropillar array for sample concentration via in-plane evaporation, Biomicrofluidics. 8 (2014) 1–9. doi:10.1063/1.4890943.

[18] Y. Zhang, L.K. Riley, M. Lin, Z. Hu, Lanthanum-based concentration and microrespirometric detection of microbes in water, Water Res. (2010). doi:10.1016/j.watres.2010.03.029.

[19] O. Rotariu, I.D. Ogden, M. MacRae, V. Bădescu, N.J.C. Strachan, An immunomagnetic separator for concentration of pathogenic micro-organisms from large volume samples, J. Magn. Magn. Mater. 293 (2005) 589–596. doi:10.1016/j.jmmm.2005.01.078.

[20] G.D. Chen, C.J. Alberts, W. Rodriguez, M. Toner, Concentration and Purification of Human Immunodeficiency Virus Type 1 Virions by Microfluidic Separation of Superparamagnetic Nanoparticles, Anal. Chem. 82 (2009) 723–728. doi:10.1021/ac9024522.

[21] S. Park, Y. Zhang, T.-H. Wang, S. Yang, Continuous dielectrophoretic bacterial separation and concentration from physiological media of high conductivity, Lab Chip. 11 (2011) 2893. doi:10.1039/c1lc20307j.

[22] S. Kiatkamjornwong, Superabsorbent Polymers and Superabsorbent Polymer Composites, ScienceAsia. 33 (2007) 39–43. doi:10.2306/scienceasia1513-1874.2007.33(s1).039.

[23] W.-F. Lee, R.-J. Wu, Superabsorbent polymeric materials. I. Swelling behaviors of crosslinked poly(sodium acrylate-co-hydroxyethyl methacrylate) in aqueous salt solution, J. Appl. Polym. Sci. 62 (1996) 1099–1114. doi:10.1002/(SICI)1097-4628(19961114)62:7<1099::AID-APP16>3.0.CO;2-1.

[24] Mark Elliott, Superabsorbent Polymers, 573 (1994) 128–140. doi:10.1021/bk-1994-0573.

[25] E.M. Ahmed, Hydrogel: Preparation, characterization, and applications: A review, J. Adv. Res. 6 (2015) 105–121. doi:10.1016/j.jare.2013.07.006.

[26] D. Valade, L.K. Wong, Y. Jeon, Z. Jia, M.J. Monteiro, Polyacrylamide hydrogel membranes with controlled pore sizes, J. Polym. Sci. Part A Polym. Chem. 51 (2013) 129–138. doi:10.1002/pola.26311.

[27] X. Xie, J. Bahnemann, S. Wang, Y. Yang, M.R. Hoffmann, "Nanofiltration" Enabled by Super-Absorbent Polymer Beads for Concentrating Microorganisms in Water Samples, Sci. Rep. 6 (2016) 1–8. doi:10.1038/srep20516.

[28] D. Shi, Y. Gao, L. Sun, M. Chen, Superabsorbent poly(acrylamide-co-itaconic acid) hydrogel microspheres: Preparation, characterization and absorbency, Polym. Sci. Ser. A. 56 (2014) 275–282. doi:10.1134/S0965545X14030146.

[29] S. Bednarz, A. Błaszczyk, D. Błażejewska, D. Bogdał, M. Cao, Y. Durant, L.E. Coleman, N. a. Meinhardt, Z. Hehn, D. Nowak, J. Pethe, J. Li, T.B. Brill, A. Note, S. Polowiński, C.F. Sch, G. Swift, H. Company, T. Imoto, S. Nagai, K. Yoshida, P.E.L. Schofer, B.E. Tate, K. Yokota, T. Hirabayashi, T. Takashima, L.Yu. Yu, H.M. Shen, Z.L. Xu, Polymerization of itaconic acid, Polimery. 5 (1975) 1197–1205. doi:10.1007/BF02283833.

[30] L.J. Böni, R. Zurflüh, M.E. Baumgartner, E.J. Windhab, P. Fischer, S. Kuster, P.A. Rühs, Effect of ionic strength and seawater cations on hagfish slime formation, Sci. Rep. 8 (2018) 1–12. doi:10.1038/s41598-018-27975-0.

[31] M.H.B. Daniel, A. Montebelo, Effects of urban sewage on dissolved oxygen, dissolved inorganic and organic carbon, and electrical conductivity of small streams along a gradient of urbanization in the Piracicaba river basin, Water, Air, Soil …. 136 (2002) 189–206. http://link.springer.com/article/10.1023/A:1015287708170.

[32] R.A. Griffen, J.J. Jurinach, Estimation of activity co-efficent from the electrical conductivity of natural agnote systems in soil extracts, Soil Sc. 116 (1973) 26–30.

[33] A.M. Kropinski, A. Mazzocco, T.E. Waddell, E. Lingohr, R.P. Johnson, Enumeration of Bacteriophages by Double Agar Overlay Plaque Assay, in: 2009: pp. 69–76. doi:10.1007/978-1-60327-164-6_7.

[34] A. Osselaere, R. Santos, V. Hautekiet, P. De Backer, K. Chiers, Deoxynivalenol Impairs Hepatic and Intestinal Gene Expression of Selected Oxidative Stress , Tight Junction and Inflammation Proteins in Broiler Chickens ,

but Addition of an Adsorbing Agent Shifts the Effects to the Distal Parts of the Small Intestine, 8 (2013) 1–7. doi:10.1371/journal.pone.0069014.

[35] X.X. Chen, G.G. Shan, J. Huang, Z.Z. Huang, Z.Z. Weng, Synthesis and properties of acrylic-based superabsorbent, J. Appl. Polym. Sci. 92 (2004) 619–624. doi:10.1080/10601320701351268.

[36] F. Prieto, E. Barrado, M. Vega, L. Deban, Measurement of electrical conductivity of wastewater for fast determination of metal ion concentration, Russ. J. Appl. Chem. 74 (2001) 1321–1324. doi:10.1023/A:1013710413982.

[37] S.M. Cormier, G.W. Suter, L. Zheng, Derivation of a benchmark for freshwater ionic strength, Environ. Toxicol. Chem. 32 (2013) 263–271. doi:10.1002/etc.2064.

[38] R.A. Griffin, J.J. Jurinak, Estimation of activity coefficients from the electrical conductivity of natural aquatic systems and soil extracts, Soil Sci., 116, 26-30. http://dx.doi.org/10.1097/00010694-197307000-00005.

[39] R.S. Cates, Influence of Crosslink Density on Swelling and Conformation of Surface-Constrained Poly(n-isopropylacrylamide) Hydrogels, 2010. doi:10.1017/CBO9781107415324.004.

[40] P.J. Flory, J. Rehner Jr, Statistical mechanics of cross-linked polymer networks II. Swelling, J Chem Phys. 11 (1943) 521–526.

[41] A.D. Tyler, L. Mataseje, C.J. Urfano, L. Schmidt, K.S. Antonation, M.R. Mulvey, C.R. Corbett, Evaluation of Oxford Nanopore's MinION Sequencing Device for Microbial Whole Genome Sequencing Applications, Sci. Rep. (2018). doi:10.1038/s41598-018-29334-5.

[42] J.L. Cashdollar, L. Wymer, Methods for primary concentration of viruses from water samples: A review and meta-analysis of recent studies, J. Appl. Microbiol. 115 (2013) 1–11. doi:10.1111/jam.12143.

[43] D.A. Kuzmanovic, I. Elashvili, C. Wick, C. O'Connell, S. Krueger, Bacteriophage MS2: Molecular weight and spatial distribution of the protein and RNA components by small-angle neutron scattering and virus counting, Structure. 11 (2003) 1339–1348. doi:10.1016/j.str.2003.09.021.

[44] H. Katayama, A. Shimasaki, H. Katayama, A. Shimasaki, S. Ohgaki, Development of a Virus Concentration Method and Its Application to Detection of Enterovirus and Norwalk Virus from Coastal Seawater Development of a Virus Concentration Method and Its Application to Detection of Enterovirus and Norwalk

Virus from Coastal, Appl. Environ. Microbiol. 68 (2002) 1033–1039. doi:10.1128/AEM.68.3.1033.

[45] V.P. Harden, J.O. Harris, The isoelectric point of bacterial cells., J. Bacteriol. 65 (1953) 198–202.

[46] B. Michen, T. Graule, Isoelectric points of viruses, J. Appl. Microbiol. 109 (2010) 388–397. doi:10.1111/j.1365-2672.2010.04663.x.

[47] G. V. Sherbet, M.S. Lakshmi, Characterisation of Escherichia coli cell surface by isoelectric equilibrium analysis, BBA - Biomembr. 298 (1973) 50–58. doi:10.1016/0005-2736(73)90008-4.

Supporting Information

1. Fabrication of poly (acrylamide-co-itaconic acid) beads using inverse suspension polymerization in a batch reactor

At room temperature, 40 mL of water was added to a well-mixed oil phase containing 185 mL cyclohexane, 65 mL tetrachloroethylene, 0.75 g Span-80 and 0.375 g Tween-60 in a 500-mL flask. The stirring speed was set to be 180 rpm and the water phase was inverse suspended into the oil phase by stirring. At the same time, the flask was heated by a water bath to 80°C. When the temperature is reached, the system was kept at this temperature for the full polymerization of the water phase. After two hours, heat was removed, and when the system was cooled to below 50°C, SAP beads were precipitated by adding ethanol. Harvested beads were washed with pure ethanol and dried in a vacuum oven overnight.

2. Water absorption rate of the SAP beads and model fits

To investigate the influence of monomer composition on the water absorption rate of SAP, three models for diffusion of water into a SAP spheres have been applied to evaluate the absorption performance. Expressions for radius expansion over time by these models are summarized in Table S2. Data of the swelling behavior of i) low sodium SAP bead in DI water, ii) low sodium SAP bead in 0.1M ionic strength water, iii) high sodium SAP beads in 0.1M ionic strength water are plotted and fitted to these three models through least squares fitting (Fig. S2).

In these models, a diffusion coefficient is used as a fitting parameter. According to the assumptions and calculations used by these models, corresponding diffusion coefficients do not have the same units and scales for these three models, but we can compare the best fitting diffusion coefficients within each model to imply the rate of diffusion of different SAP spheres in different water samples. These three models do not provide prefect fits for our experimental data, but the general curves for the radius change over time predicted by the models correlate with our experimental data. By reading the best-fitting diffusion coefficients, most models show a decrease in diffusion coefficients when the SAP swells in water with higher ionic strength, which can be accounted for by the reduced cation concentration

difference inside and outside the SAP sphere, and thus the reduced osmotic force. However, when increasing the sodium content in SAP, all models show that the diffusion coefficients increase by around 50%, which is conform to the increase of osmotic force.

The fit of these models to our experimental data is not perfect mainly for two reasons. First, the diffusion of water into SAP spheres involves the decrease of osmotic force, increase of the polymer retention force, and the electrostatic force between negatively-charged polymer chains, which is much more complex than what the models can describe. Also, all models only adopt one parameter which decreases the flexibility of these models. Therefore, to better describe the swelling behavior of SAP, a more detailed model would have to be developed.

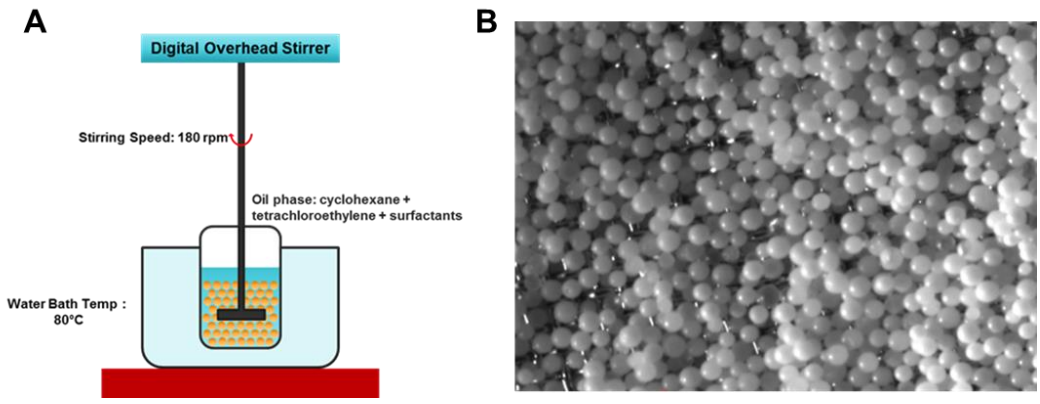

Figure S1. A) Schematics of the fabrication process of SAP beads using inverse suspension polymerization in a batch reactor. B) microscope image of beads fabricated by inverse suspension polymerization with average diameter of 120 µm.

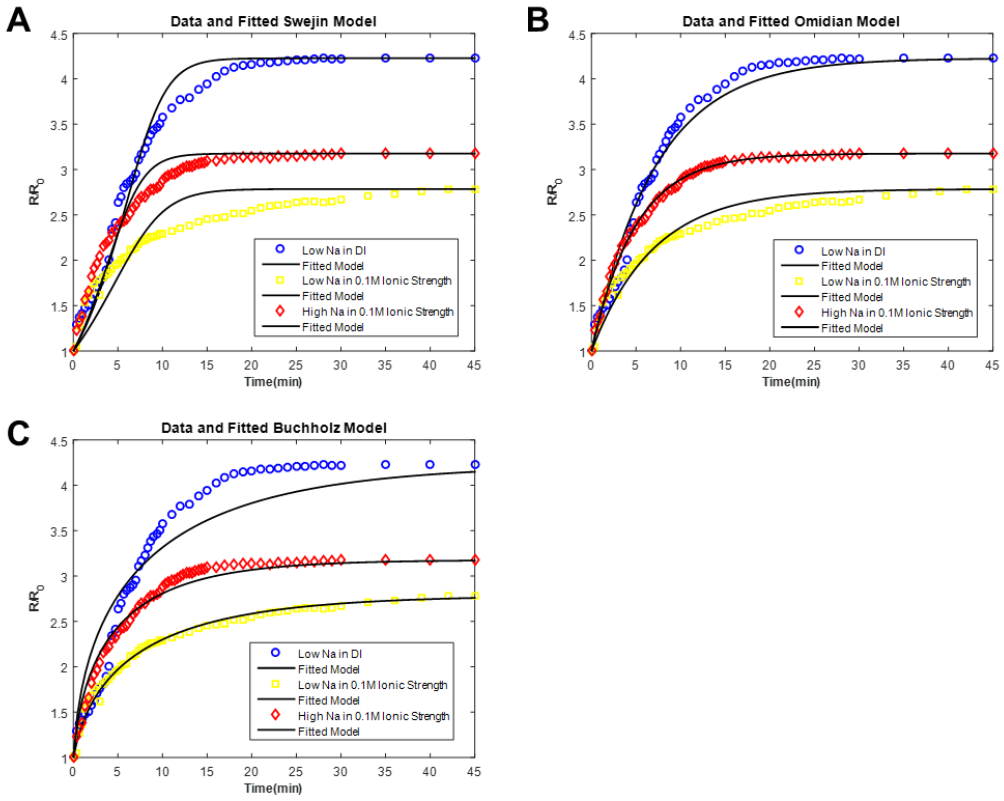

Figure S2. Comparison of experimental data and the three employed models to evaluate the absorption rate of SAP beads (diameter change verses time).

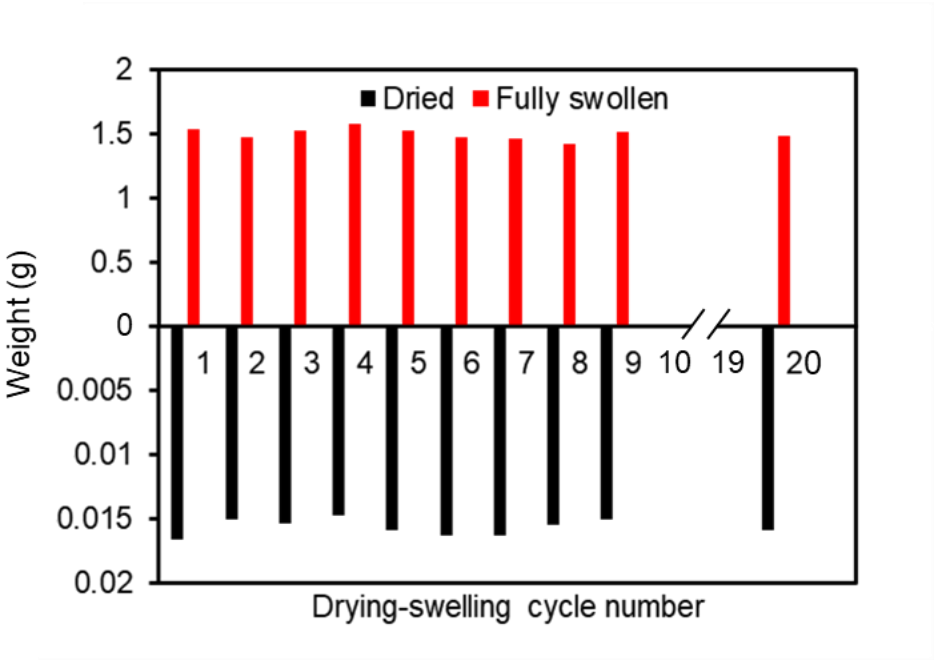

Figure S3. Weight change of 100 SAP beads for 20 drying-swelling cycles. Their mass when completely dried and swollen was measured and compared and no weight or water absorbency loss was observed.

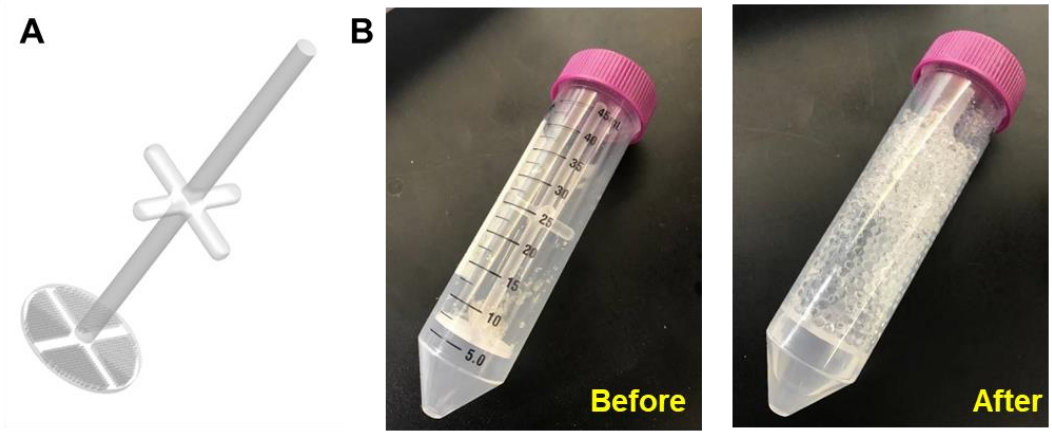

Figure S4. A) Design of the filter in the tube system. The filter has a mesh size of 300 μm, and was fabricated by 3D-printing. B) Pictures of the tube system before and after use. Dried SAP beads were pre-loaded in the tube. When the concentration was completed, concentrated sample is ready to be collected in the lower chamber.

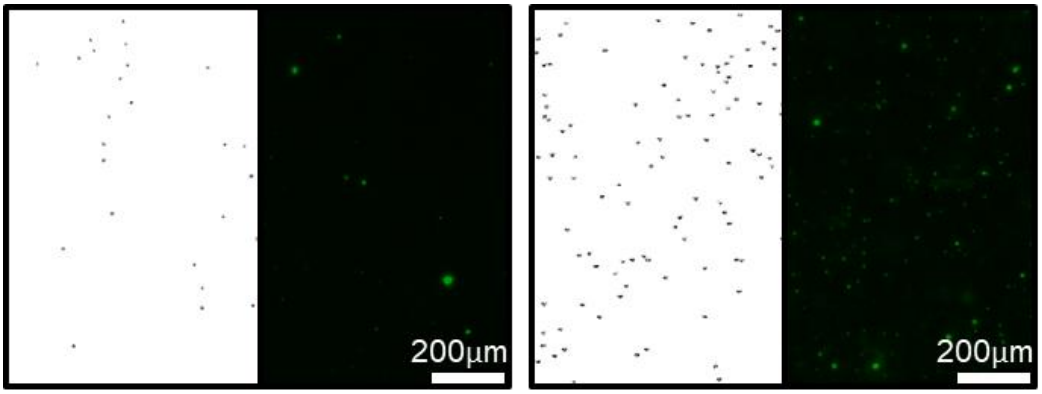

Figure S5. Fluorescence microscope images of *E. coli* concentration before and after concentration. The left side of the images were processed by ImageJ for counting. For a 10-fold concentration, an average recovery efficiency of 87% is achieved.

Figure S6. Centrifuge adapted from a salad spinner for concentration tests.

Figure S7. Fabricated SAP blocks for water absorption studies.

Table S1-1. Primer and probe sequences for the 16s rRNA qPCR assay[1]

16s rRNA Primer/probe	**Sequence (5'-3')**
Forward primer	CGGTGAATACGTTCYCGG, where Y is either C or T
Reverse primer	GGWTACCTTGTTACGACTT, where W is either A or T
TaqMan probe	FAM-CTTGTACACACCGCCCGTC

Table S1-2. MS2 primer and probe sequences for the RT-qPCR assay[2]

MS2 Primer/probe	**Sequence (5'-3')**
Forward primer	ATTCCGACTGCGAGCTTATT
Reverse primer	TTCGACATGGGTAATCCTCA
TaqMan probe	FAM-ATTCCCTCAGCAATCGCAGCAAACT-BHQ1

Table S2. Models used to evaluate the swelling of one SAP sphere:

Equation	Reference
$\frac{R}{R_0} = \left(\frac{R_m}{R_0} - 1\right)\left(1 - e^{-kt}\right) + 1$	Omidian et al. (1998)[3]
$\frac{dQ}{dt} = \frac{\pi^2 D}{R_0}(Q_{max} - Q_o)$	Buchholz (1998)[4]
$\frac{R}{R0} = \sqrt[3]{\frac{1}{1-\theta(t)}}$ $where\ \theta(t) = \theta_{max} - (\theta_{max} - \theta_0)e - kt\ ereee$	Sweijen et al. (2017)[5,6]

Note: Q in Buchholz's model represents the mass of absorbed water to the mass of dry SAP, which can be rewritten in terms of R (assuming water is incompressible), and R(t) can be yielded by numerical integration.

E. coli

Before concentration (cell/mL)	After concentration (cell/mL)				
	#1	#2	#3	Mean	STD
3.95E+04	2.33E+05	4.93E+05	6.21E+05	4.49E+05	1.98E+05
1.20E+05	1.46E+06	2.01E+06	4.52E+06	2.66E+06	1.63E+06
1.02E+06	1.29E+07	1.74E+07	2.45E+07	1.83E+07	5.85E+06

MS2

Before concentration (PFU/mL)	After concentration (PFU/mL)				
	#1	#2	#3	Mean	STD
1.15E+05	2.07E+06	1.09E+06	1.61E+06	1.59E+06	4.90E+05
8.80E+05	1.19E+07	6.88E+06	7.19E+06	8.66E+06	2.81E+06
9.88E+06	8.85E+07	7.14E+07	8.30E+07	8.10E+07	8.73E+06

Table S3. Quantification data of samples before and after concentration experiments using qPCR and RT qPCR for *E. coli* and MS2. All concentration

experiments were performed as individual triplicates, and all samples were run as triplicates on the plate. Standard curves with known gradient concentrations were run on each plate for the quantification with reaction efficiency between 90% and 110%

References:

(1) Suzuki, M. T.; Taylor, L. T.; DeLong, E. F. Quantitative Analysis of Small-Subunit RRNA Genes in Mixed Microbial Populations via 5'-Nuclease Assays. Appl. Environ. Microbiol. 2000.

(2) Huang, X.; Lin, X.; Urmann, K.; Li, L.; Xie, X.; Jiang, S.; Hoffmann, M. R. Smartphone-Based in-Gel Loop-Mediated Isothermal Amplification (GLAMP) System Enables Rapid Coliphage MS2 Quantification in Environmental Waters. Environ. Sci. Technol. 2018, 52 (11), 6399–6407.

QUASR AND MOLECULAR BEACON-BASED IN-GEL LOOP-MEDIATED ISOTHERMAL AMPLIFICATION (MGLAMP) PLATFORM FOR DIGITAL DETECTION OF SARS-COV-2 AND PATHOGENIC BACTERIA IN LARGE-VOLUME ENVIRONMENTAL WATER SAMPLES

Xunyi Wu, Yanzhe Zhu, Jing Li and Michael R. Hoffmann*

Author Statement

The manuscript was written through contributions of all authors. M.R.H. and J.L. conceived the concept for this study. J.L. and Y.Z. designed the study, J.L. X.W. and Y.Z. performed experiments, J.L. X.W. and Y.Z. analyzed the data, and X.W. wrote the manuscript.

3.0. Abstract

The quantification of SARS-CoV-2 in wastewater contributes to wastewater-based epidemiology (WBE), which helps the monitoring of prevalent infections within a community and early detections of contamination. However, quantification of SARS-CoV-2 applied in WBE relies on the availability of specialized equipment and personnel for environmental (i.e., freshwater and wastewater) sample preparation, processing, and analysis. However, these procedures are currently prioritized to meet the demand for clinical sample analyses. Here we demonstrated the usage of our portable membrane-based in-gel loop-mediated isothermal amplification (mgLAMP) system for absolute quantification of SARS-CoV-2 in environmental water samples within a 1h-timeframe for point-of-use (POU) testing and data management. The performance of mgLAMP was compared with the performance of the reverse-transcription quantitative polymerase chain reaction (RT-qPCR) method. The limit of detection (LOD) for mgLAMP for SARS-CoV-2 quantification in Milli-Q water was found to be 1 copy/mL, while in surface water collected from Kathmandu, Nepal, the LOD was 50 copies/mL. Both LODs were 100-fold lower than those obtained for RT-qPCR analyses in corresponding matrices. A 3D-printed portable device, which integrates incubation and

illumination, was developed to simultaneously allow for POU operation and simultaneous analysis of 9 mgLAMP assays. Quantitative results of the virus concentration can be sent to a smart phone or stored in an online database for cloud analysis. Compared to alternative detection methods, our platform has a very high level of tolerance against inhibitors due to the restriction effect of the hydrogel matrix. This allows for the highly sensitive detection in either clinical samples or environmental samples.

Keywords: digital LAMP, pathogen detection, point of use, membrane

3.1. Introduction

The world is currently facing an unprecedented public health burden due to Coronavirus COVID-19. As of May 10th, 2021, more than 158,612,000 cases and more than 3,299,000 deaths have been reported according to COVID-19 Dashboard by the Center for Systems Science and Engineering at Johns Hopkins University, with numbers still growing. Since infected individuals, whether symptomatic or asymptomatic, shed SARS-CoV-2 virus in their stool and the virus finally entered wastewater treatment plants[1,2], the quantification of SARS-CoV-2 in wastewater affords the ability to monitor the prevalence of infections among a given population[3,4] and also provide for an early detection of contamination via wastewater-based epidemiology (WBE). Wastewater-based epidemiology can also be applied to surface water samples for cases for which wastewater is discharged into freshwater including rivers, lakes, and estuaries without proper treatment[5,6]. However, quantification of SARS-CoV-2 applied in WBE relies on the availability of specialized equipment and personnel for environmental[7] sample preparation, processing, and analysis that are currently prioritized to meet the demand for clinical samples analyses. Therefore, ultrasensitive, rapid, and cost-effective microbial detection platforms for point-of-sampling testing (POST) are urgently

needed for monitoring the arrival, spread and decline of the SARS-CoV-2 virus in environmental samples. Corresponding control strategies could then be used for infection mitigation based on the testing results.

Quantitative reverse transcription PCR (RT-qPCR) is currently mostly used for COVID-19 detection as the gold standard for both clinical and environmental samples[1]. Since the application of this detection method is often hindered by supply shortages of reagents and thermal-cycling equipment, relative long sample-to-answer time (4-5 hours) and lack of professional lab labor[8], RT-qPCR is not suitable for point-of-sampling testing for SARS-CoV-2, especially for environmental water samples. To simplify the process of RT-qPCR for on-site usage, methods have been developed to simplify the RNA extraction step before nucleic amplification[9,10]. Alternative nucleic amplification methods such as reverse-transcription loop-mediated isothermal amplification (RT-LAMP), which requires shorter times and a more convenient analytical setups[2,8,11]. For example, onsite detection platforms have been recently developed[12], but they have mainly targeted analysis of clinical samples. Other nucleic acid detection methods that were amplification-free were also developed, by using biosensors based on gold nanoparticles (AuNPs) or use of immunofluorescence lateral flow strips with probes targeting specific regions of the SARS-CoV-2 genome[13–15]. Sensors that detect spike proteins of SARS-CoV-2 virus

particles using nanoplasmonic resonance or membrane-engineered mammalian cells with antibodies for simplified workflows were also developed[16,17]. However, these assays are not as sensitive yet as nucleic acid-based methods. Furthermore, the aforementioned detection methods are not optimized for environmental samples since they often require extra sample pretreatment and additional concentration steps[18] for environmental water samples with multiple inhibitors and low target concentrations. Moreover, current SARS-CoV-2 detection platforms are not optimized for on-site field use, and they usually do not have capacity to detect large volume of water samples larger than 1 mL.

Herein, we report on a membrane-based in-gel loop-mediated isothermal amplification (mgLAMP) system to enable the absolute quantification of SARS-CoV-2 in environmental water samples within 1 h using an integrated analytical prototype device. We also designed QUASR (for quenching of unincorporated amplification signal reporters[19]) probes for the LAMP amplification for higher specificity and fluorescence contrast. Compared to alternative detection methods, our platform has a high level of tolerance against inhibitors due to the restriction effect of the hydrogel matrix, allowing for a very sensitive detection method for wastewater samples.

3.2. Materials and Methods

3.2.1 SARS-CoV-2 Sample Preparation

Inactivated SARS-CoV-2 strains were obtained from ATCC (VR-1986HK; ATCC, Manassas, VA) or ZeptoMetrix (NATSARS(COV2)-ST; Buffalo, NY) with known concentrations and stored at -20 °C or 4 °C according to the manufactures' instructions. Before each test, SARS-CoV-2 samples were serially diluted using nuclease-free water (Thermo Scientific, Waltham, MA) for positive controls and were spiked in environmental water samples as described in the following section. SARS-CoV-2-spiked water samples were incubated with 5 mM $Na_4P_2O_7$ at room temperature for 10 min and then sonicated (46kHz, 30W) for 3 min in ice bath. The concentrations of used SARS-CoV-2 suspensions were measured by RT-qPCR assays[20]. If RNA extraction was performed for pure SARS-CoV-2 samples, the DSP Viral RNA Mini Kit (Qiagen BioSciences Inc., Germantown, MD)) was used following its manufacturer's instructions. RNeasy PowerWater Kit (Qiagen BioSciences Inc., Germantown, MD) was used to extract SARS-CoV-2 RNA spiked in environmental water samples following manufacturer's instructions.

3.2.2. SARS-CoV-2 Filtration

SARS-CoV-2 samples were filtered through a 13 mm Track-etched PC (PCTE) membrane with a 0.08 μm pore size on top of a 13 mm Hydrophilic polyester (PETE) membrane (mesh spacer). All PCTE membranes and PETE membranes used in this study were obtained from the SterliTech Corporation (Kent, WA). The PETE membrane was used as a drain disc to hold the PCTE membrane to prevent the shape change of the PCTE membrane during the filtration. The membrane and its drain disc were put in to a 13 mm Swinnex filter holder (MilliporeSigma, Burlington, MA). For the negative control of Milli-Q and positive control of SARS-CoV-2-spiked Milli-Q samples, only this step of filtration is deployed. For wastewater samples, a three tier filtration process was used as depicted in in **Fig. 4**. The first tier of 3-μm and the second tier of 0.1 μm PCTE membranes were set up as pre-filters to remove larger solids in wastewater samples. For surface fresh water such as river water, 2 tier filtration was performed with the first tier of 1 μm PCTE membrane as pre-filter. Filtrations with spiked samples were performed by a syringe pump (74905-02, Cole-Parmer, US) with inlet speed of 0.5 mL/mL. Negative controls and positive controls were directly filtered by syringe pushed by hand.

3.2.3. mgLAMP Assay

After filtration, the 0.08 μm membrane was dried at room temperature and glued on a glass slide using 1.1 μL of 50% PBS buffer (Corning™, USA) and 50% Glycerol (Sigma-Aldrich, USA) mixture. A Frame-Seal™ in situ PCR and Hybridization Slide Chamber (9 × 9 mm; Bio-Rad, Hercules, CA) was placed on the membrane to hold the mixture of PEG gel and LAMP reaction mix.

Four-arm PEG acrylate (molecular weight (MW) of 10,000 Laysan Bio, Arab, AL) and thiol-PEG-thiol (MW of 3,400; Laysan Bio, Arab, AL) were used to form the PEG gel at a mole ratio of 1:2. For each mgLAMP assay of 30 μL, the composition of the reaction mix was as follows: 10 μL of 2× WarmStart LAMP Master Mix, 1 U/mL RNase Inhibitor, Murine, 20 U/mL Antarctic Thermolabile UDG, 700 μM dUTP, 0.5 % Triton X-100 (T8787; Sigma Aldrich, St. Louis, MO),1.6 μM FIP, 1.6 μM FAM-BIP, 0.2 μM F3/B3, 0.4 μM LB, 2.4 μM optimal quencher qBIP-15nt, and nuclease-free water, plus 5% (w/v) PEG gel. All LAMP reagents were purchased from New England Biolabs (Ipswich, MA) and all primers, probes and quenchers were obtained from Integrated DNA Technologies (Coralville, IA) unless otherwise specified. In total, 11 sets of LAMP primers were tested for their

detection limit using the reagent recipe and thermocycling protocols from the original literatures. All LAMP primers tested are listed in the **Table S2**. in the supplementary information. Complementary QUASR (Quenching of Unincorporated Amplification Signal Reporters)[19] fluorescent probes (FAM-FIP or FAM-BIP) and quenchers (qFIP or qBIP) were designed using IDT OligoAnalyzer™ Tool (https://www.idtdna.com/pages/tools/oligoanalyzer) and added to the reaction mix at a final concentration of 1.6, 2.4 and 3.2 μM. The optimal QUASR probe we chose which was modified by the BIP primer for SARS-CoV-2 was (6-FAM)-5-

CAGAGACAGAAGAAACAGCAAACTGATTGTTGCAATTGTTTGGAG-3'

and the quencher was 5-TTTCTTCTGTCTCTG-3-(3IABkFQ).

A 30 μL mixture of PEG gel and LAMP reaction mix was loaded into the frame seal chamber and was covered by a transparent qPCR film (Genesee Scientific, San Diego, CA). The hydrogel mix was left at room temperature (20 °C) for 5 min for gelation and then incubated on a PCR machine (MJ Research PTC-100, Watertown, MA) at 65 °C for 30 min for LAMP reactions.

3.2.4. Fluorescence Reading and Analysis

After the LAMP reaction, the gel within the frame seal chamber was illuminated by an E-Gel Safe Imager (Invitrogen, Carlsbad, CA), and the amplicon dots were captured with a Google Pixel 4 Cellphone with its build-in camera. To compare the performance of the cellphone camera, the gel with amplicons was also illuminated and imaged using a Leica DMi8 fluorescence microscope (Leica Co., Germany). Amplicons were enumerated and the concentration of SARS-CoV-2 was back-calculated.

3.2.5. Quantitative Reverse Transcription PCR (RT-qPCR)

Performance of the mgLAMP of SARS-CoV-2 was compared to RT-qPCR. The extraction and detection of SARS-CoV-2 were performed according to the guidelines provided by the US Centers for Disease Control and Prevention (CDC)[20].

Relevant primer and probe sets were purchased from IDT (SARS-CoV-2 (2019-nCoV) CDC qPCR Probe Assay), the assay targeting the N gene was carried out in a 20-μL reaction mixture consists of 10 μL qScript XLT One-Step RT-qPCR ToughMix(2X) (Quantabio, Beverly, MA), 1.5 μL combined primer/probe mix, 2

μL of template DNA, and nuclease-free-water. The RT-qPCR assays were performed using a 6300 Realplex4 qPCR platform (Eppendorf, Hamburg, Germany), and the thermocycling involves reverse transcription for 10 minutes at 50 °C followed by 3 minutes of initialization at 95 °C, and 45 cycles of denaturation at 95 °C for 3 seconds followed by annealing/extension at 55 °C for 30 seconds. Quantitative results were analyzed by the build-in software of the Eppendorf qPCR platform.

3.2.6. Water Samples

Surface freshwater samples were collected from the Godawari Khola (river) 15 km from Kathmandu, Nepal (see **Fig. S1** for the geological location of the river) and wastewater samples were collected from the raw influent and primary effluent from a local wastewater treatment plant in Los Angeles. The conductivities and pH values of environmental water samples were measured with an electrical pH/conductivity meter (Orion Star A215; Thermo Scientific, Waltham, MA). Inactivated SARS-CoV-2 was spiked in water samples directly.

3.3. Results and Discussion

3.3.1. Workflow of mgLAMP

The mgLAMP system developed by our group allows for an easy use by people without previous training. **Fig. 1** schematically illustrates the workflow of mgLAMP for rapid microorganism detection and quantification from raw samples (input) to quantitative results (output): (i) The environmental sample (1-100 mL) is enriched by forcing it through a PCTE filtration membrane. The PCTE membrane has the required pore size to retain SARS-CoV-2 viral particles and to filter out small particles and larger molecular aggregates including potential LAMP inhibitors. The filtered membrane is then transferred on a glass slide and fixed by a frame-sealing to form a reaction chamber. (ii) The LAMP reagent mix is prepared and partitioned in to two equal volumes. The two aliquots are then mixed with a four-arm PEG acrylate and thiol-PEG-thiol monomers powders, respectively. The reaction mixture of the two PEG gels is mixed thoroughly and then loaded into the chamber at a 1-to-1 ratio. (iii) The chamber is sealed with a plastic film and the loaded mixture is cross-linked within minutes at room temperature. (iv) The sample slide is inserted into the Caltech mgLAMP prototype device for incubation at 65°C for 30 min in order to achieve LAMP amplification. (v) The Caltech prototype is

adapted for direct endpoint fluorescence imaging of the sample slide carrying 9 simultaneous samples. The photographic images are captured by thee smartphone camera of subquent quantification.

3.3.2. Selection and Optimization of LAMP Primers and Probes

In total, 11 sets of LAMP primers that were reported in the literature[11,12,21–23] were screened based on their detection limit, target gene ,and suitability for probe design. During the time frame of this research, the latest LAMP-related research of SARS-CoV-2 was followed closely and the primer list was updated accordingly. Details about all 11 LAMP primer sets can be found in **Table S2.** Among the 11 primer sets, set 7, 10, 11 which targeted the N (Nucleocapsid) gene of SARS-CoV-2 had lower detection limits of one or two orders of magnitude with a stable performance (i.e., fewer false negative results) as shown in **Fig. S2.**

The LAMP protocols developed for SARS-CoV-2 most often used LAMP dyes as the probe. However, the signal-to-noise ratios of the LAMP dye generated within the hydrogel matrix was unsatisfactory in that it was hard to distinguish between fluorescence from the amplicons and the background fluorescence[24]. In addition, as

the fluorophores of the LAMP dye bind to the amplified nucleic acid strands, the poor specificity of the LAMP dye presented another problem. In order to resolve this problem, we designed two specific fluorescent probes based on molecular beacons and QUASR probes.

In-tube test results showed that compared to the molecular beacons, the QUASR probes had higher fluorescence yields and higher signal-to-noise ratios (**Fig. S3**.). We hypothesized that this outcome resulted from the proximity of the quencher and reporting fluorophore for molecular beacons, while the quencher is released apart from the reporting fluorophore completely for QUASR. When a molecular beacon hybridizes with its target sequence, the hairpin-loop structure opens, and the reporter and the quencher at the end of the molecular beacon are also separated, resulting the emission of fluorescence signal by the reporter[25–27]. The quenchers of molecular beacons may still have quenching effects on the fluorescence of the reporting fluorophore after the amplification, therefore reducing the fluorescence intensity. However, for QUASR, one of the internal primers (FIP or BIP) is labeled with a fluorophore (FAM was used in this study) while the fluorescent probe is quenched by a complementary sequence with a quencher (Iowa Black FQ or IBFQ was used in this end) at the 3′ end. Since the melting temperature (Tm) of the

complex is at least 10 °C lower than the LAMP amplification temperature, FAM modified inner primers work just as regular inner primers during amplification. If amplification happens, incorporated FAM-inner primers will lead to fluorescence since they form stable double-strand structures and will not be quenched with the complementary quencher, thus producing a much stronger fluorescence signal[19].

Design of the QUASR probes required that we considered the possibility of the quencher forming dimer, which would decrease the quenching effect. Among the primer sets with best detection limits, primer set 11 was observed to be the best one for use as a QUASR probe since the complimentary sequences to the inner primers were unlikely to self-hybridize, thus allowing for an optimized quenching effect. Two quenchers with different lengths of 12 nt and 17 nt for FIP and 10 nt and 15 nt for BIP were designed, making a total of 4 QUASR sets (FAM-FIP with qFIP-12nt and qFIP-17nt, and FAM-BIP with qBIP-10nt and qBIP-15nt). Since the concentration of FAM-FIP or FAM-BIP was 1.6 μM, quenchers with concentrations of 1.6 μM, 2.4 μM, 3.2 μM were tested, and all tests were performed in duplicates. As shown on **Fig. 2.**, most of the FAM-IP and quenchers had suitable responses at higher spiked concentration. However, some of the combinations had unsatisfactory results when the target concentrations were decreased. In these cases,

it was hard to distinguish between the positive samples and the negative controls. Moreover, when the quencher concentration was equal to the FAM-IP concentration, occasional false positives resulted due to an insufficient quenching such that some of the negative controls also gave fluorescence response. At the lowest target concentration of ~200 copies per reaction in a tube, all QUASR combinations gave unsatisfactory results. Among all the combinations, the FAM-BIP with qBIP-15nt had the best performance in terms of detection limit, fluorescent intensity, and contrast with NTC.

3.3.3. Membrane Selection and Filtration

PCTE membranes were used to filter out SARS-CoV-2 particles. After filtration, mgLAMP was performed on the membrane. Theoretically, membranes with smaller pore sizes should be able to capture more SARS-CoV-2 particles, which would in turn lower the detection limit. However, during filtration, pressure within the filter increases as the pore size is decreased. The pressure increase makes it more difficult to filter while inducing fluid leaks during filtration unit, and damaging of viral structures at a high pressure. We tested the recovery rates of PCTE membranes

were determined for membrane pore sizes of 200 nm, 100 nm, 80 nm, and 50 nm as shown in **Fig. S4.** RNA was collected from the membranes after filtration of spiked SARS-CoV-2 samples and running RT-qPCR assays for the extracted RNA samples. Comparing all of the PCTE membrane pore sizes, the highest recovery rate occurred with the 80 nm pore size membranes. Even though the recovery rate was less than 30%. However, it does not imply that the membrane retained less than 30% of spiked particles. Instead, the lower recovery was most likely due to RNA losses during the extraction process from the membrane for the subsequent RT-qPCR analysis. Since the RNA losses during extraction should be approximately the same for all samples, the qualitative comparison between different pore sizes should be valid.

Since the average size of SARS-CoV-2 is around 100 nm[28], the recovery efficiencies of PCTE membranes of pore sizes 100 nm and 80 nm used in our mgLAMP assays at different spiked concentrations. These results are shown on **Fig. 3**. For the spiked concentrations, the recovery off of the 80 nm membrane exceeded the recovery of 100 nm membrane with an average of 60.2% ± 34.0%. The Caltech mgLAMP method does not need to extract viruses from the membrane since mgLAMP is an *in situ* analytical method on the membrane, which results in lower

losses of the target due to an extraction processes, and thus leads to lower detection limits. The mgLAMP results indicate a very high recovery rate using the 80 nm pore size membrane. The LOD per reaction for mgLAMP analysis was close to that observed for the in-tube tests. This result suggests that the primer efficiency was the major factor for the LOD.

For environmental samples such as raw wastewater influent, a dislodging step was added before the 3-tier filtration as a sample pretreatment step before the mgLAMP assay (**Fig. 4.**). The dislodging step is designed to release attached viruses from wastewater sludge surfaces by using tetra-sodium pyrophosphate with a 3-minute sonication. After dislodging, the wastewater was forced through the 3 tier filtration unit to remove particles on different sizes. For raw wastewater influents, 3 μm and 0.1 μm membrane filters were used in the first and second filtration was needed to ensure sufficient viral numbers on the third membrane (80 nm), which was then used for mgLAMP assay. Based in the RT-qPCR results, the second filtration step blocked ~60% of the total SARS-CoV-2 viruses. This required us to increase the area of the second membrane to block more solids and allow for a larger number of viruses to pass through. However, for the Nepalese surface water samples, a 2-tier filtration with one 13mm and 1-μm pore-sized membrane was used for the first

filtration step in order to achieve reliable and quantitative mgLAMP assays. The filtration strategies depend on an evaluation of water matrices that considers the size distribution of the particles within the collected samples after the dislodging step. Fresh water samples, which have larger and more homogeneous particles require less pre-filtration even though the total dissolved solid (TSS) content may be high. For example, most of the particles in Nepalese surface water after treatment were found to be around 500 nm. They were readily separated from the viral particles with a one-tier pre-filtration, while particles in primary effluent after initial wastewater treatment had sizes close to the 100 nm membrane pores. They were more difficult to separate from the viral particles. This resulted in more inhibitors into the reaction system. In the future, dynamic light scattering (DLS) be used to determine the filtration tiers and membrane pore sizes along with an optimal size for the pre-filtration step.

3.3.4. Performance of mgLAMP on SARS-CoV-2 Quantification

Figures 5A-E show that the LAMP was successfully performed in the PEG gel matrices on the PCTE membrane for the surface water collected in Nepal. Clearly

separated amplicon dots with high fluorescence yields were observed after 30 minutes of LAMP reaction time as detected with the fluorescence microscope and smartphone camera (**Fig. 5A-E**). No signals were observed for the template controls (**Fig. 5F**). The amplicon dot sizes tended to be smaller when the concentration increased within one membrane cell, although the fluorescent dots were clearly separated from each other. The numbers of amplicons could have varied from 1 to 10000 for each cell reaction. Given that a single amplicon represented one successful amplification of the target sequence, the dynamic range of mgLAMP was relatively broad. The concentration of target SARS-CoV-2 in the sample could then be calculated by counting the positive amplicons. An excellent linear correlation between the measured concentrations from the mgLAMP amplicon dots (**Fig. 5G**) with concentrations of the spiked SARS-CoV-2 viral particles in both Milli-Q water and surface water (e.g., $R^2 \geq 95\%$). The detection limit in Milli-Q water was as low as 1 copy/mL. However, due to the high TSS value of more than 400 mg/L, and the target loss during required dislodging and pre-filtration step, the detection limit of mgLAMP method for SARS-CoV-2 in surface water was substantially higher at 50 copies/mL. However, since membrane filtration tends to decrease the detection limit, but the combination of the gel with LAMP amplification increases the tolerance towards environmental inhibitors. Regardless

of the background matrix of the natural or engineered water, the mgLAMP detection method had a 100-fold lower detection limit compared to RT-qPCR quantification.

3.3.5. Quantification of Bacteria including *E. coli* and *S.* Typhi

In addition to SARS-CoV-2 quantification, mgLAMP was also used for quantification of non-pathogenic *E. coli* and pathogenic *S.* Typhi. PCTE membranes with a 0.2 μm pore size were used to filter and capture bacteria given that the characteristic size of *E. coli* and *S.* Typhi of 1.0 μm. For the bacterial analyses, lysozyme was added into the mgLAMP reaction mix. Lysozyme degrades the peptidoglycans of the bacterial cell walls. It has been shown to be effective for cell lysis and nucleic acid release[29]. Molecular beacons developed by Lin et al. were used as probes in the reaction system as they generated strong fluorescent signals for bacteria[30,31]. Details about the preparation, filtration and mgLAMP reaction for the bacterial samples are found in the supplementary information section.

As depicted in in **Fig. 6 a-h**, mgLAMP was used successfully on the bacterial samples. For the bacterial sample detection, mgLAMP also produced separated

amplicon dots that appeared after 30 minutes of the LAMP reaction as detected using either the fluorescence microscope or the smartphone camera (**Fig. 3 a-h**). A linear correlation was observed between mgLAMP amplicon dots with different concentrations of spiked cells for the bacterial pathogens. The sensitivity was down to a single membrane cell with a dynamic range of ~0.4-40000 cells/mL (**Fig. 6i-j**). However, the detection efficiency was lower when the spiked concentrations were high. For example, the detection efficiency of *E. coli* at the range 4×10^1 to 4×10^3 cells/mL, was 4.74 times the efficiency at the range of 4×10^1 to 4×10^4 cells/mL. Although the mgLAMP platform has lower detection limits and high sensitivity, the limited space within a single PEG gel membrane cell nay lead to some limitations at the upper detection limit.

The versatility of mgLAMP for both viral and bacterial samples shows that the Caltech prototype device has the potential to be used for the detection of a variety of pathogenic microorganisms. With future improvements in the filtration protocol and the reaction mix employed, the mgLAMP amplification methods should provide low-cost, point-of-use monitoring solutions for detection and quantification of microbes that that are the vectors of life-threatening infectious diseases.

3.4. Conclusions

In this study, a membrane-based in-gel loop-mediated isothermal amplification system was developed for the rapid and cost-effective quantification of SARS-CoV-2 at the point of collection in the ambient environment. We developed a simple workflow for our detection system to aid in the point-of-use testing and we designed customized QUASR probes to obtain stronger fluorescent signals with higher specificity. We carefully selected PCTE membranes with 80-nm pore size for best recovery of SARS-CoV-2 and developed filtration strategies for different environmental water matrices. The resulting detection limit of the mgLAMP was found to be lower than the LOD obtained with RT-qPCR regardless of the specific nature of the water samples. The Caltech prototype system is a promising tool for use in field studies, especially for environmental surveillance and source tracking of waterborne pathogens. The mgLAMP-based system can rapidly and easily detect target pathogens in various environmental water samples. Coupled with analysis on a cloud server, the regional distribution of waterborne pathogens could be visualized. This approach provides for the monitoring and eventual control of waterborne pathogens from multiple sources.

Figures

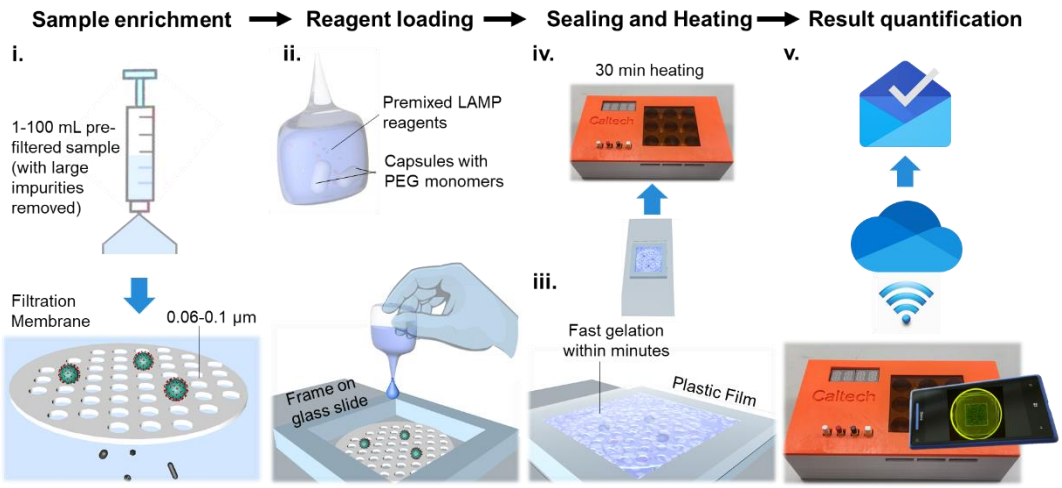

Figure 1. The schematic workflow of mgLAMP from sample-input to result-output for target microorganism detection. (This figure was created by Yanzhe Zhu, who granted permission for its use in this dissertation.)

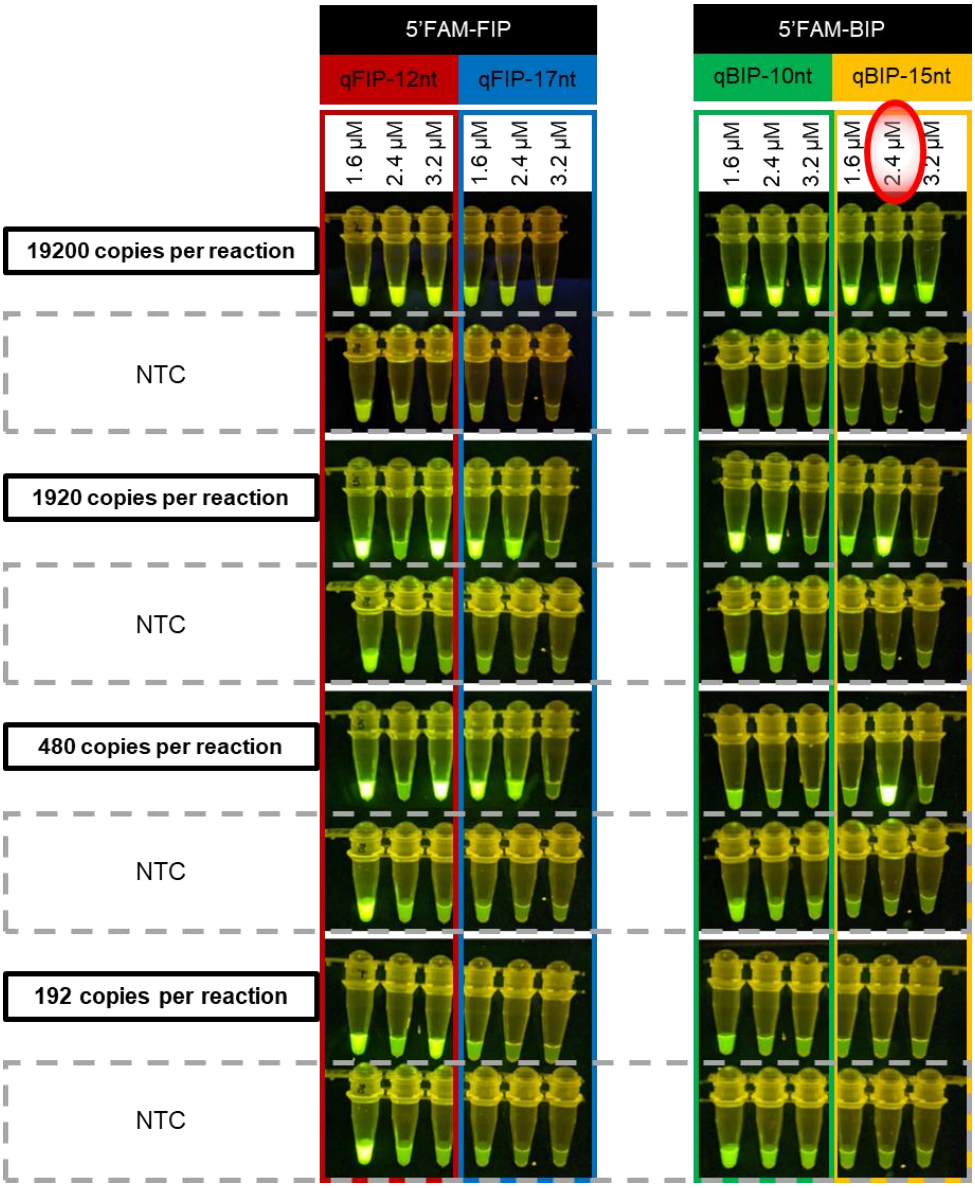

Figure 2. Performance of 4 QUASR combinations with different quencher concentrations. From left to right, each color box represents a combination of FAM-

IP with quenchers of different lengths. Within each color box from left to right, the quencher concentrations increase from 1.6 μM to 3.2 μM. From up to down, different concentrations of SARS-CoV-2 RNA were added and amplified, with negative control of RNase free water to show the fluorescence contrast of quenching.

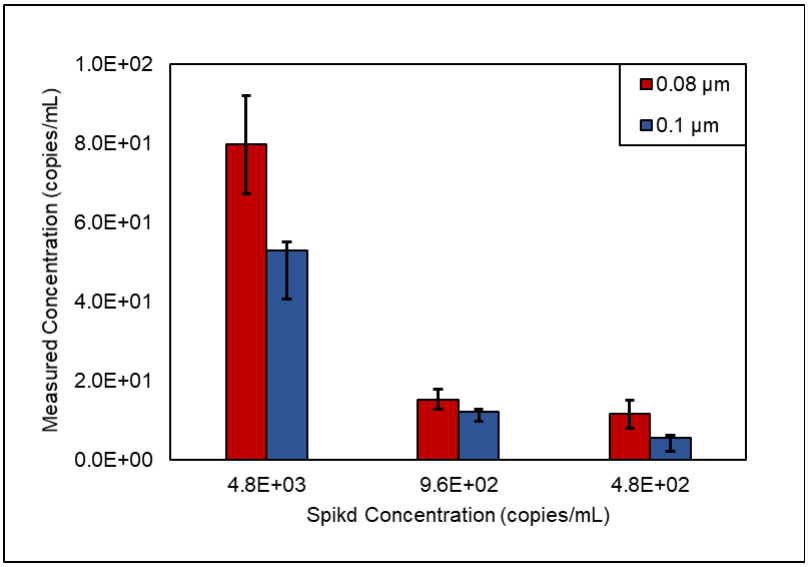

Figure 3. Comparison on the SARS-CoV-2 recovery between 0.08- and 0.1-µm PCTE membranes at different concentrations for mgLAMP.

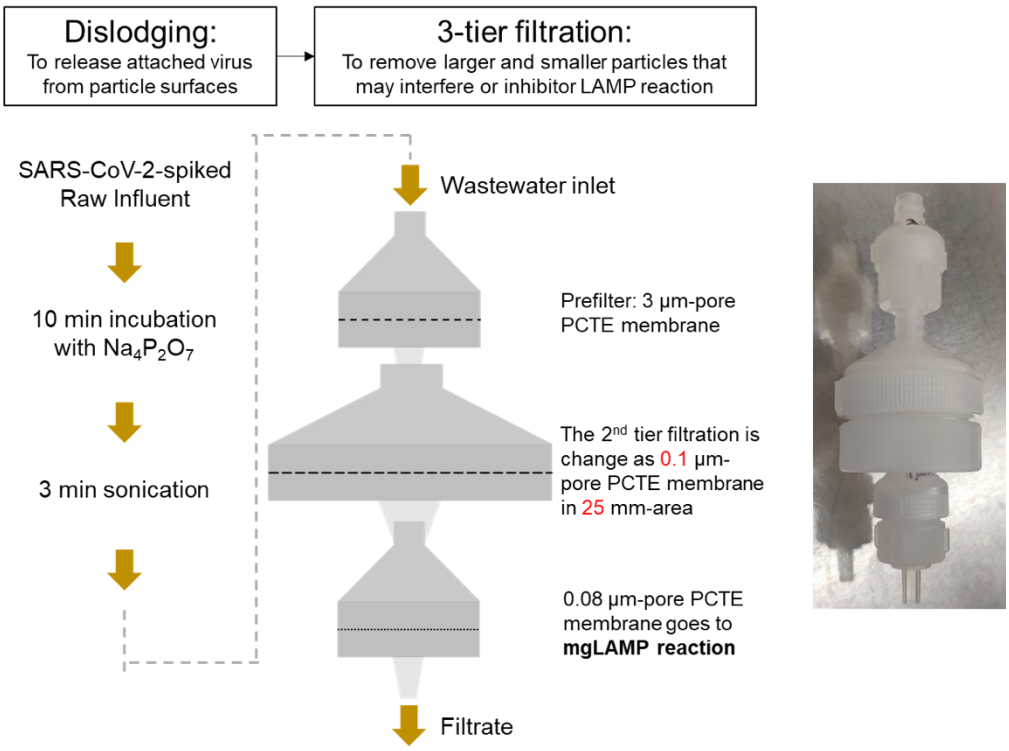

Figure 4. Pretreatment process including dislodging process and 3-tier filtration (schematic illustration and actual photo) for environmental water and wastewater samples. (This figure was created by Yanzhe Zhu and Jing Li, who granted permission for its use in this dissertation.)

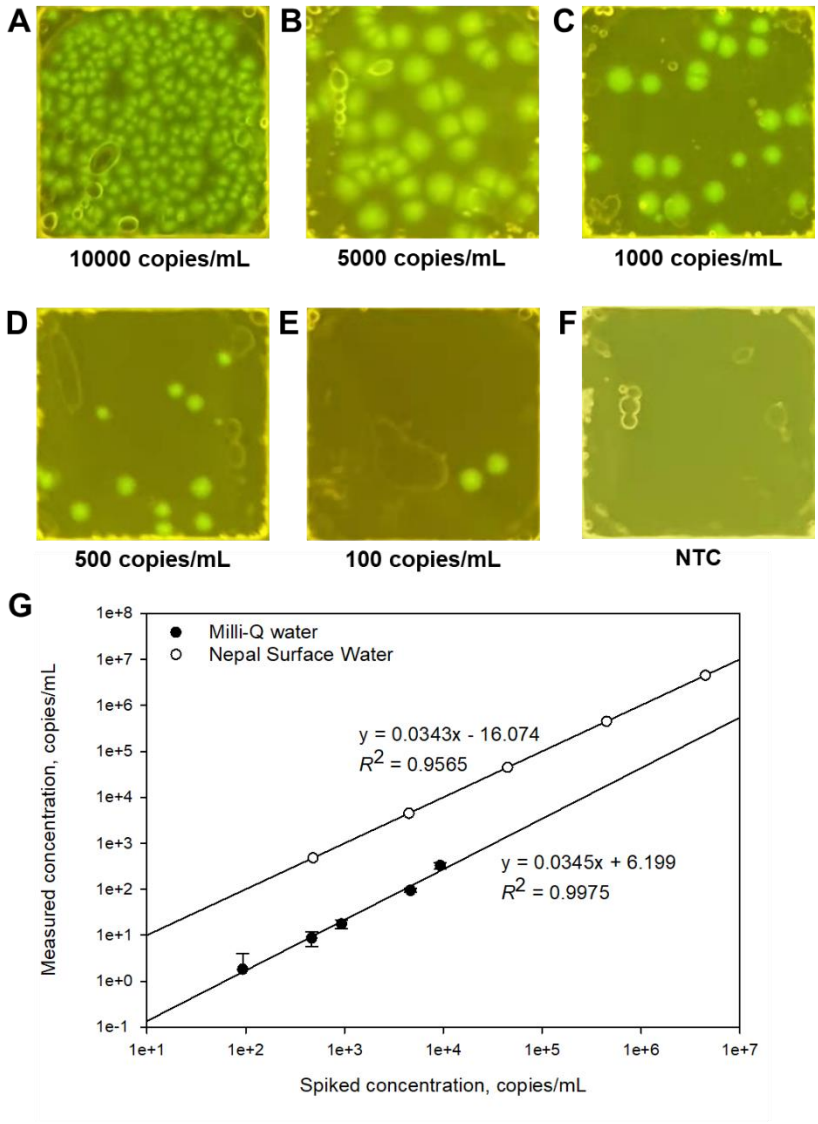

Figure 5. (A-E) were mgLAMP amplicon dots for different SARS-CoV-2 concentrations spiked into Nepal surface water samples and (F) is the no template

control. All images were taken by the google pixel 3 under the E-gel Safe imager. (G) Comparisons of measured SARS-CoV-2 to the spiked concentrations in both Milli-Q water and Nepal surface water. (This figure was created by Jing Li, who granted permission of its use in this dissertation.)

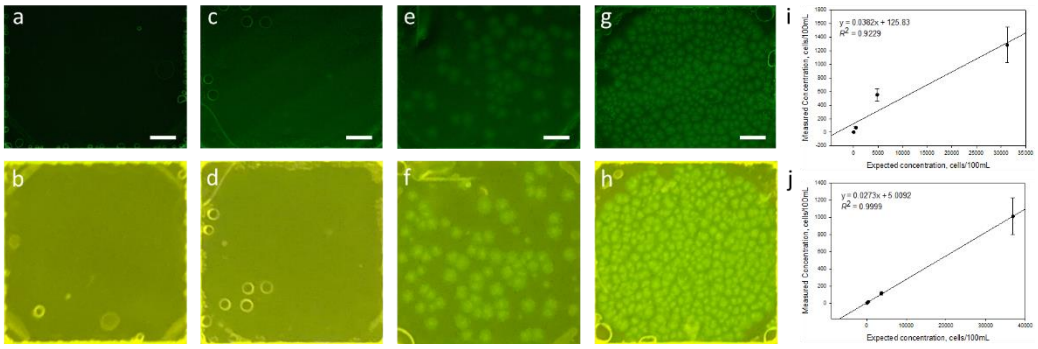

Figure 6. (**a-h**) were mgLAMP amplicon dots for different *E. coli* concentrations. Top panel images (**a, c, e, g**) were taken by fluorescence microscope while bottom panel images (**b, d, f, h**) were taken by the google pixel 3 under the E-gel Safe imager. (**a, b**) No template control, (**c, d**) low template concentration of around 5 dots/assay, (**e, f**) medium template concentration of around 50 dots/assay, (**g, h**) high template concentration of around 500 dots/assay. Scale bar, 1 mm. Comparisons of measured *E. coli* (**i**) and *S.* Typhi (**j**) to the spiked concentrations. (This figure was created by Jing Li, who granted permission of its use in this dissertation.)

References

(1) Farkas, K.; Hillary, L. S.; Malham, S. K.; McDonald, J. E.; Jones, D. L. Wastewater and Public Health: The Potential of Wastewater Surveillance for Monitoring COVID-19. *Curr. Opin. Environ. Sci. Heal.* **2020**, *17*, 14–20.

(2) Philo, S. E.; Keim, E. K.; Swanstrom, R.; Ong, A. Q. W.; Burnor, E. A.; Kossik, A. L.; Harrison, J. C.; Demeke, B. A.; Zhou, N. A.; Beck, N. K.; et al. A Comparison of SARS-CoV-2 Wastewater Concentration Methods for Environmental Surveillance. *Sci. Total Environ.* **2021**, *760*, 144215.

(3) Ahmed, W.; Angel, N.; Edson, J.; Bibby, K.; Bivins, A.; O'Brien, J. W.; Choi, P. M.; Kitajima, M.; Simpson, S. L.; Li, J.; et al. First Confirmed Detection of SARS-CoV-2 in Untreated Wastewater in Australia: A Proof of Concept for the Wastewater Surveillance of COVID-19 in the Community. *Sci. Total Environ.* **2020**, *728*, 138764.

(4) Gonzalez, R.; Curtis, K.; Bivins, A.; Bibby, K.; Weir, M. H.; Yetka, K.; Thompson, H.; Keeling, D.; Mitchell, J.; Gonzalez, D. COVID-19 Surveillance in Southeastern Virginia Using Wastewater-Based Epidemiology. *Water Res.* **2020**, *186* (January), 116296.

(5) Baldovin, T.; Amoruso, I.; Fonzo, M.; Buja, A.; Baldo, V.; Cocchio, S.; Bertoncello, C. SARS-CoV-2 RNA Detection and Persistence in Wastewater Samples: An Experimental Network for COVID-19 Environmental Surveillance in Padua, Veneto Region (NE Italy). *Sci. Total Environ.* **2021**, *760*, 143329.

(6) Adelodun, B.; Ajibade, F. O.; Ibrahim, R. G.; Bakare, H. O.; Choi, K. S. Snowballing Transmission of COVID-19 (SARS-CoV-2) through Wastewater: Any Sustainable Preventive Measures to Curtail the Scourge in Low-Income Countries? *Sci. Total Environ.* **2020**, *742*, 140680.

(7) Randazzo, W.; Truchado, P.; Cuevas-Ferrando, E.; Simón, P.; Allende, A.; Sánchez, G. SARS-CoV-2 RNA in Wastewater Anticipated COVID-19 Occurrence in a Low Prevalence Area. *Water Res.* **2020**, *181*.

(8) Lalli, M. A.; Langmade, S. J.; Chen, X.; Fronick, C. C.; Sawyer, C. S.; Burcea, L. C.; Wilkinson, M. N.; Fulton, R. S.; Heinz, M.; Buchser, W. J.; et al. Rapid and Extraction-Free Detection of SARS-CoV-2 from Saliva with Colorimetric LAMP. *medRxiv* **2020**, 1–34.

(9) Smyrlaki, I.; Ekman, M.; Lentini, A.; Rufino de Sousa, N.; Papanicolaou, N.;

Vondracek, M.; Aarum, J.; Safari, H.; Muradrasoli, S.; Rothfuchs, A. G.; et al. Massive and Rapid COVID-19 Testing Is Feasible by Extraction-Free SARS-CoV-2 RT-PCR. *Nat. Commun.* **2020**, *11* (1), 1–12.

(10) Wee, S. K.; Sivalingam, S. P.; Yap, E. P. H. Rapid Direct Nucleic Acid Amplification Test without Rna Extraction for Sars-Cov-2 Using a Portable Pcr Thermocycler. *Genes (Basel).* **2020**, *11* (6), 1–13.

(11) González-González, E.; Lara-Mayorga, I. M.; Rodríguez-Sánchez, I. P.; León, F. Y. De; García-Rubio, A.; Garciaméndez-Mijares, C. E.; Guerra-Alvarez, G. E.; García-Martínez, G.; Aguayo-Hernández, J. A.; Márquez-García, E. Scaling Diagnostics in Times of COVID-19: Colorimetric Loop-Mediated Isothermal Amplification (LAMP) Assisted by a 3D-Printed Incubator for Cost-Effective and Scalable Detection of SARS-CoV-2. *medRxiv* **2020**.

(12) Ganguli, A.; Mostafa, A.; Berger, J.; Aydin, M. Y.; Sun, F.; Stewart de Ramirez, S. A.; Valera, E.; Cunningham, B. T.; King, W. P.; Bashir, R. Rapid Isothermal Amplification and Portable Detection System for SARS-CoV-2. *Proc. Natl. Acad. Sci. U. S. A.* **2020**, *117* (37), 22727–22735.

(13) Wang, D.; He, S.; Wang, X.; Yan, Y.; Liu, J.; Wu, S.; Liu, S.; Lei, Y.; Chen, M.; Li, L.; et al. Rapid Lateral Flow Immunoassay for the Fluorescence Detection of SARS-CoV-2 RNA. *Nat. Biomed. Eng.* **2020**, *4* (12), 1150–1158.

(14) Alafeef, M.; Dighe, K.; Moitra, P.; Pan, D. Rapid, Ultrasensitive, and Quantitative Detection of SARS-CoV-2 Using Antisense Oligonucleotides Directed Electrochemical Biosensor Chip. *ACS Nano* **2020**, *14* (12), 17028–17045.

(15) Mao, K.; Zhang, H.; Yang, Z. Can a Paper-Based Device Trace COVID-19 Sources with Wastewater-Based Epidemiology? *Environ. Sci. Technol.* **2020**, *54* (7), 3733–3735.

(16) Mavrikou, S.; Moschopoulou, G.; Tsekouras, V.; Kintzios, S. Development of a Portable, Ultra-Rapid and Ultra-Sensitive Cell-Based Biosensor for the Direct Detection of the SARS-CoV-2 S1 Spike Protein Antigen. *Sensors* **2020**, *20* (11), 3121.

(17) Huang, L.; Ding, L.; Zhou, J.; Chen, S.; Chen, F.; Zhao, C.; Xu, J.; Hu, W.; Ji, J.; Xu, H.; et al. One-Step Rapid Quantification of SARS-CoV-2 Virus

Particles via Low-Cost Nanoplasmonic Sensors in Generic Microplate Reader and Point-of-Care Device. *Biosens. Bioelectron.* **2021**, *171*, 112685.

(18) Sherchan, S. P.; Shahin, S.; Ward, L. M.; Tandukar, S.; Aw, T. G.; Schmitz, B.; Ahmed, W.; Kitajima, M. First Detection of SARS-CoV-2 RNA in Wastewater in North America: A Study in Louisiana, USA. *Sci. Total Environ.* **2020**, *743*, 140621.

(19) Ball, C. S.; Light, Y. K.; Koh, C. Y.; Wheeler, S. S.; Coffey, L. L.; Meagher, R. J. Quenching of Unincorporated Amplification Signal Reporters in Reverse-Transcription Loop-Mediated Isothermal Amplification Enabling Bright, Single-Step, Closed-Tube, and Multiplexed Detection of RNA Viruses. *Anal. Chem.* **2016**, *88* (7), 3562–3568.

(20) CDC Division of Viral Diseases. CDC 2019-Novel Coronavirus (2019-NCoV) Real-Time RT-PCR Diagnostic Panel 2019-NCoVEUA-01 CDC-006-00019, Revision: 06. **2020**, 80.

(21) Lamb, L. E.; Ph, D.; Oak, R.; States, M. I. U.; Lamb, L. E.; Ph, D.; Lamb, L. E.; Ph, D.; Bartolone, S. N. The Lancet Rapid Detection of Novel Coronavirus (COVID-19) by Reverse Transcription-Loop- Mediated

Isothermal Amplification. *medRxiv* **2020**.

(22) Zhang, Y.; Odiwuor, N.; Xiong, J.; Sun, L.; Nyaruaba, R. O.; Wei, H.; Tanner, N. A. Rapid Molecular Detection of SARS-CoV-2 (COVID-19) Virus RNA Using Colorimetric LAMP. *medRxiv* **2020**.

(23) El-Tholoth, M.; Bau, H. H.; Song, J. A Single and Two-Stage, Closed-Tube, Molecular Test for the 2019 Novel Coronavirus (COVID-19) at Home, Clinic, and Points of Entry. *ChemRxiv* **2020**.

(24) Quyen, T. L.; Ngo, T. A.; Bang, D. D.; Madsen, M.; Wolff, A. Classification of Multiple DNA Dyes Based on Inhibition Effects on Real-Time Loop-Mediated Isothermal Amplification (LAMP): Prospect for Point of Care Setting. *Front. Microbiol.* **2019**, *10* (October), 1–12.

(25) Poddar, S. K. Detection of Adenovirus Using PCR and Molecular Beacon. *J. Virol. Methods* **1999**, *82* (1), 19–26.

(26) Zhang, P.; Beck, T.; Tan, W. Design of a Molecular Beacon DNA Probe with Two Fluorophores. *Angew. Chemie - Int. Ed.* **2001**, *40* (2), 402–405.

(27) Lin, X.; Huang, X.; Zhu, Y.; Urmann, K.; Xie, X.; Hoffmann, M. R.

Asymmetric Membrane for Digital Detection of Single Bacteria in Milliliters of Complex Water Samples. *ACS Nano* **2018**. *12* (10), 10281–10290

(28) Laue, M.; Kauter, A.; Hoffmann, T.; Möller, L.; Michel, J.; Nitsche, A. Morphometry of SARS-CoV and SARS-CoV-2 Particles in Ultrathin Plastic Sections of Infected Vero Cell Cultures. *Sci. Rep.* **2021**, *11* (1), 3515.

(29) Lin, X.; Huang, X.; Urmann, K.; Xie, X.; Hoffmann, M. R. Digital Loop-Mediated Isothermal Amplification on a Commercial Membrane. *ACS Sensors* **2019**, *4* (1), 242–249.

(30) Huang, X.; Lin, X.; Urmann, K.; Li, L.; Xie, X.; Jiang, S.; Hoffmann, M. R. Smartphone-Based in-Gel Loop-Mediated Isothermal Amplification (GLAMP) System Enables Rapid Coliphage MS2 Quantification in Environmental Waters. *Environ. Sci. Technol.* **2018**, *52* (11), 6399–6407.

Supporting Information

Text 1 Bacteria sample Preparation

All bacterial strains were purchased from the American Type Culture Collection (ATCC, Manassas, VA). *E. coli* (ATCC 10798) was used as model indicator bacteria in this study and cultured in LB broth in the shaking incubator for ~14 h at 37 °C at 200 rpm. *Salmonella* Typhi (CVD 909) was used as model pathogenic bacteria and was cultivated in TS broth with in the incubator for ~14 h at 35 °C at 200 rpm. Before each test, cells were harvested, washed and serially diluted to 10^4-10^6 cells·mL^{-1} using phosphate-buffered saline (PBS) (pH 7.4) (Corning™, USA). The concentrations of used bacteria suspensions were measured by fluorescence enumeration. The washed bacterial sample was stained with 1× SYBR Green and incubated in dark for 20 min. Stained bacterial sample was filtered through a PCTE membrane with a 0.2 μm pore size (SterliTech), and the membrane was placed on a glass slide. The cell number was then counted under a fluorescence microscope (Leica DMi8, Leica Co., Germany). If DNA extraction was performed, the PureLink™ Genomic DNA Mini Kit was used following its manufacturer's instructions.

Text 2 Bacteria Sample Filtration

Bacterial samples were filtered through a 13mm PCTE membrane with a 0.2 μm pore size on top of a 13mm PETE membrane (mesh spacer). All PCTE membranes and PETE membranes used in this study were ordered from SterliTech Corporation (Kent, WA). The PETE membrane was used as a drain disc to hold the PCTE membrane to prevent the shape change of the PCTE membrane during the filtration. The membrane and its drain disc were put in to a 13mm Swinnex Filter Holder obtained from MilliporeSigma (Burlington, MA). Filtrations were performed by syringe pushed by hand for 1mL of bacterial samples and were performed by a syringe pump (74905-02, Cole-Parmer, US) for 10−100 mL of bacterial samples.

Text 3 Bacterial mgLAMP Reaction System

For each mgLAMP assay of 30 µL, the composition of the reaction mix is as follows: 3 µL of 10× LAMP buffer, 6 mM MgSO4, 1.4 mM dNTP, 640 U/mL Bst 2.0 WarmStart polymerase, 1.5 mg/mL BSA, 2 mM NaF, 0.1 mg/mL lysozyme 1.6 µM FIB/BIP, 0.2 µM F3/B3, 0.8 µM LF/ LB, and nuclease-free water, plus 10% (w/v) hydrogel. Four-arm PEG acrylate (molecular weight (MW) of 10,000 Laysan Bio, Arab, AL) and thiol-PEG-thiol (MW of 3,400; Laysan Bio, Arab, AL) were used to form the PEG gel at a mole ratio of 1:2. LAMP primers used are listed in Table S1. All LAMP reagents were purchased from New England Biolabs (Ipswich, MA) and all primers, probes and quenchers were obtained from Integrated DNA Technologies (Coralville, IA) unless otherwise specified.

Complementary fluorescent probe (molecular beacon) were custom designed and added to the reaction mix at a final concentration of 0.4 µM. Customized molecular beacons were designed using PrimerExplorer V4 (http://primerexplorer.jp/elamp4.0.0/index.html). The molecular beacon for *E. coli* is:

(6-FAM)-5-CACCTTATCAATCTCGATATCCATGAAGGTG-(3IABkFQ) and the molecular beacon for *S.* Typhi is:

(6-FAM)-5-AGGAACTCGGATGGCTTCGTTCCT-3-(3IABkFQ).

Table S1. LAMP Primers for *E. col* and *S*. Typhi

Target	Primer name	Sequence (5'-3')	Reference
E. coli	F3	GCCATCTCCTGATGACGC	Hill et al., 2008
	B3	ATTTACCGCAGCCAGACG	
	FIP (F1c+F2)	CATTTTGCAGCTGTACGCTCGCAGCC CATCATGAATGTTGCT	
	BIP (B1c+B2)	CTGGGGCGAGGTCGTGGTATTCCGA CAAACACCACGAATT	
	LF	CTTTGTAACAACCTGTCATCGACA	
	LB	ATCAATCTCGATATCCATGAAGGTG	
S. Typhi	F3	GACTTGCCTTTAAAAGATACCA	Fan et al., 2015
	B3	AGAGTGCGTTTGAACACTT	
	FIP (F1c+F2)	AACTTGCTGCTGAAGAGTTGGACCGA ATGACTCGACCATC	
	BIP (B1c+B2)	CCTGGGGCCAAATGGCATTATGCACT AAGTAAGGCTGG	
	LF	TCGGATGGCTTCGTTCCT	
	LB	CAAGGGTTTCAAGACTAAGTGGTTC	

Table S2. 11 LAMP primers sets tested for this study.

Primer Set No.	Target gene	Primer	Sequence
1	N gene	FIP (5'-3')	CCACTGCGTTCTCCATTCTGGTAAATGCACCCCGCATTACG
			CGCGATCAAAACAACGTCGGCCCTTGCCATGTTGAGTGAGA
		F3 (5'-3')	TGGACCCCAAAATCAGCG
		B3 (5'-3')	GCCTTGTCCTCGAGGGAAT
		LF (5'-3')	TGAATCTGAGGGTCCACCAA
		LB (5'-3')	TTACCCAATAATACTGCGTCTTGGT
2		FIP (5'-3')	AGCGGTGAACCAAGACGCAGGGCGCGATCAAAACAACG
		BIP (5'-3')	AATTCCCTCGAGGACAAGGCGAGCTCTTCGGTAGTAGCCAA
		F3 (5'-3')	CCAGAATGGAGAACGCAGTG
		B3 (5'-3')	CCGTCACCACCACGAATT
		LF (5'-3')	TTATTGGGTAAACCTTGGGGC
		LB (5'-3')	TAACACCAATAGCAGTCCAGATGA
3	The consensus sequences of 23 different strains were established to identify areas of sequence conservation.	FIP (5'-3')	AGAGCAGCAGAAGTGGCACAGGTGATTGTGAAGAAGAAGAG
		BIP (5'-3')	TCAACCTGAAGAAGAGCAAGAACTGATTGTCCTCACTGCC
		F3 (5'-3')	TCCAGATGAGGATGAAGAAGA
		B3 (5'-3')	AGTCTGAACAACTGGTGTAAG
		LF (5'-3')	CTCATATTGAGTTGATGGCTCA
		LB (5'-3')	ACAAACTGTTGGTCAACAAGAC
4	ORF1a	F3 (5'-3')	CTGCACCTCATGGTCATGTT
		B3 (5'-3')	AGCTCGTCGCCTAAGTCAA
		FIP (5'-3')	GAGGGACAAGGACACCAAGTGTATGGTTGAGCTGGTAGCAGA
		BIP (5'-3')	CCAGTGGCTTACCGCAAGGTTTTAGATCGGCGCCGTAAC
		LF (5'-3')	CCGTACTGAATGCCTTCGAGT
		LB (5'-3')	TTCGTAAGAACGGTAATAAAGGAGC
5		F3 (5'-3')	TCATCAAACGTTCGGATGCT
		B3 (5'-3')	TATGGCCACCAGCTCCTT
		FIP (5'-3')	CGACCGTACTGAATGCCTTCGAGAACTGCACCTCATGGTCAT
		BIP (5'-3')	AGACACTTGGTGTCCTTGTCCCAGAAGAACCTTGCGGTAAGC
		LF (5'-3')	CTGCTACCAGCTCAACCATAAC
		LB (5'-3')	TCATGTGGGCGAAATACCAGT
6		F3 (5'-3')	CTGCACCTCATGGTCATGTT
		B3 (5'-3')	GATCAGTGCCAAGCTCGTC
		FIP (5'-3')	GAGGGACAAGGACACCAAGTGTGGTAGCAGAACTCGAAGGC
		BIP (5'-3')	CCAGTGGCTTACCGCAAGGTTTTAGATCGGCGCCGTAAC
		LF (5'-3')	ACCACTACGACCGTACTGAAT
		LB (5'-3')	TTCGTAAGAACGGTAATAAAGGAGC
7	N gene	F3 (5'-3')	TGGCTACTACCGAAGAGCT
		B3 (5'-3')	TGCAGCATTGTTAGCAGGAT
		FIP (5'-3')	TCTGGCCCAGTTCCTAGGTAGTCCAGACGAATTCGTGGTGG
		BIP (5'-3')	AGACGGCATCATATGGGTTGCACGGGTGCCAATGTGATCT
		LF (5'-3')	GGACTGAGATCTTTCATTTTACCGT
		LB (5'-3')	ACTGAGGGAGCCTTGAATACA
8		F3 (5'-3')	ACCGAAGAGCTACCAGACG
		B3 (5'-3')	TGCAGCATTGTTAGCAGGAT
		FIP (5'-3')	TCTGGCCCAGTTCCTAGGTAGTTCGTGGTGGTGACGGTAA
		BIP (5'-3')	AGACGGCATCATATGGGTTGCACGGGTGCCAATGTGATCT
		LF (5'-3')	CCATCTTGGACTGAGATCTTTCATT
		LB (5'-3')	ACTGAGGGAGCCTTGAATACA
9	Complete genome sequences of various COVID-19 were aligned and analyzed to identify conserved sequences.	F3 (5'-3')	TGCTTCAGTCAGCTGATG
		B3 (5'-3')	TTAAATTGTCATCTTCGTCCTT
		FIP (5'-3')	TCAGTACTAGTGCCTGTGCCCACAATCGTTTTTAAACGGGT
		BIP (5'-3')	TCGTATACAGGGCTTTTGACATCTATCTTGGAAGCGACAACAA
		LF (5'-3')	CTGCACTTACACCGCAA
		LB (5'-3')	GTAGCTGGTTTTGCTAAATTCC
10	N gene	FIP (5'-3')	GCCAGCCATTCTAGCAGGAGCAACAGTTAAGAAATTCAACTCC
		BIP (5'-3')	GATGCTGCTCTTGCTTTGCTACCAGACATTTTGCTCTCAA
		F3 (5'-3')	GTTCCTCATCACGTAGTCG
		B3 (5'-3')	GTTTGGCCTTGTTGTTGTT
		LB (5'-3')	GCTGCTTGACAGATTGAACCAG
11		FIP (5'-3')	TAAGGCTTGAGTTTCATCAGCCTTACGCATACAAAACATTCCCA
		BIP (5'-3')	CAGAGACAGAAGAAACAGCAAACTGATTGTTGCAATTGTTTGGAG
		F3 (5'-3')	GTCATTTTGCTGAATAAGCATAT
		B3 (5'-3')	GAGTCAGCACTGCTCATG
		LB (5'-3')	GTGACTCTTCTTCCTGCTGCAGATT

Table S2. Cont.

Probe	Limit of detection	Dynamic range	Time to answer	Treated volume/uL	Sample matrix	Refernce
Eva Green	625	~625 to 2 × 10^5	50 min	1 µL	Plasmids containing the complete N gene	González-González et al. 2020
SYBR Green	1.02 fg	to 10 ng	30 min	NA	human serum, urine, saliva, oropharyngeal swabs, and nasopharyngeal swabs	Lamb et al. 2020
YTO®-9 double-stranded DNA binding dye	120 copies/3 uL	~120 million copies down to ~120 copies (per 25 µL reaction)	30 min	3 µL	DNA fragments containing these two regions were synthesized as gBlocks	Zhang et al. 2020
EvaGreen® dye	fewer than 100 targets per reaction volume	70000 targets per reaction volume	50 min	1 µL	Synthesized DNA (619bp) containing the targeted sequence to mimic the COVID-19 target	El-Tholoth et al. 2020
EvaGreen® dye	50 RNA copies	up to 10^8 copiesper µL	30 min	2 µL	Genomic RNA for SARS-Related Coronavirus 2 and clinical samples	Ganguli et al. 2020

Table S3. FAM modified inner primers and corresponding quenchers of different lengths.

Name	Sequence
5'FAM-FIP	/56-FAM/TAAGGCTTGAGTTTCATCAGCCTTACGCATACAAAACATTCCCA
12nt-qFIP-3'IBFQ	ACTCAAGCCTTA/3IABkFQ/
17nt-qFIP-3'IBFQ	ATGAAACTCAAGCCTTA/3IABkFQ/
5'FAM-BIP	/56-FAM/CAGAGACAGAAGAAACAGCAAACTGATTGTTGCAATTGTTTGGAG
10nt-qBIP-3'IBFQ	TCTGTCTCTG/3IABkFQ/
15nt-qBIP-3'IBFQ	TTTCTTCTGTCTCTG/3IABkFQ/

Figure S1. Surface water sampling location of the Godawari river in Kathmandu, Nepal.

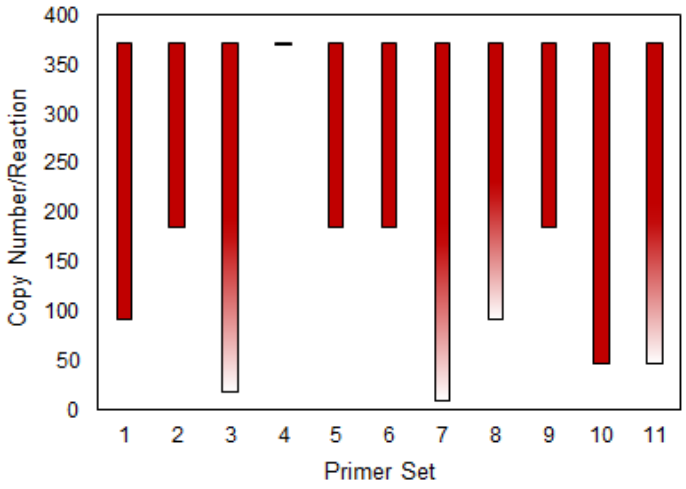

Figure S2. Detection limits of 11 primer sets. Bars with transparent ends mean that false negative occurred at detection of the lowest copy numbers.

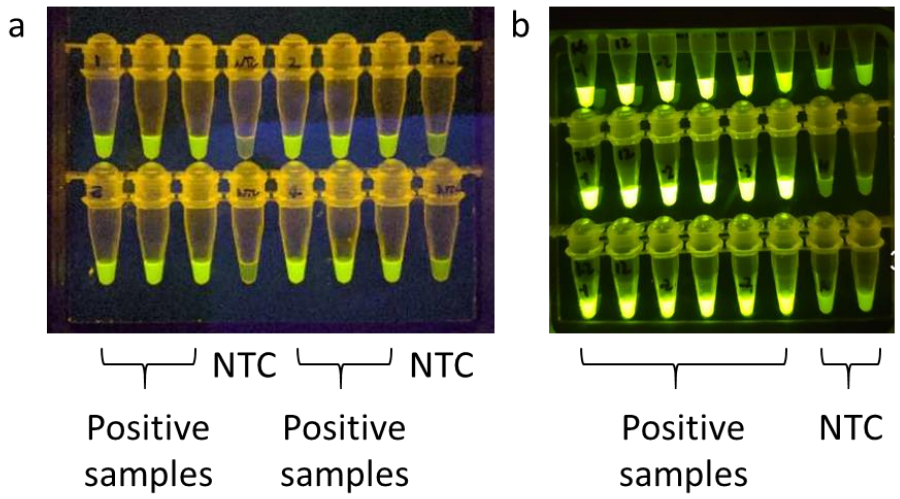

Figure S3. Fluorescence outputs of (a) molecular beacons and (b) QUASR probes. QUASR probes showed higher fluorescence yield and higher signal-to noise ratio. (This figure was created by Jing Li, who granted permission of its use in this dissertation.)

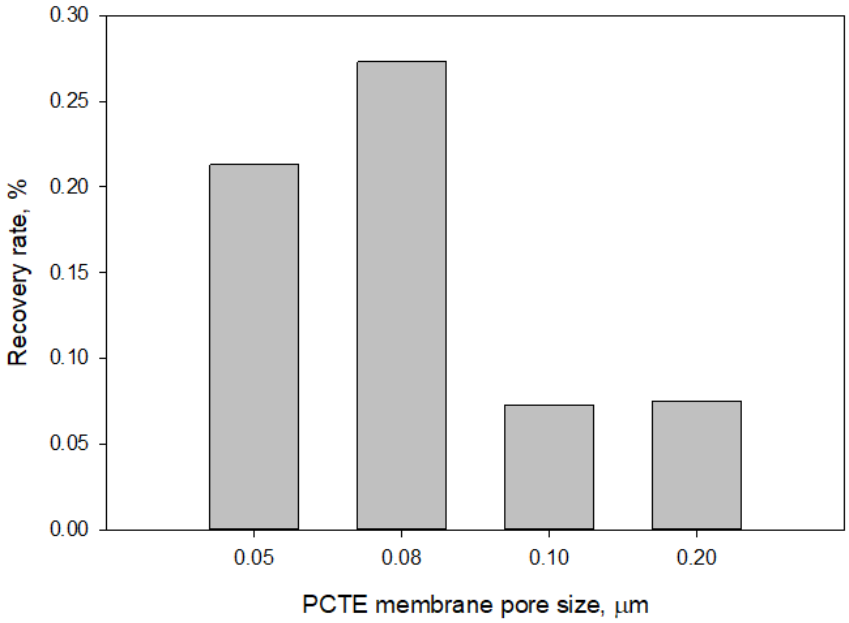

Figure S4. SARS-CoV-2 recovery rates of PCTE membranes with different pore sizes. (This figure was created by Jing Li, who granted permission of its use in this dissertation.)

References:

(1) Hill, J.; Beriwal, S.; Chandra, I.; Paul, V. K.; Kapil, A.; Singh, T.; Wadowsky, R. M.; Singh, V.; Goyal, A.; Jahnukainen, T.; Johnson, J. R.; Tarr, P. I.; Vats, A. Loop-Mediated Isothermal Amplification Assay for Rapid Detection of Common Strains of Escherichia Coli. *J. Clin. Microbiol*. **2008**, 46, 2800-2804.

(2) Fan, F.; Yan, M.; Du, P.; Chen, C.; Kan, B. Rapid and Sensitive Salmonella Typhi Detection in Blood and Fecal Samples Using Reverse Transcription Loop-Mediated Isothermal Amplification. *Foodborne Pathog. Dis*. **2015,** 12, 778-786.

(3) González-González, E.; Lara-Mayorga, I. M.; Rodríguez-Sánchez, I. P.; León, F. Y. De; García-Rubio, A.; Garciaméndez-Mijares, C. E.; Guerra-Alvarez, G. E.; García-Martínez, G.; Aguayo-Hernández, J. A.; Márquez-García, E. Scaling Diagnostics in Times of COVID-19: Colorimetric Loop-Mediated Isothermal Amplification (LAMP) Assisted by a 3D-Printed Incubator for Cost-Effective and Scalable Detection of SARS-CoV-2. *medRxiv* **2020**.

(4) Lamb, L. E.; Ph, D.; Oak, R.; States, M. I. U.; Lamb, L. E.; Ph, D.; Lamb, L. E.; Ph, D.; Bartolone, S. N. Rapid Detection of Novel Coronavirus (COVID-19) by Reverse Transcription-Loop- Mediated Isothermal Amplification. *medRxiv* **2020**.

(5) Zhang, Y.; Odiwuor, N.; Xiong, J.; Sun, L.; Nyaruaba, R. O.; Wei, H.; Tanner, N. A. Rapid Molecular Detection of SARS-CoV-2 (COVID-19) Virus RNA Using Colorimetric LAMP. *medRxiv* **2020**.

(6) El-Tholoth, M.; Bau, H. H.; Song, J. A Single and Two-Stage, Closed-Tube, Molecular Test for the 2019 Novel Coronavirus (COVID-19) at Home, Clinic, and Points of Entry. *ChemRxiv* **2020**.

(7) Ganguli, A.; Mostafa, A.; Berger, J.; Aydin, M. Y.; Sun, F.; Stewart de Ramirez, S. A.; Valera, E.; Cunningham, B. T.; King, W. P.; Bashir, R. Rapid Isothermal Amplification and Portable Detection System for SARS-CoV-2. *Proc. Natl. Acad. Sci. U. S. A.* **2020**, *117* (37), 22727–22735.

CO-OCCURRENCE PATTERNS OF *VIBRIO CHOLERAE* AND *ESCHERICHIA COLI* IN VARIOUS ENVIRONMENTAL SETTINGS

Xunyi Wu, Jing Li, and, Michael R. Hoffmann*

Author Statement

The manuscript was written through contributions of all authors. M.R.H, J.L., and X.W. conceived the concept for this study. J.L. and X.W. designed the study, X.W. performed experiments, and X.W. wrote the paper.

4.0. Abstract

Regular environmental surveillance of waterborne pathogens is required to ensure the safety of water and protect human health. Due to the diverse range of pathogenic bacteria in environmental waters, regular monitoring of a range of pathogens may be impractical due to the lack of qualified personnel or the availability of advanced instrumentation. Therefore, microbial indicator organisms are most often used to manage waterborne health risks. In this study, the interactions of *Vibrio cholerae* (*V. cholerae*), the etiologic agent of cholera, with *Escherichia coli* (*E. coli*), the most commonly used indicator organism for waterborne pathogens including *V. cholerae*, was investigated through evaluating the survival and growth of both bacteria under different temperatures and nutrition deprivation using plate culturing and real-time polymerase chain reaction (qPCR). During co-growth, it is challenging for *V. cholerae* to maintain an initial population advantage since *E. coli* could utilize substrates for growth and respiration more effectively. As observed during competitive growth, *V. cholerae* retreats into a viable-but–non-culturable state under environmental stress over 3-5 days while *E. coli* remains viable for more than 14 days. It is clear that *V. cholerae* competes with *E. coli* depending on the water source suggesting that bacterium-bacterium interactions are influenced by

multiple physicochemical and biochemical parameters present in a given ambient water body are contributing factors regulating the proliferation of *V. cholerae*.

4.1. Introduction

Waterborne pathogenic bacteria are responsible for a series of diseases, being a major public health concern worldwide[1–3]. Health issues related to pathogenic bacteria have become extremely severe in many developing regions because of limited clean water supplies and poor sanitation conditions[4,5]. Children, the elderly, and people with impaired immune systems are especially susceptible to these diseases. Moreover, diseases caused by waterborne pathogens have the potential to spread and infect large numbers of individuals within a certain region in a short time, posing serious risks to many local communities[6,7]. One of the leading etiologic pathogenic bacteria is *Vibrio cholerae* (*V. cholerae*). Some strains of *V. cholerae* secrete cholera toxin (CT), which is the causative agent of cholera as a disease[8,9]. During the bacterial infection on human intestine, mucous production is enhanced, which leads to diarrhea, vomiting, and extreme dehydration. Cholera is estimated to cause around 2.8 million cases of illness and 91,000 deaths worldwide annually[10]. For example, a cholera outbreak in Haiti in mid-October 2010 led to around 665,000 confirmed cases and 8,183 people died[11]. Many developing regions around the world are under the continuous threat of cholera (e.g., 1045

reported cases of cholera and 24 related deaths took place in Ethiopia between mid-December 2019 and February 2020[12]).

Just as many other pathogenic bacteria, *V. cholerae* is mainly transmitted through the fecal-oral route: from fecal materials secreted by infected persons to healthy persons though unclean drinking water or contaminated food[5]. Moreover, after being released to the environment. *V. cholerae* can persist in multiple aquatic environmental reservoirs for weeks or months, which further increase the difficulty to eradicate the transmission of this disease[13,14]. Therefore, regular environmental surveillance of pathogenic bacteria including *V. cholerae* is required to ensure the safety of water and protect human health. Precise detection and quantification methods for waterborne pathogens including traditional culture-based methods and more recent nucleic acid amplification diagnosis are regularly used in surveillance programs to periodically measure the concentrations of target pathogens and to evaluate the potential risks[15]. Nevertheless, there can be a diverse range of pathogenic bacteria in environmental waters, and regular monitoring of so many pathogens individually may be impractical due to the lack of qualified labor and easy and reliable methods. Thus, a microbial indicator organism is often used as the primary method for managing waterborne health risks[16,17].

Microbial indictors are microorganisms that are more abundant and more readily detected and thus used to indicate the probable presence of pathogenic organisms. *Escherichia coli* (*E. coli*) is the most commonly used indicator due to its high correlation with fecal contamination[18–20]. There is a high concentration of *E. coli* in the intestines of vertebrate animals. Fecal bacteria are released into the environment as fecal matter. Thus, the presence of *E. coli* in environmental waters can indicate the possibility of fecal contamination occurrence as well as fecal pathogenic risks[21,22]. Compared to many pathogenic bacteria, which have low concentration in environmental waters and are often difficult to detect, *E. coli*'s concentration is as a surrogate indicator. Acceptable microbial indicator requirements have been established by the World Health Organization, the US Environmental Protection Agency, and the US Food and Drug Administration among other agencies[23–25]. However, the growth, persistence and survival of the indicator bacteria with other fecal pathogens can vary as a function of the specific environmental setting, and therefore, may control the correlation between *E. coli* and *V. cholerae* or other pathogenic bacteria.[16,26].

In this study, the interactions of *V. cholerae* with *E. coli* will be investigated through evaluating the survival and growth of both bacteria under lab conditions

with different initial proportions. We also looked at the persistence of *E. coli* and *V. cholerae* in environmental water samples including surface water samples and drinking water samples for 7 to 14 days. Moreover, a special focus was given to the development of viable but non-culturable (VBNC) state in *V. cholerae* that usually fail to grow on culture media but remain metabolically active to persist during unfavorable conditions under survival competition. We highlight that *V. cholerae* interacts *E. coli* differently under different water conditions suggesting that bacterium-bacterium interactions influenced by multiple parameters of ambient water would be a contributing mechanism in regulating the proliferation of *V. cholerae.* Besides understanding more about the correlation between this microbial indicator and the risk of this fecal pathogen, this study also aims to use the information of this bacterium-bacterium interactions to provide inspirations on how to design better bottom-up control practices towards *V. cholerae* and other waterborne pathogens using microbial indicators.

4.2. Materials and Methods

4.2.1. Cultivation of E. coli and V. Cholerae

E. coli (ATCC 10798) and *V. Cholerae* (ATCC 14035) used in this study were purchased at lyophilized state and stored at -80 °C. These bacterial strains were first propagated from lyophilized state according to the manufacture's procedures, and then cultured in Luria-Bertani broth (BD Difco™, USA) at 37 °C overnight to reach the stationary phase. Before each test, bacterial cells were harvested by centrifuging for 2 minutes at 6000 RCF, washed and serially diluted to 10^4-10^6 cells·mL^{-1} using phosphate-buffered saline (pH 7.4) (Corning™, USA).

4.2.2. Water Sample Collection and Processing

Two representative locations of water sources were selected and sampled at May 2019. One environmental water samples were collected from a turtle pond on the Caltech campus (Pasadena, CA, USA) and the other from the snow creek in mammoth mountains (Mammoth, CA, USA) (with ionic strengths of 15 and 5 mmol·L^{-1}, respectively[27]). Two samples of 500 mL each were collected using sterile

plastic or glass bottles. Samples were transported to the laboratory using cold chain and stored at 4 °C. Water temperature was measured in each water source. The conductivities and pH values of environmental water samples were measured with an electrical pH/conductivity meter (Orion Star A215, Thermo Scientific, US) and ionic strengths were quantified using Griffin's equation[28]. 20 μL of each collected water samples were plated on Luria-Bertani agar (BD Difco™, USA) to evaluate the initial concentration of local microorganisms within 48 h after sample collection. Before the seeding of *E. coli* and *V. Cholerae*, environmental water samples are sterilized by autoclaving.

4.2.3. Phenotypic and Molecular-based Quantification of *E. coli* and *V. Cholerae*

20 μL of enrichment cultures or water samples of *E. coli* and *V. Cholerae* were plated onto Luria-Bertani agar (BD Difco™, USA) and thiosulfate citrate bile salts sucrose (TCBS; BD Difco™, USA) agar plates and incubated for 18 to 20 hours at 37 °C. All results were expressed in number of colony-forming units (CFU) per 100 mL. Optical density at a wavelength of 600 nm (OD600) was also measured using

Nanodrop 2000 (Thermo Scientific, USA) for estimating the concentration of bacteria to monitor the growth.

Concentrations of *E. coli* and *V. cholerae* were also molecularly quantified by quantitative PCR (qPCR) using a 6300 Realplex4 qPCR platform (Eppendorf, Hamburg, Germany). Bacterial DNAs were first extracted using the PureLink® Genomic DNA Mini Kit (Invitrogen, USA) before amplification according to the manufacturer's manual. Relevant primer sets and probes are listed in Table 1. For *E. coli*, the qPCR assay targeting the rfb gene cluster partial sequences was carried out in a 20-µL reaction mixture consists of 10 µL PerfeCTa® qPCR ToughMix® (Quanta BioSciences Inc.), 0.2 µM forward primer, 0.2 µM reverse primer, 0.1 µM TaqMan probe, 2 µL of template DNA, and nuclease-free-water. The qPCR thermocycling involves 10 minutes of initialization at 95 °C, and 40 cycles of denaturation at 95 °C for 15 seconds followed by annealing at 56 °C for 30 seconds and extension at 72 °C for 30 seconds. A final hold at 72 °C for 5 min was added.

For *V. cholerae*, the qPCR assay targeting the nonclassical hemolysin (hlyA) sequence was carried out in a 20-µL reaction mixture consists of 10 µL PerfeCTa® qPCR ToughMix® (Quanta BioSciences Inc.), 0.3 µM forward primer, 0.3 µM reverse primer, 0.05 µM TaqMan probe, 2 µL of template DNA, and nuclease-free-

water. The qPCR thermocycling involves 10 minutes of initialization at 95 °C, and 40 cycles of denaturation at 95 °C for 20 seconds followed by annealing/extension at 60 °C for 60 seconds. All qPCR reactions for each DNA sample were undertaken in duplicate or triplicate and the nuclease-free water was used as negative controls for all qPCR assays.

4.2.4. Monitoring of Growth and Maintenance of *E. coli* and *V. Cholerae*

E. coli and *V. Cholerae* at different initial proportions from 200:1 to 1: 50 were seeded in LB broth with a total initial concentration of 10^7 cells/mL. 1 mL of co-culture samples was taken from the beginning of the seeding, after 1, 2, 3, 5, 7, 9, and 24 hours. Taken co-culture samples were processed and quantified using the method mentioned in the previous section.

To evaluate the viability of *V. cholerae* during co-culture, a propidium monoazide (PMA) pretreatment step was used[29]. First, PMA solution (Biotium Inc., USA) was added to samples to a final concentration of 80 μM. Samples with PMA was incubated in the dark at 4 °C for 10 min, and then exposed to light (1000 W/m^2, Sun 2000, Abet Technologies Inc.) for 10 min on ice box to activate PMA.

To evaluate the maintenance of *E. coli* and *V. Cholerae* in environmental samples, pure *E. coli* and *V. Cholerae* as well as mixed cultures as different proportions were seeded to environmental water samples. The microorganism concentrations were measured after 1, 2, 3, 4, 5 and 6 days using both phenotypic and molecular-based quantification methods.

4.3. Results and Discussion

4.2.1. Growth of *E. coli* and *V. Cholerae* in Co-cultures

As fecal bacteria, *E. coli* and *V. Cholerae* share many common characteristics including their preferred growth conditions. That is one of the major reason why *E. coli* is commonly used as a fecal bacterial indicator for *V. cholerae* in environmental waters and to estimate the potential pathogenic risks[30]. Under their most preferred growth conditions in lab conditions (37 °C, 200 rpm, in LB broth), both bacteria showed similar growth curves (Fig. S1.), reaching a stationary phase in ~ 10 hours with a doubling time around 20 minutes. When *E. coli* and *V. Cholerae* were growing in co-cultures, the bacterial populations also showed similar growth curves regardless of the constituent proportions when the total initial seeding concentrations remained similar. As shown on Figure 1., the growth of the total bacterial concentration of *E. coli* and *V. Cholerae* was quite stable.

Theoretically, if the growth rate of both bacteria remained the same during co-culture, their relative proportions should also remain stable during growth. If so, we could use the endpoint measurement of the concentrations of *E. coli* to *V. Cholerae* to estimate the concentrations when *E. coli* and *V. Cholerae* were initially

released. When *E. coli* and *V. Cholerae* were seeded at a similar level (1:1 and 4:1), their growth rates seemed quite stable during the whole periods before reaching stationary phase (**Fig. 2.**). Considering that in most environmental water samples, the concentration of *E. coli* is usually much higher than the concentration of *V. Cholerae*, *E. coli* given initial growth advantages by increasing its concentration to 100 and 200 folds of the concentrations of *V. Cholerae*. As shown on **Fig. 2C** and **2D,** *E. coli* could maintain these initial advantages until the endpoint at the stationary phase. However, if we gave initial growth advantages to *V. Cholerae* to *E. coli* by 20 fold or even 50 fold, it was challenging for *V. Cholerae* to maintain the advantages. The concentrations of *E. coli* and *V. Cholerae* became closer during growth, and at stationary phase the number of *V. Cholerae* can only be about three times of the number *E. coli* although the initial proportions were as high as 50 times.

Therefore, if on-site detection finds that the concentration of *E. coli* is similar to or greater than the number of *V. Cholerae*, the data can be used to estimate the original source proportions of individual bacterial contaminants. However, when *V. Cholerae* is found to be dominant, since *V. Cholerae* cannot maintain a growth advantage, it may have been introduced initially at a much higher concentration than *E. coli.*

4.2.2. Maintenance of *E. coli* and *V. Cholerae* in Environmental samples

To evaluate the persistence of *E. coli* and *V. Cholerae* in environmental waters, co-cultures had been seeded to different environmental water samples at their preferred temperature (37 °C) and at lower temperature (4 °C). Some literature reported a longer survival period of fecal bacteria at low temperature[31]. In our case, *E. coli* showed very strong survival potential, as it could persist in both preferred temperature and low temperature for more than 2 weeks, with a relatively lower concentration at lower temperature. *V. Cholerae,* however, although showed longer survival at lower temperature for 5 days compared to that at 37 °C. It could not be detected by phenotypic methods after then (**Fig. 3.**). The inability to detect it using culturing methods could be attributed to the induced VBNC state due to the stress of low temperature and low nutrition[14].

4.2.3. Resuscitation of *V. Cholerae*

A resuscitation study was conducted after *V. Cholerae* was induced to VBNC state under environmental stress to examine the resuscitation potential of this pathogen. Preliminary research showed that *E. coli* resuscitated much more easily than *V.*

Cholerae after 1 and 6 months, counting from the time when they became no longer culturable. *E. coli* cells, when responding to appropriate environmental stimuli, such as a temperature upshift or the addition of nutrients, quickly turned to metabolically active and culturable in no matter pure or mixed cultures within 24 hours. However, *V. Cholerae* can only be easily resuscitated from pure culture and the timescale for resuscitation was usually several days. In preliminary experiments from mixed cultures, about 50% of V. Cholerae resuscitated in its preferred growth conditions. Many pathogens in the VBNC state are not infectious, but they can retain virulence potential and become infectious following resuscitation to an actively metabolizing state. As a robust microbial indicator, *E. coli*'s resuscitation is expected, but the potential for the possible resuscitation of other pathogenic microorganisms should also be factored into account.

Tables and Figures

Table 1. qPCR Primers and Probes for *E. coli* and *V. Cholerae*

Target	Primer/ Probe	Sequence (5'-3')	Reference
E. coli K12 rfb	Forward primer	TAA AGT AAC CTT GAT CGA AG	Adapted from Lu et al., 2014[32]
	Reverse Primer	ATT CCT AAA GAA AGT ATC TAT TC	
	TaqMan Probe	/56-FAM/AA CGT ACC AGC ATA AAT GAT CCT /3BHQ_1/	
V. Cholerae hlyA	Forward primer	TGC GTT AAA CAC GAA GCG AT	Adapted from Lyon, 2001[33]
	Reverse Primer	AAG TCT TAC ATT GTG CTT GGG TCA	
	TaqMan Probe	/56-FAM/TC AAC CGA TGC GAT TGC CCA AGA /3BHQ_1/	

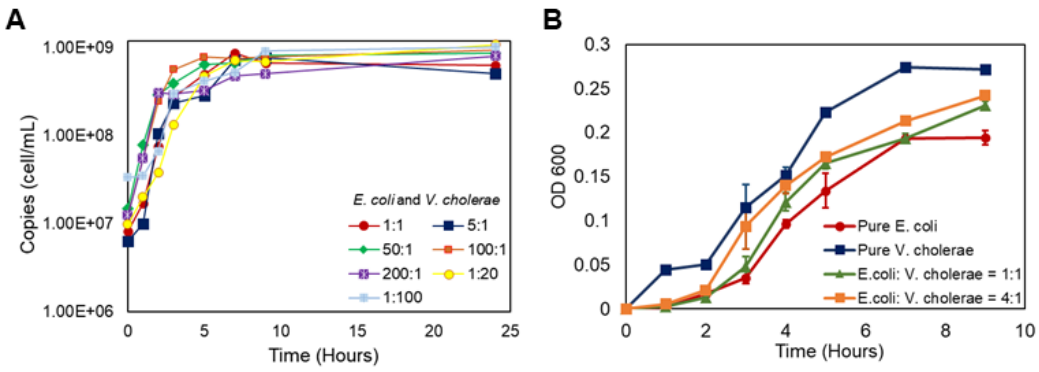

Figure 1. Total bacteria concentration in co-culture of *E. coli* and *V. cholerae*. Measured by A) real-time PCR and B) OD 600.

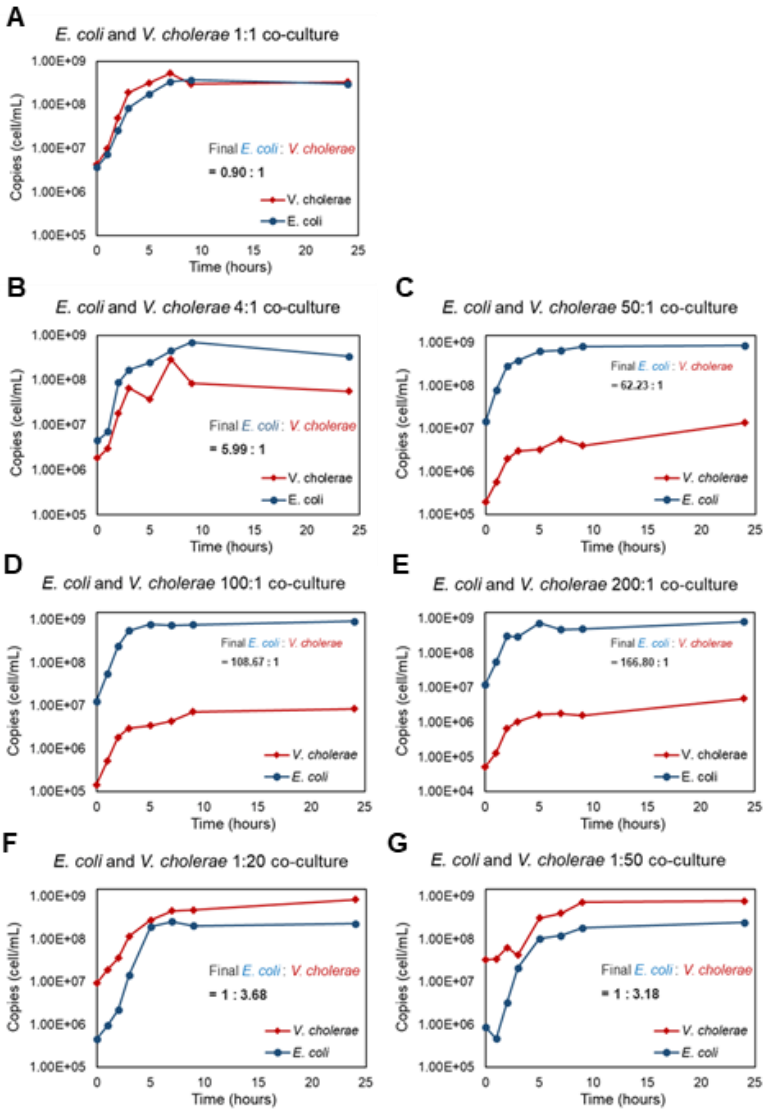

Figure 2. Growth of *E. coli* and *V. cholerae* in LB broth at 37 °C with different initial proportions: initial seeding proportions of *E. coli* and *V. cholerae* are at A) 1:1; B) 4:1; C) 50:1: D) 100:1; E) 200:1; F) 1:20; G) 1:50.

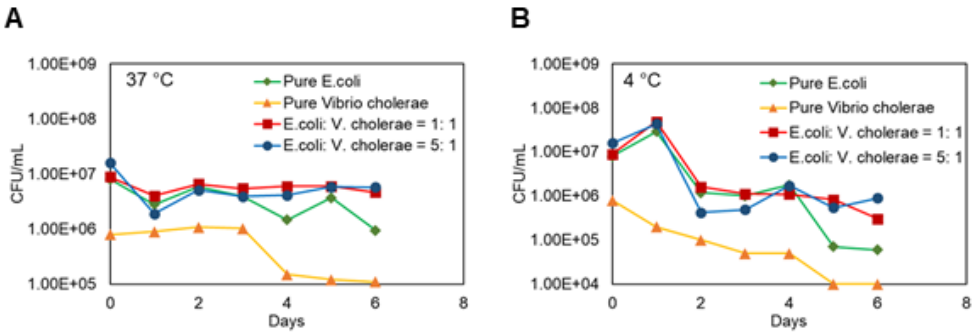

Figure 3. Maintenance of *V. cholerae* and *E. coli* in aquatic environment at different temperatures in snow creek water: A) at 37 °C; B) at 4 °C.

References

(1) Leclerc, H.; Schwartzbrod, L.; Dei-Cas, E. Microbial Agents Associated with Waterborne Diseases. *Critical Reviews in Microbiology*. 2002, pp 371–409.

(2) Ramírez-Castillo, F.; Loera-Muro, A.; Jacques, M.; Garneau, P.; Avelar-González, F.; Harel, J.; Guerrero-Barrera, A. Waterborne Pathogens: Detection Methods and Challenges. *Pathogens* **2015**, *4* (2), 307–334.

(3) World Health Organization. Drinking-water http://www.who.int/news-room/fact-sheets/detail/adolescent-pregnancy.

(4) Prüss-Ustün, A.; Bartram, J.; Clasen, T.; Colford, J. M.; Cumming, O.; Curtis, V.; Bonjour, S.; Dangour, A. D.; De France, J.; Fewtrell, L.; et al. Burden of Disease from Inadequate Water, Sanitation and Hygiene in Low- and Middle-Income Settings: A Retrospective Analysis of Data from 145 Countries. *Trop. Med. Int. Heal.* **2014**, *19* (8), 894–905.

(5) Leclerc, H.; Schwartzbrod, L.; Dei-Cas, E. Microbial Agents Associated with Waterborne Diseases. *Crit. Rev. Microbiol.* **2002**, *28* (4), 371–409.

(6) Diseases, W. Water Sanitation Hygiene Water-Related Diseases. **2020**, 3–5.

(7) Gunda, N. S. K.; Mitra, S. K. Rapid Water Quality Monitoring for Microbial Contamination. *Electrochem. Soc. Interface* **2017**, *25* (4), 73–78.

(8) Silva, A. J.; Benitez, J. A. Vibrio Cholerae Biofilms and Cholera Pathogenesis. *PLoS Negl. Trop. Dis.* **2016**, *10* (2), 1–25.

(9) Gómez-Aldapa, C. A.; Refugio Torres-Viela, M.; Amaya-Acosta, M. A.; Rangel-Vargas, E.; Villaruel-López, A.; Castro-Rosas, J. Behavior of Thirteen Foodborne Bacteria on Whole Hass Avocado and Potential of Roselle Calyx Extracts as Alternative Disinfectant Agents of Avocado. *J. Food Saf.* **2017**, *37* (4), 1–8.

(10) Ali, M.; Nelson, A. R.; Lopez, A. L.; Sack, D. A. Updated Global Burden of Cholera in Endemic Countries. *PLoS Negl. Trop. Dis.* **2015**, *9* (6), 1–13.

(11) WHO. WHO | Cholera in Haiti. *Who*. 2015.

(12) Ethiopia - Cholera Outbreak (Ethiopian Authorities, UNICEF, DG ECHO Partners) (ECHO Daily Flash of 21 January 2020) - Ethiopia _ ReliefWeb.

(13) Vezzulli, L.; Pruzzo, C.; Huq, A.; Colwell, R. R. Environmental Reservoirs of Vibrio Cholerae and Their Role in Cholera. *Environ. Microbiol. Rep.* **2010**, *2* (1), 27–33.

(14) Lutz, C.; Erken, M.; Noorian, P.; Sun, S.; McDougald, D. Environmental Reservoirs and Mechanisms of Persistence of Vibrio Cholerae. *Front. Microbiol.* **2013**, *4* (12), 1–15.

(15) Leclerc, H.; Edberg, S.; Pierzo, V.; Delattre, J. M. Bacteriophages as Indicators of Enteric Viruses and Public Health Risk in Groundwaters. *Journal of Applied Microbiology*. 2000. *88* (1), 5-21.

(16) Abia, A. L. K.; Ubomba-Jaswa, E.; Momba, M. N. B. Competitive Survival of Escherichia Coli, Vibrio Cholerae, Salmonella Typhimurium and Shigella Dysenteriae in Riverbed Sediments. *Microb. Ecol.* **2016**, *72* (4), 881–889.

(17) Straub, T. M.; Chandler, D. P. Towards a Unified System for Detecting Waterborne Pathogens. *J. Microbiol. Methods* **2003**, *53* (2), 185–197.

(18) Ashbolt, N.; Grabow, W.; Snozzi, M. Indicators of Microbial Water Quality. In *WHO Water Quality: Guidelines, Standards and Health*; 2001.

(19) Saxena, G.; Bharagava, R. N.; Kaithwas, G.; Raj, A. Microbial Indicators, Pathogens and Methods for Their Monitoring in Water Environment. *J. Water Health* **2015**, *13* (2), 319–339.

(20) Edberg, S. C.; Rice, E. W.; Karlin, R. J.; Allen, M. J. Escherichia Coli: The Best Biological Drinking Water Indicator for Public Health Protection. *J. Appl. Microbiol.* **2000**. (29), 106S-116S.

(21) Truchado, P.; Hernandez, N.; Gil, M. I.; Ivanek, R.; Allende, A. Correlation between E. Coli Levels and the Presence of Foodborne Pathogens in Surface Irrigation Water: Establishment of a Sampling Program. *Water Res.* **2018**, *128*, 226–233.

(22) Price, R. G.; Wildeboer, D. E. Coli as an Indicator of Contamination and Health Risk in Environmental Waters. In *Escherichia coli - Recent Advances on Physiology, Pathogenesis and Biotechnological Applications*; InTech, 2017; Vol. i, p 13.

(23) USEPA [United States Environmental Protection Agency]. National Primary Drinking Water Regulations https://www.epa.gov/ground-water-and-drinking-water/national-primary-drinking-water-regulations.

(24) WHO. WHO | Guidelines for Safe Recreational Water Environments. **2013**, *1*, 118–127.

(25) FDA. Standards for the Growing, Harvesting, Packing, and Holding of Produce for Human Consumption. *Fed. Regist.* **2014**, *77* (171), 1–196.

(26) Truchado, P.; Hernandez, N.; Gil, M. I.; Ivanek, R.; Allende, A. Correlation between E. Coli Levels and the Presence of Foodborne Pathogens in Surface Irrigation Water: Establishment of a Sampling Program. *Water Res.* **2018**, *128*, 226–233.

(27) Daniel, M. H. B.; Montebelo, A. Effects of Urban Sewage on Dissolved Oxygen, Dissolved Inorganic and Organic Carbon, and Electrical Conductivity of Small Streams along a Gradient of Urbanization in the Piracicaba River Basin. *Water, Air, Soil.* **2002**, *136*, 189–206.

(28) Griffen, R. A.; Jurinach, J. J. Estimation of Activity Co-Efficent from the Electrical Conductivity of Natural Agnote Systems in Soil Extracts. *Soil Sc.* **1973**, *116*, 26–30.

(29) Xie, X.; Wang, S.; Jiang, S. C.; Bahnemann, J.; Hoffmann, M. R. Sunlight-

Activated Propidium Monoazide Pretreatment for Differentiation of Viable and Dead Bacteria by Quantitative Real-Time Polymerase Chain Reaction. *Environ. Sci. Technol. Lett.* **2016**, *3* (2), 57–61.

(30) Jofre, J.; Lucena, F.; Blanch, A. R.; Muniesa, M. Coliphages as Model Organisms in the Characterization and Management of Water Resources. *Water (Switzerland)*. **2016**, *8* (5), 199.

(31) Craig, D. L.; Fallowfield, H. J.; Cromar, N. J. Enumeration of Faecal Coliforms from Recreational Coastal Sites: Evaluation of Techniques for the Separation of Bacteria from Sediments. *J. Appl. Microbiol.* **2002**, *93* (4), 557–565.

(32) Lu, J.; Gerke, T. L.; Buse, H. Y.; Ashbolt, N. J. Development of an Escherichia Coli K12-Specific Quantitative Polymerase Chain Reaction Assay and DNA Isolation Suited to Biofilms Associated with Iron Drinking Water Pipe Corrosion Products. *J. Water Health* **2014**, *12* (4), 763–771.

(33) Lyon, W. J. TaqMan PCR for Detection of Vibrio Cholerae Ö1, O139, Non-O1, and Non-O139 in Pure Cultures, Raw Oysters, and Synthetic Seawater†. *Appl. Environ. Microbiol.* **2001**, *67* (10), 4685–4693.

Supporting Information

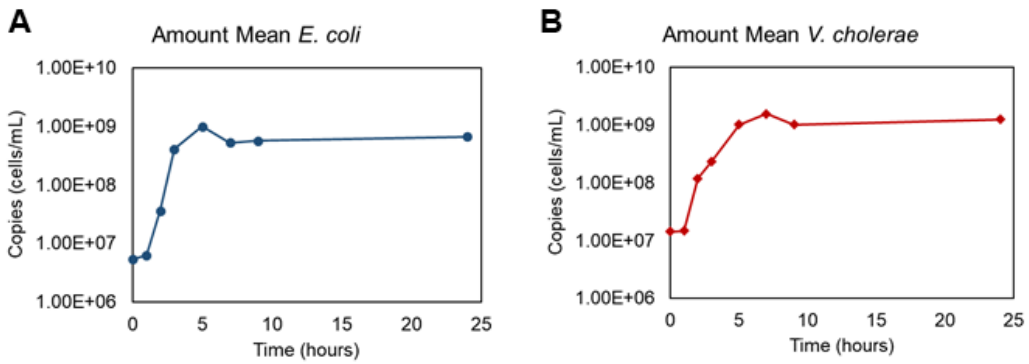

Figure S1. Growth of pure culture of *E. coli* and *V. cholerae* in LB broth at 37°, 200 rpm.

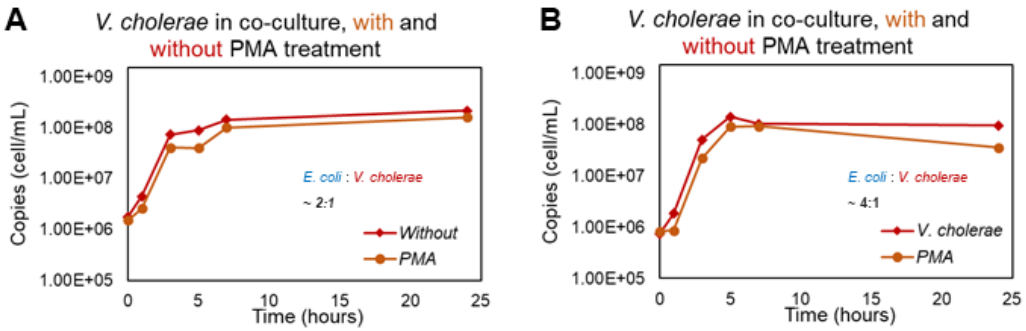

Figure S2. Viability of *V. cholerae* during growing in co-culture with initial *E. coli* and *V. cholerae* proportion at A) 2:1 and B) 4:1.

Chapter 5

CONCLUSION AND OUTLOOK

In this thesis, novel, easy-to-use, and cost-effective solutions were developed for improved waterborne pathogen control, especially under resource-limited conditions: a portable 3D-printed system with super-absorbent polymer (SAP) microspheres for sample enrichment, and a membrane-based in-gel loop-mediated isothermal amplification (mgLAMP) system for absolute quantification were developed, and interactions between microbial indicator and waterborne pathogens were explored. The major contributions of this dissertation are as follows:

1) **Tailored SAP microspheres coupled with a hand-powered tube system were developed to achieve efficient and rapid concentration of environmental microorganisms.** We improved the water absorbing ability of SAP microspheres in highly ionic water samples in terms of both speed and efficiency. We developed a low-cost, portable, hand-powered centrifuge tube system to complement our tailored SAP microspheres. The integrated system greatly facilitates the concentration of water samples in low-resource settings. We envision that this system could be applied to the field for efficient microbial concentration and promote rapid on-site microbial

analysis.

2) **A membrane-based in-gel loop-mediated isothermal amplification system (**mgLAMP**) was developed for rapid and cost-effective in-field quantification of SARS-CoV-2.** mgLAMP can rapidly and easily detect target pathogens in multiple environmental samples. Coupled with analysis on cloud servers, regional distributions of waterborne pathogens could be visualized, providing valuable information on the monitoring and controlling of waterborne pathogens and eliminating the health risk. mgLAMP could be a promising solution in field studies, especially for environmental surveillance and source tracking of waterborne pathogens.

3) **The interactions of *V. cholerae,* as a waterborne pathogen, with *E. coli*, as the most commonly used indicator, was investigated**. We measured the survival and growth rates of both bacteria under different temperatures and nutrition deprivations. The differences in bacterium-bacterium interactions of *V. cholerae* and *E. coli* suggested that environmental stress in ambient water matrices has to be taken into consideration while using microbial indicator to estimate the risk of waterborne pathogens.

In summary, this dissertation constructed a workflow for the surveillance of waterborne pathogens with simplified strategies to concentrate, quantify, and monitor pathogens on site with limited resources.

Looking forward, further works are still needed to facilitate the process of pathogen detection. I hereby suggest a few possible directions for additional projects.

Pretreatment of environmental water samples has always been a major challenge prior to the detection and quantification. While the system with tailored SAP introduced in Chapter 3 provides a simple solution to increase the concentration for easier detection, inhibitors in environmental samples might also be concentrated at the same time. Moreover, nucleic acid samples that are not extracted and purified could contaminate subsequent molecular analysis. Since the current concentration system with SAP has a flow-through tube design that is compatible with centrifuges, the system can be upgraded with membrane-filtration or centrifugation to purify the sample and to remove inhibitors. Similarly, chemical lysis or on-membrane extraction to extract nucleic acids could also be included. These improvements should largely facilitate subsequent detection steps.

For the detection method discussed in Chapter 4, LAMP with customized probes was chosen because this combination yields high fluorescent signal and specificity.

Furthermore, LAMP reactions do not require complicated thermocycling equipment unlike PCR. However, one drawback of LAMP compared to PCR is the complexity of 4-6 primers used; another drawback is that the preparation of the reagent mix can be convoluted and challenging especially for nonprofessional users. One solution is the lyophilization (freeze-drying). Reagent mix could be lyophilized with protectant chemicals and then stored at room temperature. The lyophilized reagent mix has better storage stability and transportability, while still maintaining its performance when water is added. The lyophilization of PCR reagents have been reported to be practical by multiple literatures, whereas lyophilizing LAMP reagent mix remains challenging, especially with customized probes.

Finally, since the technologies introduced in this thesis are designed to be portable and easy to use, we are expecting them to be used at the point of sample collection by nonprofessional personnel. Because of the flow-through design of both the sample pretreatment method and the detection method, these two steps could be integrated together to achieve a stronger performance with a simplified setup. Taking one step further, with the current development of automated robotics and machine learning, automated sampling, detection, and analysis for long term surveillance of target pathogens might be feasible.